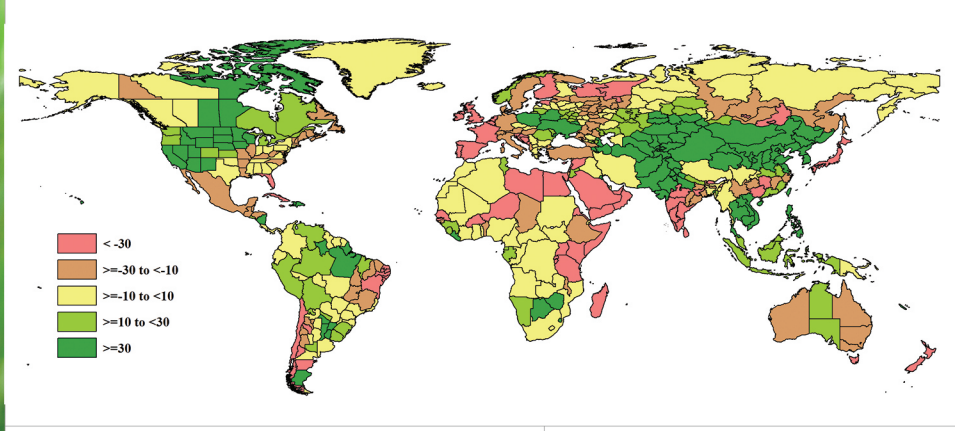

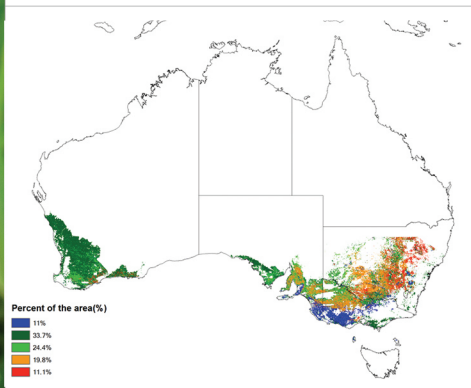

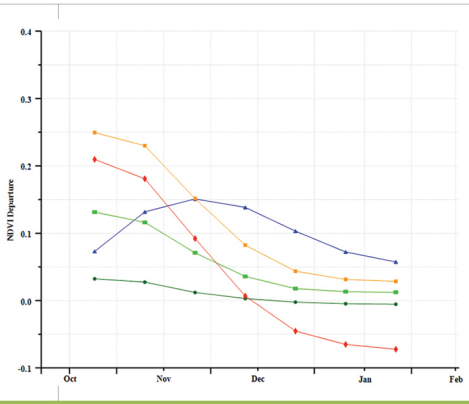

CropWatch bulletin

QUARTERLY REPORT ON GLOBAL CROP PRODUCTION

Monitoring Period: October 2016 - January 2017

Feb 28, 2017

Volume 17, No. 1 (Total No. 104)

Institute of Remote Sensing and Digital Earth (RADI)
Chinese Academy of Sciences (CAS)

February 2017
Institute of Remote Sensing and Digital Earth (RADI), Chinese Academy of Sciences
P.O. Box 9718-29, Olympic Village Science Park
West Beichen Road, Chaoyang
Beijing 100101, China

This bulletin is produced by the CropWatch research team at the Digital Agriculture Division, Institute of Remote Sensing and Digital Earth (RADI), Chinese Academy of Sciences, under the overall guidance of Professor Bingfang Wu.

Contributors are Diego de Abelleyra, Jose Bofana, Sheng Chang, Bulgan Davdai, Rene Gommes, Zhaoxin He, Mingyong Li, Olipa Lungu, Zongha Ma, Prashant Patil, Elijah Phiri, Mrinal Singha, Battestseg (Baku) Tuvdendorj, Shen Tan, Fuyou Tian, Linjiang Wang, Meiling Wang, Bingfang Wu, Qiang Xing, Jiaming Xu, Nana Yan, Mingzhao Yu, Hongwei Zeng, Miao Zhang, Xin Zhang, Xinfeng Zhao, Yang Zheng, Liang Zhu, and Weiwei Zhu.

Thematic contributors for this bulleting include: Jingxin Fang (vc1618@163.com) for the section on price prediction in China. Fengying Nie (niefengying@sohu.com) and Xuebiao Zhang for the section on food import and export outlook in 2017. English version editing was provided by Anna van der Heijden.

Corresponding author: Professor Bingfang Wu
Institute of Remote Sensing and Digital Earth, Chinese Academy of Sciences
Fax: +8610-64858721, E-mail: **cropwatch@radi.ac.cn**, **wubf@radi.ac.cn**

CropWatch Online Resources: This bulletin along with additional resources is also available on the CropWatch Website at http://www.cropwatch.com.cn.

Contents

Note: CropWatch resources, background materials and additional data are available online at www.cropwatch.com.cn.

LIST OF TABLES

LIST OF FIGURES

Abbreviations

5YA	Five-year average, the average for the four-month period for October-January from 2012 to 2016; one of the standard reference periods.
15YA	Fifteen-year average, the average for the four-month period from October-January from 2002 to 2016; one of the standard reference periods and typically referred to as “average.”
BIOMSS	CropWatch agroclimatic indicator for biomass production potential
BOM	Australian Bureau of Meteorology
CALF	Cropped Arable Land Fraction
CAS	Chinese Academy of Sciences
CWAI	CropWatch Agroclimatic Indicator
CWSU	CropWatch Spatial Units
DM	Dry matter
EC/JRC	European Commission Joint Research Centre
ENSO	El Niño Southern Oscillation
FAO	Food and Agriculture Organization of the United Nations
GAUL	Global Administrative Units Layer
GVG	GPS, Video, and GIS data
ha	hectare
kcal	kilocalorie
MPZ	Major Production Zone
MRU	Monitoring and Reporting Unit
NDVI	Normalized Difference Vegetation Index
OISST	Optimum Interpolation Sea Surface Temperature
PAR	Photosynthetically active radiation
PET	Potential Evapotranspiration
RADI	CAS Institute of Remote Sensing and Digital Earth
RADPAR	CropWatch PAR agroclimatic indicator
RAIN	CropWatch rainfall agroclimatic indicator
SOI	Southern Oscillation Index
TEMP	CropWatch air temperature agroclimatic indicator
Ton	Thousand kilograms
VCIx	CropWatch maximum Vegetation Condition Index
VHI	CropWatch Vegetation Health Index
VHIn	CropWatch minimum Vegetation Health Index
W/m^2	Watt per square meter

Bulletin overview and reporting period

This CropWatch bulletin presents a global overview of crop stage and condition between October 1 2016 and January 31 2017, a period referred to in this bulletin as the ONDJ (October, November, December, and January) period or just the "reporting period." The bulletin is the 104th such publication issued by the CropWatch group at the Institute of Remote Sensing and Digital Earth (RADI) at the Chinese Academy of Sciences, Beijing.

CropWatch analyses and indicators

CropWatch analyses are based mostly on several standard as well as new ground-based and remote sensing indicators, following a hierarchical approach. The analyses cover large global zones; major producing countries of maize, rice, wheat, and soybean; and detailed assessments of Chinese regions. In parallel to an increasing spatial precision of the analyses, indicators become more focused on agriculture as the analyses zoom in to smaller spatial units.

CropWatch uses two sets of indicators: (i) agroclimatic indicators—RAIN, TEMP, and RADPAR, which describe weather factors; and (ii) agronomic indicators—BIOMSS, VHIn, CALF, VCIx, and Cropping Intensity, describing crop condition and development. Importantly, the indicators RAIN, TEMP, RADPAR, and BIOMSS do not directly describe the weather variables rain, temperature, radiation, or biomass, but rather they are spatial averages over agricultural areas, which are weighted according to the local crop production potential. For each reporting period, the bulletin reports on the *departures* for all eight indicators, which (with the exception of TEMP) are expressed in relative terms as a percentage change compared to the average value for that indicator for the last five or fifteen years (depending on the indicator). For more details on the CropWatch indicators and spatial units used for the analysis, please see the quick reference guide in Annex C, as well as online resources and publications posted at www.cropwatch.com.cn.

This bulletin is organized as follows:

Chapter	Spatial coverage	Key indicators
Chapter 1	World, using Monitoring and Reporting Units (MRU), 65 large, agro-ecologically homogeneous units covering the globe	RAIN, TEMP, RADPAR, BIOMSS
Chapter 2	Major Production Zones (MPZ), six regions that contribute most to global food production	As above, plus CALF, VCIx, and VHIn
Chapter 3	30 key countries (main producers and exporters)	As above plus NDVI and GVG survey
Chapter 4	China	As above plus high resolution images
Chapter 5	Production outlook, disaster events, agriculture in South and Southeast Asia, and an update on El Niño.	
Online Resources	www.cropwatch.com.cn	

Regular updates and online resources

The bulletin is released quarterly in both English and Chinese. To sign up for the mailing list, please e-mail cropwatch@radi.ac.cn or visit CropWatch online at www.cropwatch.com.cn. Visit the CropWatch Website for additional resources and background materials about methodology, country agricultural profiles, and country long-term trends.

Executive summary

Introduction

The period from October 2016 to January 2017 is a relatively quiet period from an agricultural point of view. In the temperate northern hemisphere summer crops have been harvested, while winter crops have been planted and are now mostly dormant. In some tropical and equatorial countries, including the Philippines, Thailand, Vietnam and Brazil, planting of the second maize and rice generally starts around January, while in the southern hemisphere summer crops are at advanced development stages and nearing flowering, for example maize and soybean in Argentina, Brazil and South Africa.

Southern hemisphere production

Winter wheat harvesting was completed in the southern hemisphere, and the current CropWatch Bulletin provides a production estimate for the main producers: 11.245 million tons in Argentina, an increase of 5.0% over last year; 32.066 million tons in Australia (up by a spectacular 24.3%); and 7.747 million tons of winter wheat in Brazil (+10.0%). In Australia and Argentina, the output of the major production areas grew less than the areas that normally contribute little to exportable surpluses. For maize, the traditional producers and exporters in the southern hemisphere will be covered in detail in the May bulletin. The current situation for the crop, however, is promising in Brazil, the main producer in the south, but less favorable in Argentina where excess water has affected summer crops. South Africa, the third largest maize producer in the hemisphere with about 15 million tons in 2014 is currently doing well, after a rather poor performance in 2015 due to drought; CALF, the CropWatch cropped arable land fraction indicator, which assesses to what extent cropland is actually cultivated, increased by 7 percentage points. Although Australia is a minor producer of maize, CALF rose 40 percentage points over the average of the previous five years, the highest variation among all countries monitored by CropWatch. The maximum Vegetation Condition Index (VCIx), however, one of the crop performance indicators, is low for the country due to drought, which is likely to results in an altogether average output.

Global environmental conditions

Globally, CropWatch analyses identify several large areas of continental scale where conditions varied in a coherent fashion since last October. They are numbered from W01 to W05 (wet) and D01 to D10 (dry), to which the already mentioned Australia belongs. Their location is illustrated in figure 3.1.

Wet areas

The first area, W01 or northwestern America, includes major production zones of Canada and the United States (CALF, +10 percentage points) where temperature exceeded seasonal values and where prospects of winter crops are favorable. Next, in northern and central-south America (W02), some areas recorded excess rainfall, as was already mentioned for parts of Argentina. Contrary to W01, W03 (northern-central Europe) was not only wet but also cold, and crop prospects are about average. The area includes Poland (VCIx=0.88) and Ukraine, two countries where snow was unusually abundant in January. In Ukraine, VCIx was just fair (0.67) and CALF dropped by 12 percentage points compared with the recent seasons. The next area, W04, is very large and extends from the western Caspian and northwest India to eastern Asia (Qinghai province of China). It recorded about double of average precipitation, and the CropWatch biomass production potential (BIOMSS) increased accordingly. The last wet area, W05, encompasses

most of continental and maritime Southeast Asia; it had some very large rainfall increases (Cambodia, RAIN, +120%), some of which were brought about by cyclones (see also section 5.2 on disasters for details). Altogether, CALF in this area was relatively stable (extremes are -4% in Cambodia and 0% in Thailand), but VCIx was high, at least 0.87 (Cambodia, Indonesia), reaching 0.94 in Thailand. Production prospects are generally above average.

Dry areas

In America, the first identified dry area (D01) extends from the northeastern United States to the Caribbean and Honduras. The average rainfall deficit here reached 21%, with temperature (TEMP) above average by 1°C. In Mexico, which is part of the area, CALF is up 8% with VCIx=0.88, and crop prospects are favorable. In the second dry area, D02 or the western Cono Sul, an area that includes some important pastoral areas, the drop in the biomass production potential indicator (BIOMSS) reached 28% due to drought and low temperature.

The next area, D03, coincides approximately with the Western European Major Production Zone (MPZ) for which chapter 2 provides a detailed analysis. Low rainfall (-30% on average) combined with below average temperature (-1.8°C) affected mostly France where VCIx is 0.73. In other areas, considering the still early stage of the season, prospects remain average or just below.

In D04, the Eastern Mediterranean, the average rainfall deficit was 39%. Turkey, the major agricultural country in the area experienced a marked drop in CALF (-20 percentage points) with one of the lowest VCIx values (0.55). In Egypt, the most populated country in the area and a major global food importer, prospects of winter crops are below average.

Next, in Eastern Africa (D05), BIOMSS dropped 39% due to drought; in several countries 2016 was the second consecutive drought year. In Ethiopia, however, in spite of RAIN being down 26%, CALF is up 6 percentage points with a VCIx of 0.90.

D06 to D09 occur in the eastern European continent and Asia. The first covers western Russia, where RAIN was down by 21% and TEMP by -2.0°C. Considering that CALF in this area is up 16 percentage points, crop prospects remain favorable. D07, southern Siberia to Japan, is of minor global wheat production areas, where rainfall deficit in the region average is -28%, with a temperature anomaly of -1.2°C. The D08 area, which includes several Chinese provinces (Yunnan to Jiangxi) and where rainfall was 28% below average, will be mentioned again below. D09 (most of southern and eastern India) is one of the most problematic areas of the current reporting period. The deficit of rainfall reaches 46%, and this occurs after the damage caused by floods in previous months (and reported in previous CropWatch bulletins). At the same time, however, the northwestern and northern-central areas, which are mostly irrigated, benefited from above average rainfall. Altogether, considering that CALF did not change significantly, crop prospects remain fair.

Finally, D10 includes Australia, which was mentioned above, and New Zealand, where rainfall fell 52% nationwide during the reporting period.

China

China enjoyed crop conditions not unlike those of the previous season: TEMP was 0.7°C above average and RAIN was up 12%, combined with a drop in solar radiation (RADPAR, -12%).

Generally, the Northeast and Inner Mongolia regions do not have any crops in the field at this time of reporting because temperature is climatically too low for winter crops. Hibernating winter wheat occurs in all other regions, so that current water supply (as rain or snow) will eventually benefit crops after the winter dormancy phase, especially in the Loess region and Southwest China, two regions where

production prospects are favorable. The regions that will need close monitoring include Huanghuaihai (CALF, down 6 percentage points), Lower Yangtze (CALF dropped 8 percentage points, and indicators undergo a lot of spatial variability), as well as Southwest China where adverse conditions could develop in Chongqing, Guizhou, Hubei, Hunan, and especially Sichuan. In Southern China, crop condition in central Guangdong deserves close monitoring as well, due to its below average condition during the whole period, with VCIx below 0.5.

At the national level, CALF was generally stable with a bit of decreasing in comparison with the previous five years' average, and the overall expectations for the forthcoming winter wheat remain fair.

The bulletin also includes a section on domestic prices; they include a likely increase for rice and a projected decrease for maize and wheat. For soybeans, wide fluctuations are conjectured.

Chapter 1. Global agroclimatic patterns

Chapter 1 describes the CropWatch agroclimatic indicators (CWAIs) for rainfall (RAIN), temperature (TEMP), and radiation (RADPAR), along with the agronomic indicator for potential biomass (BIOMSS) for sixty-five global Monitoring and Reporting Units (MRU). Rainfall, temperature, and radiation indicators are compared to their average value for the same period over the last fifteen years (called the "average"), while BIOMSS is compared to the indicator's average of the recent five years. Indicator values for all MRUs are included in Annex A table A.1. For more information about the MRUs and indicators, please see Annex C and online CropWatch resources at www.cropwatch.com.cn.

1.1 Overview

Over the current reporting period and based on findings from all 65 MRUs, the CropWatch indicator with the largest variability in departure from average conditions is temperature (as measured by the coefficient of variation of TEMP departures from average for all 65 units), followed by rainfall (RAIN) and radiation (RADPAR). Nevertheless, global temperature was about average (-0.1°C), while rainfall was 18% above average and radiation 2% below.[1] In general, for the reporting period, no significant correlation exists between the intensity of the agroclimatic variables and their departures from average, although RAIN and TEMP, and TEMP and RADPAR, are positively correlated (R=0.41 and R=0.82, respectively), which results from well-known behavior of climate variables.

Starting with rainfall, the sections below will focus on the description of anomaly patterns (see also figures 1.1 through 1.4).

Rainfall

From October 2016 to January 2017, the global spatial variability of RAIN (figure 1.1) was far less coherent than for TEMP and RADPAR. Dry conditions prevailed mostly in the East African highlands, the Horn of Africa and Madagascar, the Nordeste, and southern Asia. Several of these areas are not in their rainfed growing seasons and normally expect limited rain during the reporting period. Marked deficits, however, should be mentioned in Asia for MRU-45 (Southern Asia, RAIN, -48%) and MRU-46 (Southern Japan and Korea, -25%), in Africa for MRU-2 (East African highlands, -40%), MRU-4 (the Horn of Africa, -44%), and MRU-5 (the main agricultural areas of Madagascar, -41%), as well as for Oceania (MRU-56, New Zealand, -52% and MRU-55, Nullarbor to Darling, -40%). The two areas that deserve mentioning in South America include MRU-27 (Western Patagonia, -44%) and again MRU-22, the Brazilian Nordeste with -30% rainfall.

The largest positive departures, some of which are also mentioned in section 5.2 on disasters affected MRU-47 (Southern Mongolia, +366%), distant MRU-48 (Punjab to Gujarat, +201%, where rainfall has benefited winter crops), as well as several areas in China from west to east (MRU-32, Gansu-Xinjiang, +156%; MRU-35, Inner Mongolia, +151%; MRU-36, the Loess region, +121%; MRU-34, Huanghuaihai, +107%; and MRU-38, Northeast China with +90%). Finally, in MRU-50 (Southeast Asia), 631 mm were recorded, an excess of 79% over average.

[1] Averages are not weighted by the areas of the MRUs.

Abnormal temperature patterns

For temperature (figure 1.2), the most striking features are below average temperature over most of Eurasia, as well as above average temperatures in northern America, eastern Asia, and in the Brazilian Nordeste. In the remaining, mostly tropical areas, close to average (Africa) and slightly below average conditions (everywhere else) are displayed.

In Eurasia, the area with below average temperatures runs from Spain and the western Mediterranean to eastern Siberia (MRU-51), encompassing 11 MRUs. The largest departures in this area are those of Eastern Siberia (MRU-51 with TEMP, -2.3°C), non-Mediterranean western Europe (MRU-60, -2.1°C), the Ural to Altai mountains (MRU-62, -1.9°C), and both the Caucasus (MRU-29) and the Ukraine to the Ural mountains (MRU-58) with -1.6°C below average.

In North America, most of the continent (except along the western coast) experienced above average temperature, most notably in the Corn Belt (MRU-13, +1.5°C) and, to a lesser extent, the Cotton Belt (MRU-14, +1.4°C), the northern Great Plains (MRU-12, +1.0°C), and, in Mexico, the Southwest and northern Highlands (MRU-18, +0.8°C). Next, in Asia, temperature departures in the area from the southern Himalayas (MRU-44) to Inner Mongolia (MRU-35) and southern China (MRU-40) were most noticeable in Southwest China (MRU-41, +0.9°C), South China (MRU-40, +1.0°C), the Lower Yangtze (MRU-37, +1.0°C), and the Loess region of China (MRU-36, +1.3°C).

In South America and the Caribbean, the only area that needs mentioning is MRU-25 (central-north Argentina) with temperatures of 1.3°C below average. MRU-22, the semi-arid north-eastern area of Brazil recorded 0.8°C above average. In the remaining areas of tropical Africa, Southeast Asia and Oceania, temperature was between 0.5°C and 1.0°C below average.

Radiation

To some extent, RADPAR patterns (figure 1.3) followed those of TEMP, with abnormally low values over most of Eurasia and the southern Mediterranean, East and Southeast Asia and Oceania, as well as North America (about -5%). Southern Asia (MRU-45), Central and South America, as well as Africa recorded mostly positive departures. Noticeable differences, however, existed especially in eastern and Southeast Asia where positive temperature departures are associated with poor radiation. The largest recorded negative departures of RADPAR occurred in China—from -21% in the Lower Yangtze area (MRU-37), to Hainan, Huanghuaihai, and Southwest China (MRUs-33, 34, and 41) with about -13% RADPAR, and the Loess region (MRU-36) and Southern China (MRU-40) with about -9%. In MRU-62 (Ural to Altai mountains) as well as mainland (MRU-50) and maritime Southeast Asia (MRU-49), radiation was about 7% lower than average; other, still significant, radiation deficits were recorded in MRU-58 (Ukraine to Ural mountains) with -5%.

Combination of factors and biomass

Using RAIN and TEMP as the main variables, this section attempts to identify areas that are characterized by more than one large departure from the reference value. RAIN and TEMP may vary in the same or opposite directions, so that the first category includes areas where both rainfall and temperature departures are high, which is to say “warmer and wetter than average.” (Both “warmer” and “wetter” are relative terms, which means that -5°C is considered warmer than -10°C, even if it is still freezing. The same applies for wetter and drier.)

"Wet and warm"

Among the significant agricultural areas, warm and wet conditions happened essentially in Asia and North America, including in particular several regions of China, such as MRU-36 (the Loess region, where rainfall exceeds average by 120% and temperature by 1.3°C, while RADPAR was 9% below average). Next is MRU-35 (Inner Mongolia) with RAIN, TEMP, and RADPAR departures reaching respectively 151%, +0.7°C, and −4%, resulting in a BIOMSS increase estimated at 91%. In Huanghuaihai (MRU-12), the indicators take the following values: RAIN, +107%; TEMP, +0.6°C; RADPAR, -13%; and +99% for BIOMSS. Similar observations can be listed for MRU-47 (Southern Mongolia, BIOMSS 168% up), MRU-32 (Gansu-Xinjiang, BIOMSS up 127%), MRU-42 (Taiwan, +16% BIOMSS) and MRU-39, Qinghai-Tibet, where the BIOMSS increase is estimated to reach 15%. In Hainan (MRU-33), BIOMSS is conjectured to rise 41% due to, mostly, precipitation that is 46% above average. In all those areas, the combined increase of RAIN and TEMP has created unusual winter conditions with a likely biomass production increase that may be realized later in the season.

Other "warm and wet" areas include MRU-30 (Pamir area, +23% in BIOMSS) in Asia and MRU-12 and MRU-18 in northern America. MRU-12 covers the northern Great Plains (RAIN, +35%; TEMP +1.0°C; RADPAR, −5%; and BIOMSS, +28%). In MRU-18, the Southwestern United States and northern Mexican highlands, BIOMSS is estimated to increase 34%.

"Dry and warm"

After "wet and warm," it is possible to identify areas "dry and warm," several of which occur in Asia, starting with MRU-37 (the Lower Yangtze), with RAIN down 12% and TEMP up 1°C. RADPAR underwent a severe drop of 21%, while BIOMSS could nevertheless increase 6%. In MRU-46 (Southern Japan and Korea), a precipitation drop of 25% was accompanied by an increase in TEMP (+0.5°C), a small loss of sunshine (RADPAR, -5%) and BIOMSS down 6%. A comparable drop in BIOMSS could occur in MRU-40 (Southern China) due to similar conditions.

On the American continent, MRU-14 (U.S. Cotton Belt to Mexican Nordeste) showed a modest drop in RAIN (-8%) but a more significant temperature increase (1.4°C), with nevertheless about average BIOMSS (-1%). The situation is not so favorable in MRU-22, the Brazilian Nordeste (mentioned several times in this bulletin), where BIOMSS is expected to drop 28%.

"Dry and cold"

The "dry and cold" category includes a long list of more than ten MRUs in different continents, starting with Eurasia (MRU-29, the Caucasus; MRU-59, Mediterranean Europe and Turkey, where RAIN dropped 23% and TEMP by 1.4°C; and MRU-60, non-Mediterranean western Europe where the indicators are -20% and -2.1°C, respectively). Low rainfall but only slight drops in TEMP are reported from MRU-28, the semi-arid Southern Cone, MRU-54 (Queensland to Victoria), MRU-55 (Nullarbor to Darling), as well as MRU-56, New Zealand, where shortage of precipitation (-51%) could entail a BIOMSS drop of 35%. In Africa, in MRU-6 (Southwest Madagascar) and MRU-5 (which includes most of the Malagasy island), drought could result in a BIOMSS drop of 10 to 20%. Finally, in MRU-4, the Horn of Africa, the BIOMSS potential is down 37%.

"Wet and cold"

In this last category of "wet and cold," MRU-38 (Northeast China), MRU-58 (Ukraine to Ural mountains), and MRU-62 (Ural to Altai mountains) are included, with indicators for the Ural to Altai mountains (at +31% for RAIN, -1.9°C for TEMP, and -7% for RADPAR) concurring to reduce the BIOMASS production potential by 20%.

Figure 1.1. Global map of October 2016-January 2017 rainfall anomaly (as indicated by the RAIN indicator) by MRU, departure from 15YA (percentage)

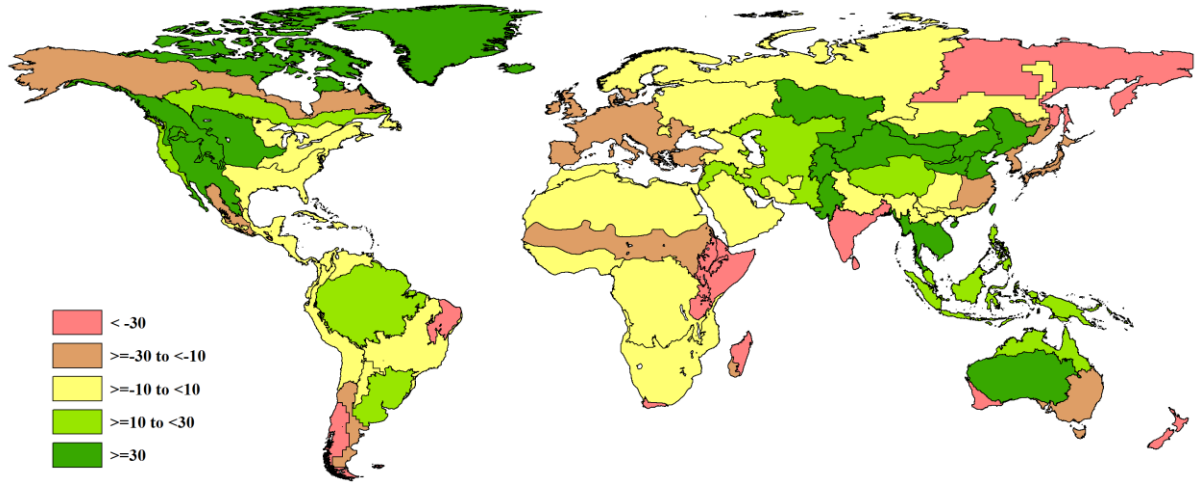

Figure 1.2. Global map of October 2016-January 2017 temperature anomaly (as indicated by the TEMP indicator) by MRU, departure from 15YA (degrees Celsius)

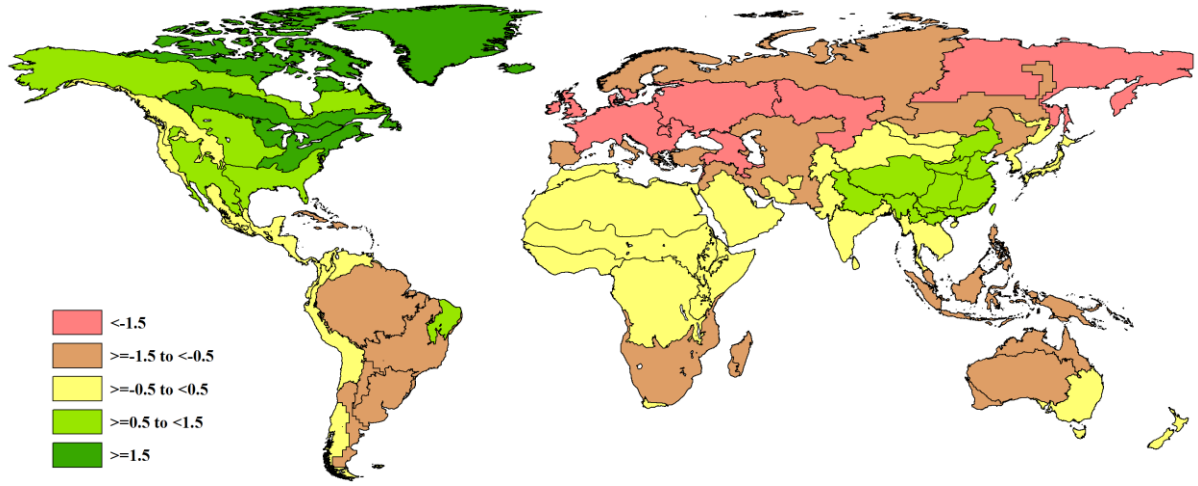

Figure 1.3. Global map of October 2016-January 2017 PAR anomaly (as indicated by the RADPAR indicator) by MRU, departure from 15YA (percentage)

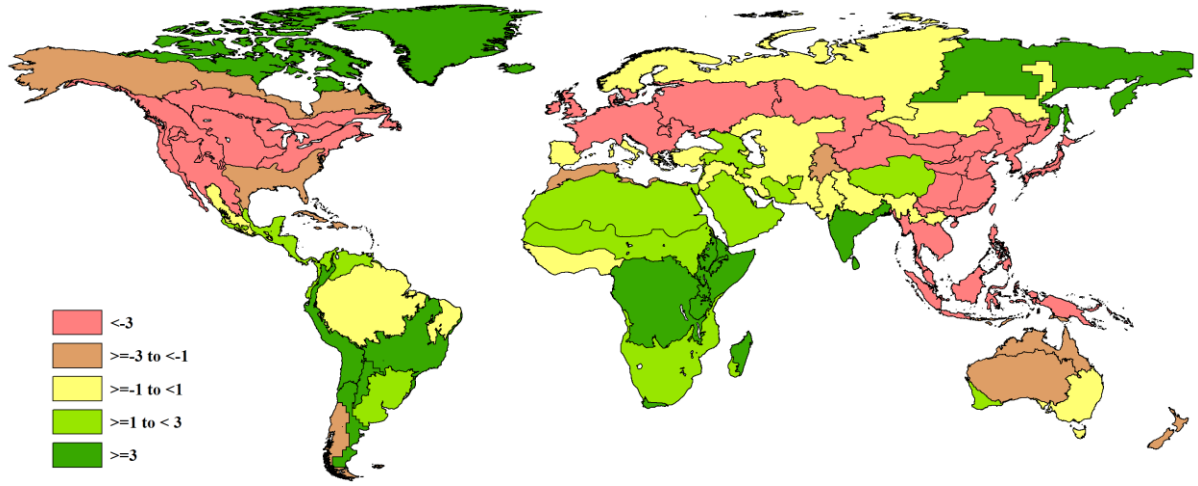

Figure 1.4. Global map of October 2016-January 2017 biomass accumulation (BIOMSS) by MRU, departure from 5YA (percentage)

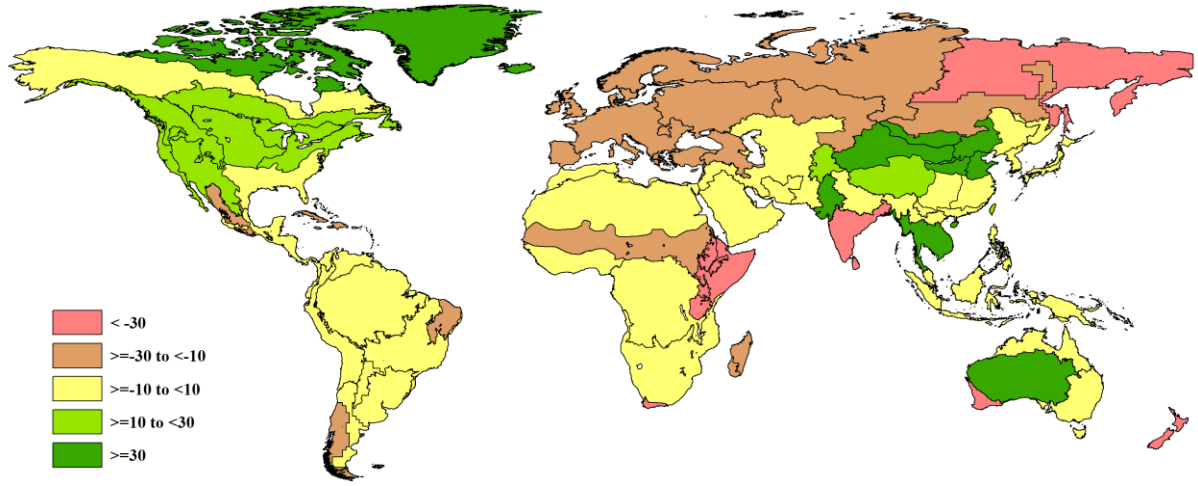

Chapter 2. Crop and environmental conditions in major production zones

Chapter 2 presents the same indicators—RAIN, TEMP, RADPAR, and BIOMSS—used in Chapter 1, and combines them with the agronomic indicators—cropped arable land fraction (CALF), maximum vegetation condition index (VCIx), and minimum vegetation health index (VHIn)—to describe crop condition in six Major Production Zones (MPZ) across all continents. For more information about these zones and methodologies used, see the quick reference guide in Annex C as well as the CropWatch bulletin online resources at www.cropwatch.com.cn.

2.1 Overview

Tables 2.1 and 2.2 present an overview of the agroclimatic (table 2.1) and agronomic (table 2.2) indicators for each of the six MPZs, comparing the indicators to their fifteen and five-year averages.

Table 2.1. October 2016-January 2017 agroclimatic indicators by Major Production Zone, current value and departure from 15YA

	RAIN		TEMP		RADPAR	
	Current (mm)	Departure from 15YA (%)	Current (°C)	Departure from 15YA (°C)	Current (MJ/m^2)	Departure from 15YA (%)
West Africa	230	6	27.1	-0.1	1167	0
South America	775	8	23.6	-0.7	1329	2
North America	310	4	6.5	1.4	538	-3
South and SE Asia	234	12	22.8	0.1	969	0
Western Europe	193	-29	4.8	-2.3	315	-2
C. Europe and W. Russia	220	9	-2.0	-1.7	225	-6

Note: Departures are expressed in relative terms (percentage) for all variables, except for temperature, for which absolute departure in degrees Celsius is given. Zero means no change from the average value; relative departures are calculated as (C-R)/R*100, with C=current value and R=reference value, which is the fifteen-year average (15YA) for the same period (October-January) for 2002-2016.

Table 2.2. October 2016-January 2017 agronomic indicators by Major Production Zone, current season values and departure from 5YA

	BIOMSS (gDM/m^2)		CALF (Cropped arable land fraction)		Maximum VCI Intensity
	Current	Departure from 5YA (%)	Current	Departure from 5YA (% points)	Current
West Africa	598	1	99	5	0.90
South America	1835	4	96	0	0.66
North America	813	12	70	11	0.92
S. and SE Asia	495	2	93	-1	0.91
Western Europe	752	-20	88	-2	0.81
Central Europe and W Russia	591	-10	74	2	0.79

Note: See note for table 2.1, with reference value R defined as the five-year average (5YA) for October-January 2012-2016.

2.2 West Africa

The seasonal variations of the water are the major climatic variable affecting crop distribution and phenology in West Africa. However, historical and economic factors have also helped create the present

distribution, especially for cash crops. The reporting period marks the end of the main harvesting season throughout the region for maize, sorghum, millet, and yams, with cereal production expected to be above average (>5%). In the north of the MPZ, which only has one rainy season, the harvesting of cereals is underway. In the west (Guinea to Liberia), an important part is played by rice, of which the harvest extends into December and sometimes even January. In the areas that tend to record bimodal rainfall (southern Côte d'Ivoire to Nigeria), the first maize crop was harvested in October, while the short season maize was harvested in early 2017. In contrast, cassava (the main staple in the region) is still growing, as reflected by the area of cropped arable land.

Based on CropWatch observations, average rainfall was recorded in 77.4% of croplands in the MPZ, with close to average temperature of 27.1°C (-0.1% compared to the five-year average) and sunshine (RADPAR, 0% deviation), which gave a slight increase of the biomass production potential (BIOMSS, +1%). The west of the region enjoyed a significant increase of precipitation over average, contributing to the overall increase of +6% for RAIN for the MPZ, which also translated into increased Niger discharge for the benefit of the Sahel, especially irrigated rice in the inner Delta and flood recession crops along the river.For the MPZ as a whole, the cropped arable land fraction (CALF) reached 99%. Precipitation is currently slowing down, marking the end of the rainy season. According to the VCIx map in relation to crop condition, average VCIx was 0.9. Climatic conditions were generally favorable across the Nigerian northern savannah agro-ecological zone. During this period, Nigeria has a good share of cropped arable land reflecting the extent of agricultural production in the region.

Generally, as the growing season was coming to a close during this reporting period, the climatic conditions were close to average, with precipitation well distributed in time. The temperature fluctuated from normal average within a +/-2°C margin after cessation of the rainy season. CropWatch indicators depict a stable and coherent climatic condition conducive for late crop harvest in early 2017 (second maize crop and cassava).

Figure 2.1. West Africa MPZ: Agroclimatic and agronomic indicators, October 2016-January 2017

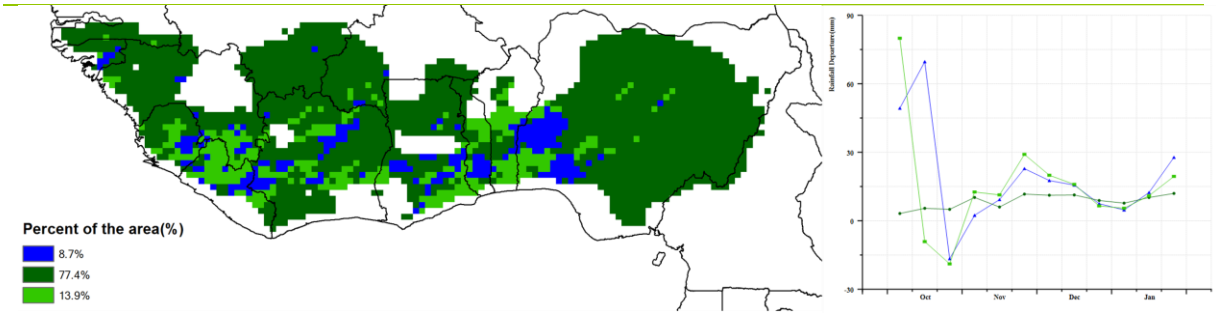

a. Spatial distribution of rainfall profiles

b. Profiles of rainfall departure from average (mm)

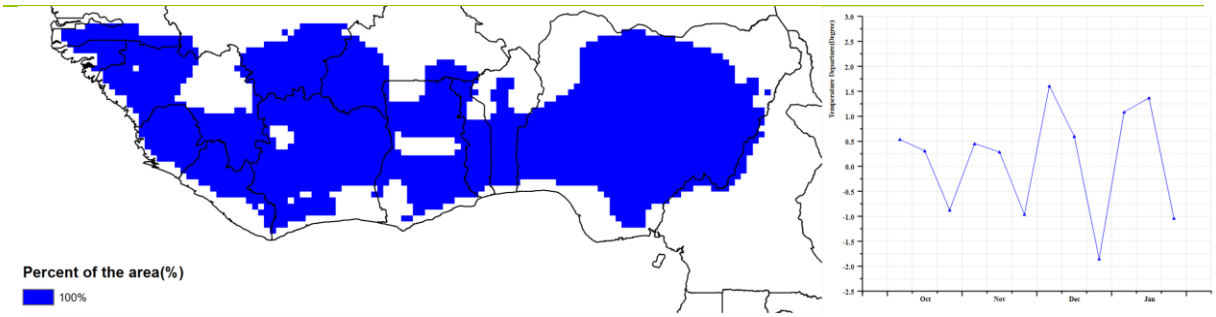

c. Spatial distribution of temperature profiles

d. Profiles of temperature departure from average (mm)

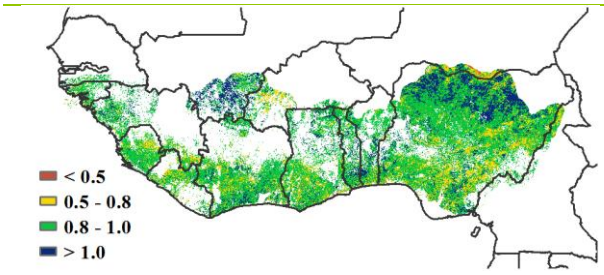

e. Maximum VCI

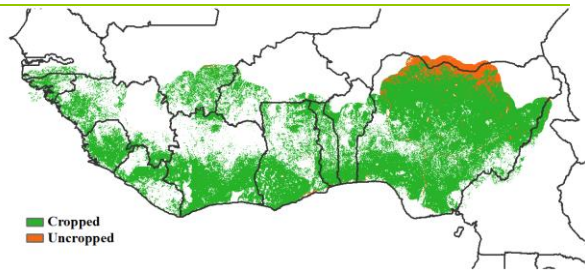

f. Cropped arable land

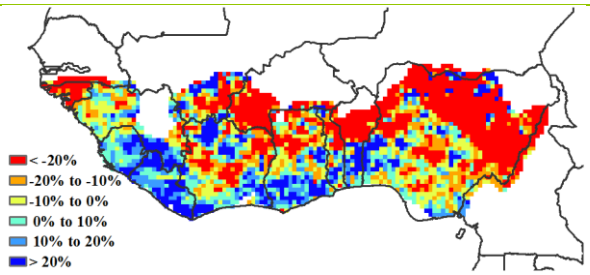

g. Biomass accumulation potential departure

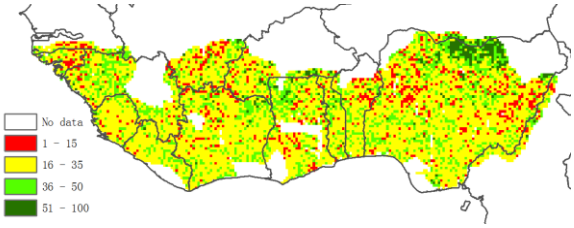

h. VHI minimum

Note: For more information about the indicators, see Annex C.

2.3 North America

In general, crop condition was average in the North American MPZ. This monitoring period covers November 2016 to January 2017, and winter crops of 2017 have been planted and reached over-wintering stages. Overall, CropWatch agroclimatic indicators show warmer than average conditions: rainfall was 4% above average and the temperature departure was +1.4°C.

The North American MPZ covers essentially the Northern Great Plains (MRU-12), Corn Belt (MRU-13), and an area from the Cotton Belt to the Mexican Noreste (MRU-13). The first MRU received abundant rainfall (35% above average), while the second and third recorded amounts that were respectively just 1% above average or a deficit (-8%). The Northern Great Plains are a main production zone of winter crops, and abundant rainfall during the current reporting period will benefit the growth of winter crops after over-wintering stages.

Temperature in the MPZ fluctuated greatly: the MPZ was dominated by warm temperature before November 2016, after which it suffered ice-storms in December and January with a temperature departure reaching -9°C. After a spell with close to average temperature, some areas, especially in the northeast recorded TEMP values 9°C above average. The warm temperature benefited the sowing of winter crops, while extreme low temperature during over-wintering was good for killing pests. The spatial variation of rainfall and temperature also resulted in differences in the biomass accumulation potentials, with negative departures recorded in the Cotton Belt to Mexican Noreste area (such as in Alabama with -9%) and positive values elsewhere.

According to the maximum vegetation condition index (VCIx) map, crop condition was below average in the lower Mississippi. Especially for Arkansas, the minimum VHI map indicates drought due to rainfall deficit (-20%). Crops are above average in the winter crop zones, including Texas, Oklahoma, Kansas and South Dakota. The fraction of cropped arable land (CALF) was significantly above average (+11.32 percentage points), while uncropped land was distributed in the Canadian Prairies and the western Great Plains.

Overall, above average conditions prevail in the North American MPZ.

Figure 2.2. North America MPZ: Agroclimatic and agronomic indicators, October 2016 – January 2017

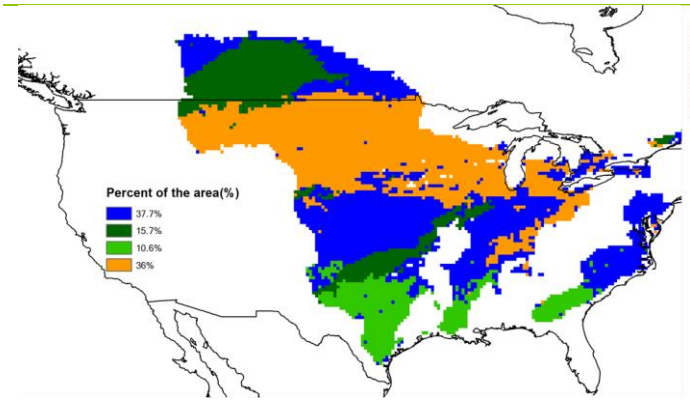

a. Spatial distribution of rainfall profiles

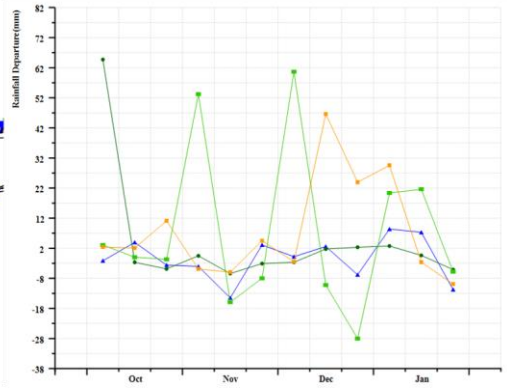

b. Profiles of rainfall departure from average (mm)

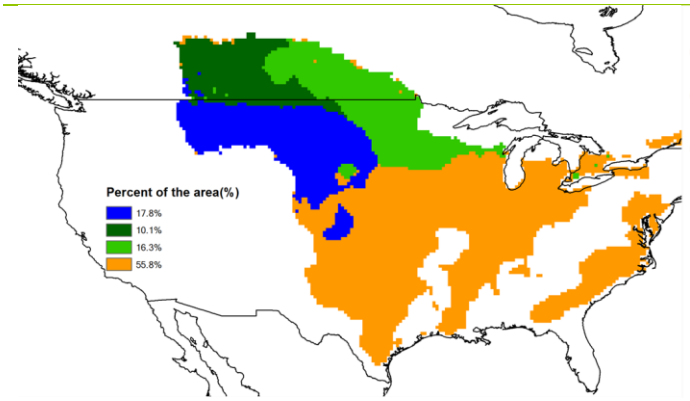

c. Spatial distribution of temperature profiles

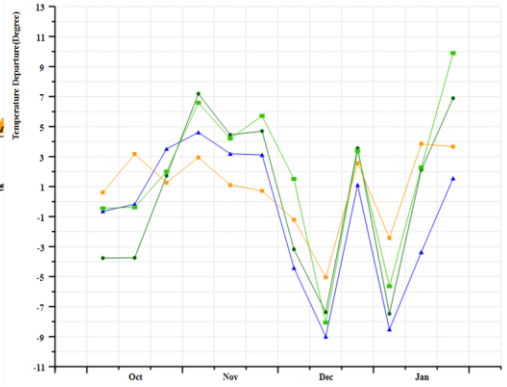

d. Profiles of temperature departure from average (mm)

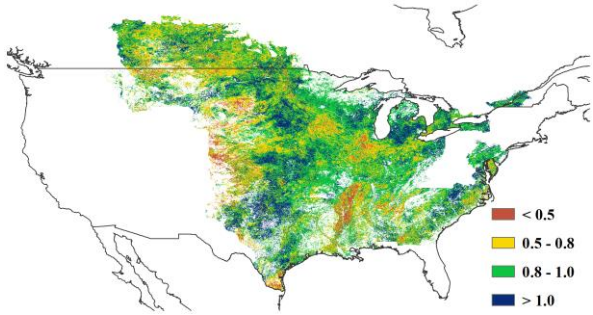

e. Maximum VCI

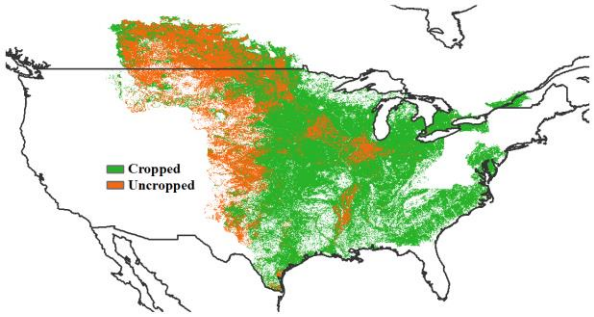

f. Cropped arable land

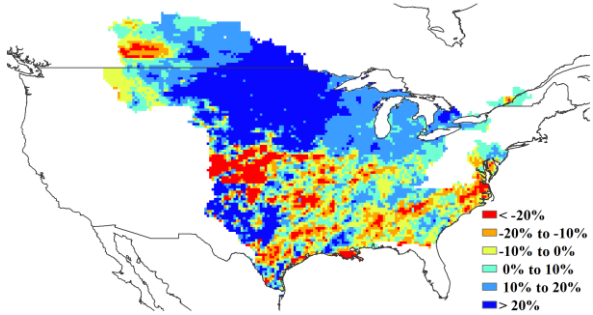

g. Biomass accumulation potential departure

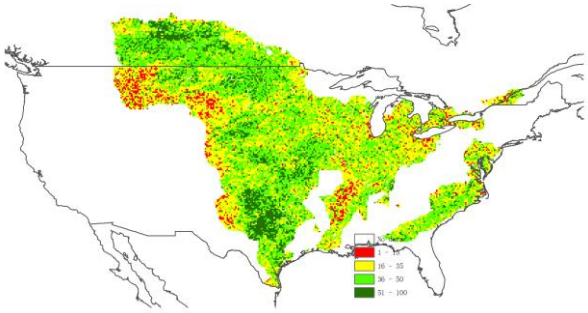

h. VHI minimum

Note: For more information about the indicators, see Annex C.

2.4 South America

The current monitoring period covers the main harvesting time of winter crops in the Pampas, as well as soybean planting, early growing stages of maize, and the planting of late maize all over the MPZ.

Rainfall (RAIN) was 8% above average, while temperature was slightly below (TEMP, -0.7°C) and radiation (RADPAR) 2% above average as well, resulting in a projected BIOMSS of about 4% above the five-year average. Maximum VCI values, however, show that expected potential production is far from the high values observed during previous seasons. When considering spatial detail, precipitation was higher than average during December and January in central and northern Argentina and in the state of Rio Grande do Sul in Brazil. The same period experienced higher than average temperatures in the Pampas and near the coast in Brazil. Maximum VCI showed higher values for Brazil than for Argentina, reflecting areas with problems in the latter (such as flooding in northeast Buenos Aires and Cordoba provinces and drought in southern Buenos Aires), with poor conditions confirmed by the BIOMSS map. In general, VHI showed similar values across the MPZ, without any relevant differences between Argentina and Brazil.

Altogether the prospects for summer crops remain favorable in Brazil, while some regions of Argentina suffered from poor conditions that may reduce their output.

Figure 2.3. South America MPZ: Agroclimatic and agronomic indicators, October 2016-January 2017

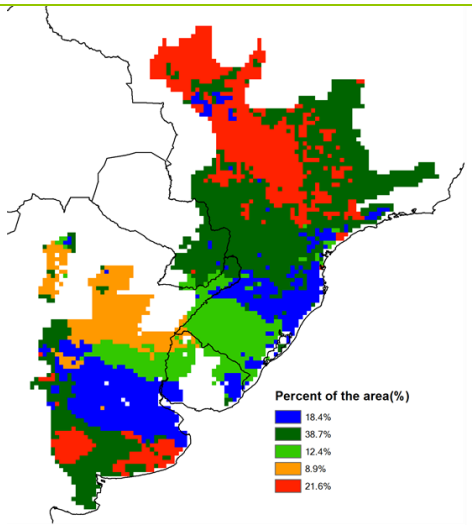

a. Spatial distribution of rainfall profiles

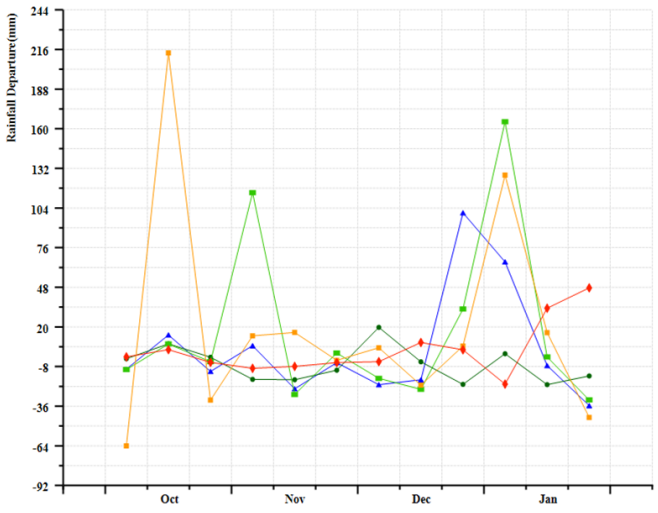

b. Profiles of rainfall departure from average (mm)

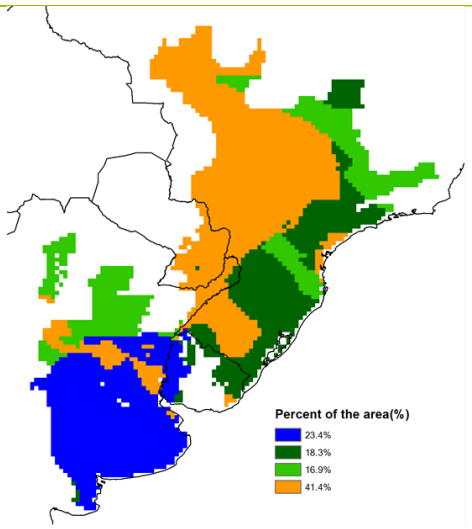

c. Spatial distribution of temperature profiles

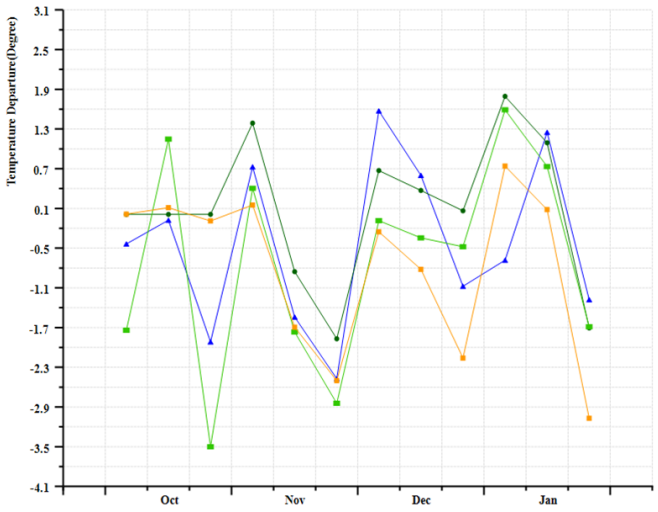

d. Profiles of temperature departure from average (mm)

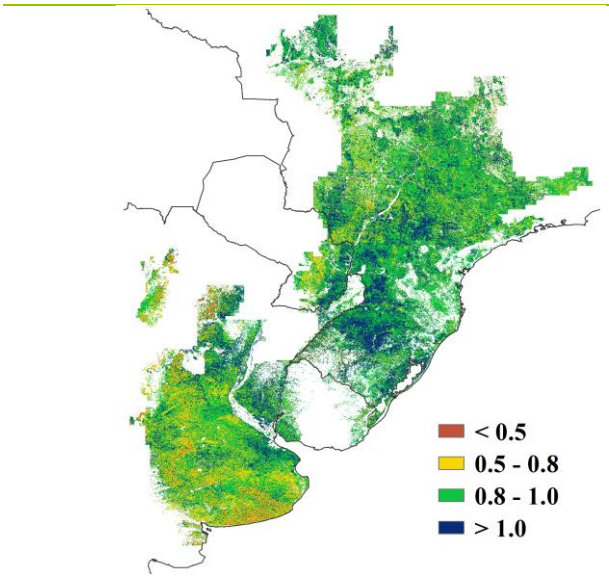

e. Maximum VCI

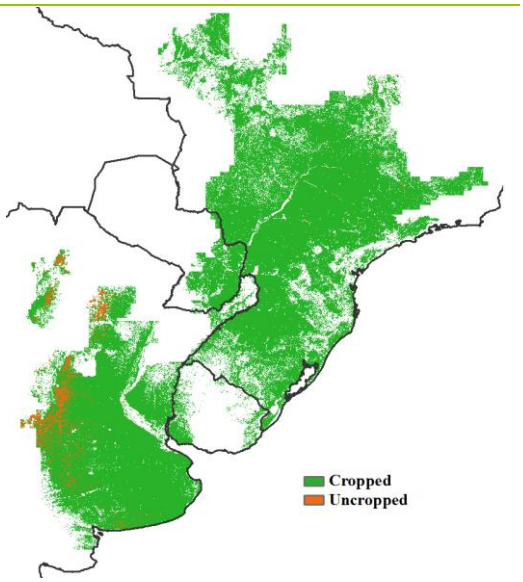

f. Cropped arable land

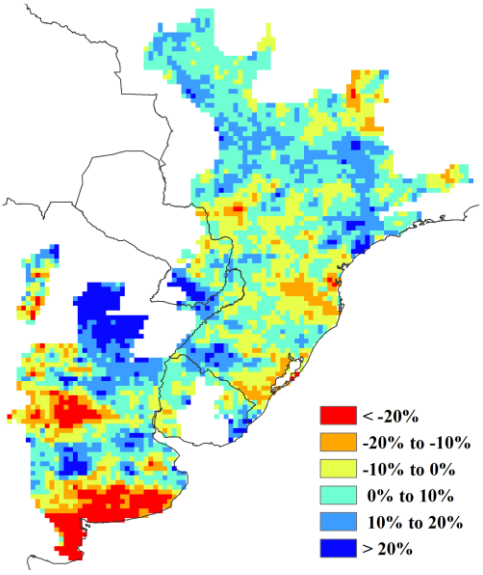

g. Biomass accumulation potential departure

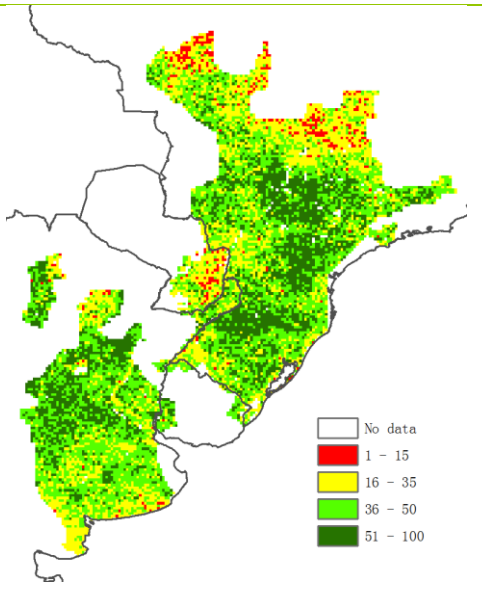

h. VHI minimum

Note: For more information about the indicators, see Annex C.

2.5 South and Southeast Asia

The reporting period covers mainly the growth and harvest of wet season crops in this MPZ. According to CropWatch indicators, the overall crop condition is average for the region, with marked differences between the dry west and the east. For the whole MPZ, rainfall was 12% above average, resulting from excess rainfall in Bangladesh (RAIN, +5%), Cambodia (+120%), Myanmar (+6%), Thailand (+82%), and Vietnam (+74%). However, in India rainfall was below average (-30%) as a whole, resulting from poor rainfall in Andhra Pradesh (-71%), Assam (-7%), Bihar (-23%), Chhattisgarh (-25%), Goa (-69%), Jharkhand (-58%), Kerala (-62%), Karnataka (-74%), Maharashtra (-42%), Madhya Pradesh (-34%), Nagaland (-15%), Odisha (-28%), Tamil Nadu (-60%), and West Bengal (-18%). A significant rainfall peak (+612 mm) occurred in the central regions of Vietnam in December, in relation with several cyclones that are described in the section on disasters (section 5.2).

The MPZ experienced average temperature and radiation. Temperature peaks were noticed only in limited areas such as northern India (+3.0°C) in December. Cold spells occurred over the MPZ in November (-1.5°C) and in late January (-0.8°C). In the north, temperature was consistently above average.

The biomass accumulation (BIOMSS) increased in the region by 2% as compared to the five-year average for the region in this same period. It was, however, down 20% in central to southern India, whereas the rest of the countries in the MPZ and western India experienced positive BIOMSS departures close to or above +20%. The largest biomass accumulation potential increases were recorded in Thailand (+38%), Vietnam (+37%), Myanmar (+10%), Cambodia (+62%), and Bangladesh (+16%). For India as a whole, BIOMSS dropped 20% below the average of the previous five years.

Maximum VCI values were high, except in parts of southern and northern India and in some parts of Vietnam, indicating poor crop condition in those areas. The minimum VHI values were distributed in a scattered manner, with lowest values in India, confirming the water stress in those areas.

Overall, agroclimatic indicators and vegetation indices show favorable crop condition throughout the region, with the exception of a large area in India and possibly parts of northern Vietnam.

Figure 2.4. South and Southeast Asia MPZ: Agroclimatic and agronomic indicators, October 2016-January 2017

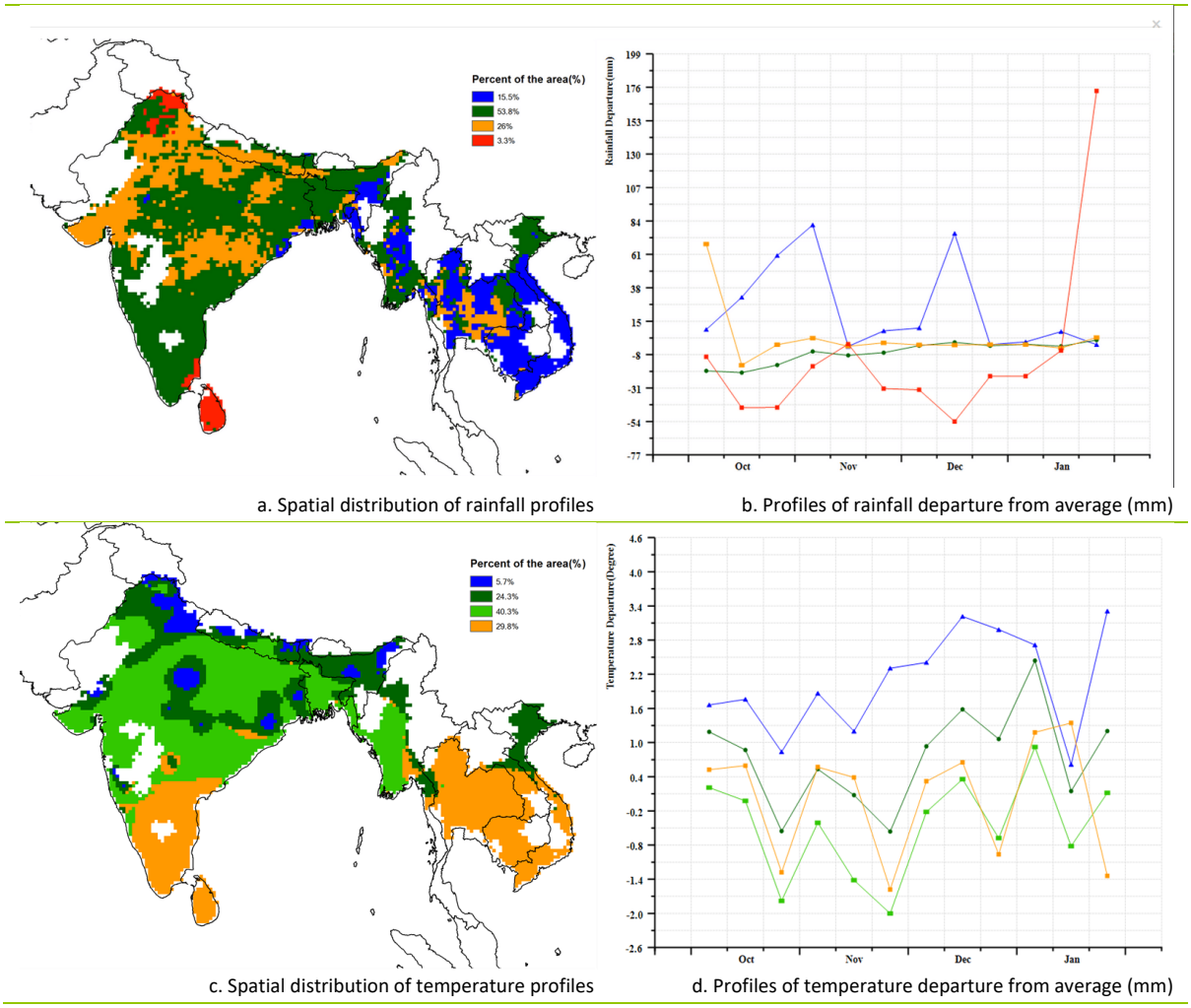

a. Spatial distribution of rainfall profiles

b. Profiles of rainfall departure from average (mm)

c. Spatial distribution of temperature profiles

d. Profiles of temperature departure from average (mm)

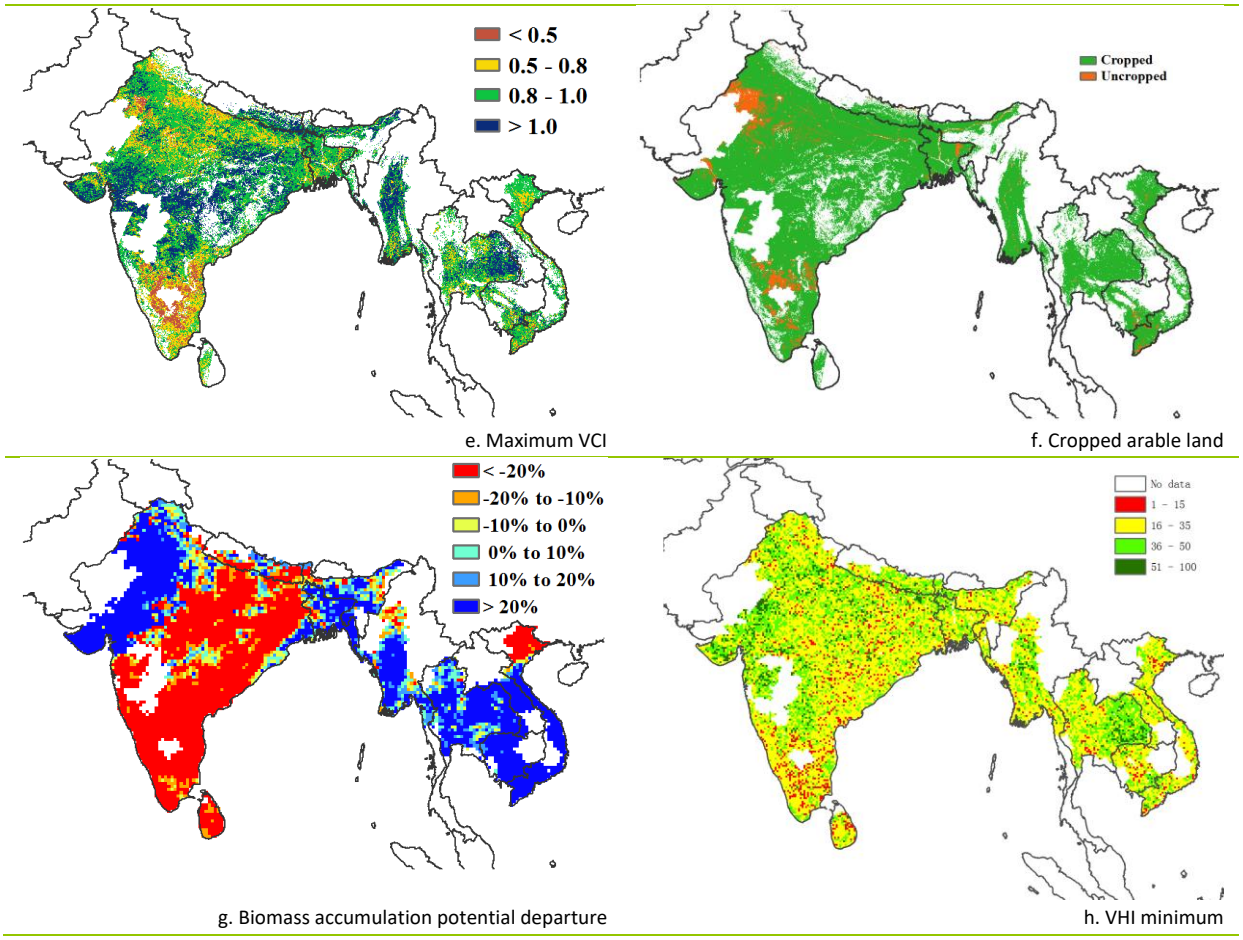

e. Maximum VCI

f. Cropped arable land

g. Biomass accumulation potential departure

h. VHI minimum

Note: For more information about the indicators, see Annex C.

2.6 Western Europe

During the current monitoring period, crop condition was below average in most parts of the continental Western European MPZ based on the integration of agroclimatic and agronomic indicators. Summer crops were completely harvested, and winter crops were planted and reached over-wintering stages. Figure 2.5 represents an overview of CropWatch agroclimatic and agronomic indicators for this MPZ.

The agroclimatic indicators show that total rainfall was 29% below average, with exceptional positive departures over most of the Czech Republic, Austria, Slovakia, Hungary, middle-northern Germany, and eastern Denmark from October to early November, in northern Italy in mid-October, and in south and southeast France and northern Spain in late November. Occasional and scattered snowfall started early (November) and was more abundant in 2016-17 than in previous years; it also persisted longer than usual due to cold weather. Starting from the first week of January to the end of the month, the snow covered almost the whole MPZ from the east to the eastern fringe of France (Alsace), the country that experienced the largest negative temperature anomaly of the MPZ.

Substantially drier-than-usual conditions in early October in France and western Germany hampered the sowing of winter cereals. In northeastern Austria and northern Italy, heavy rains in the first half of October somewhat delayed part of the harvest of grain and maize and the sowing of winter crops, but benefited the emergence of winter crops that had been sown earlier. Temperatures over the whole MPZ were below average (-2.3°C), and temperature profiles indicate that above average temperatures were observed in northern Germany and Denmark from mid-November to early January. Radiation was 2% below average.

Due to the continuous rainfall deficit, especially after November, and coupled with the impact of low temperature (in particular in France, the United Kingdom, and Spain), the biomass accumulation potential BIOMSS was 20% below the recent five-year average. The lowest values (-20% and below) occur over most parts of the continental Western European MPZ (mainly concentrated in France, the United Kingdom, the south and east of Spain, and the south and northwest of Germany). In those regions, values for minimum VHI also confirm the water deficit to a certain extent. In contrast, BIOMSS was above average (sometimes exceeding a 10% departure) in parts of Austria, Slovakia, Hungary, central Spain, northern Italy, and northeast Germany.

Maximum VCI was relatively low in most of Spain, France, the United Kingdom, Germany, Czech Republic, northern Italy, southeast Hungary, southwest Slovakia, and northern Austria. Average VCIx for the MPZ was 0.81. Overall, 88% of arable land in the MPZ was cropped during this reporting period, 2 percentage points below average. Most uncropped arable land was concentrated in Spain and scattered in northern and southern Italy, central and southern France, southeast Hungary, and southwest Slovakia.

Overall, crop condition is currently average or below average along an east-west gradient.

Figure 2.5. Western Europe MPZ: Agroclimatic and agronomic indicators, October 2016-January 2017

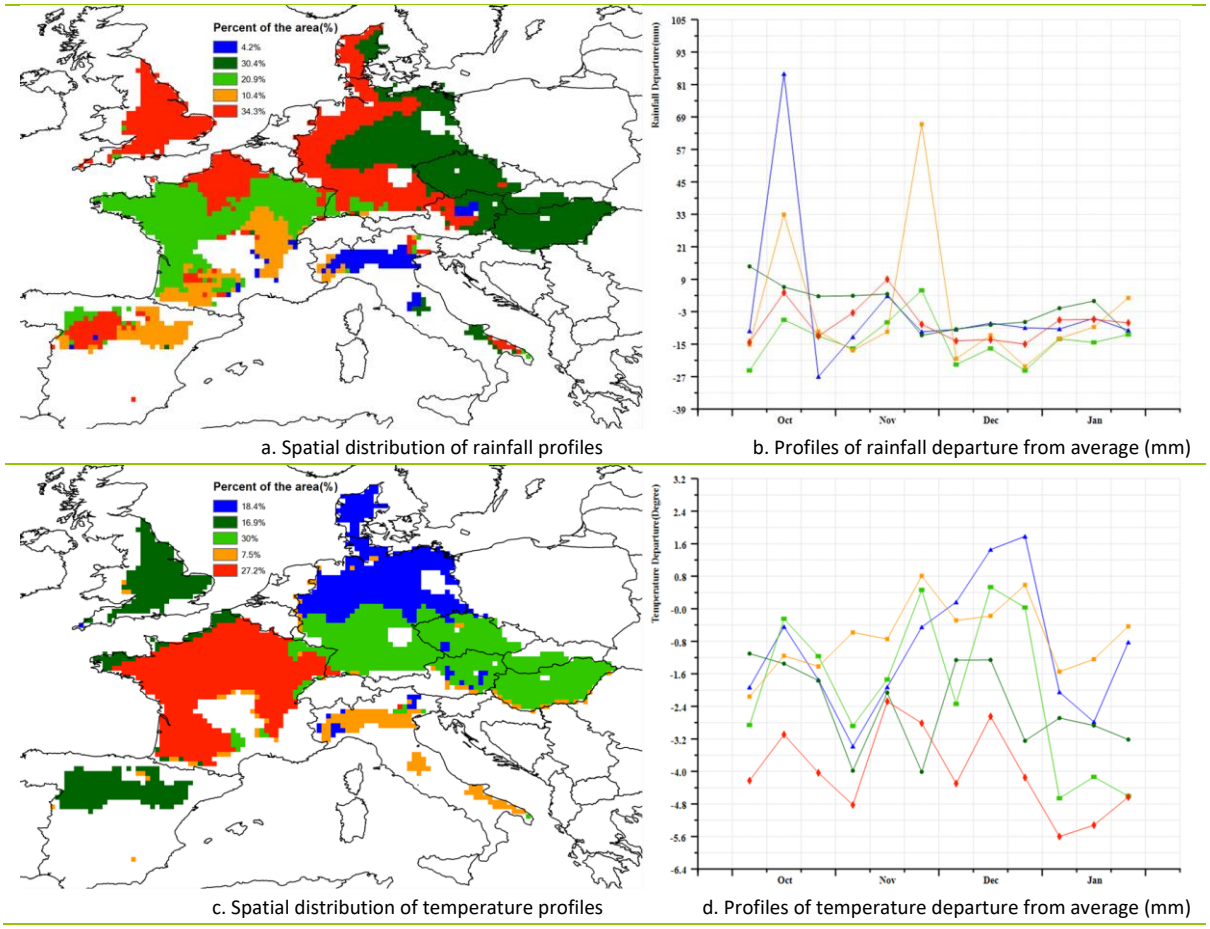

a. Spatial distribution of rainfall profiles

b. Profiles of rainfall departure from average (mm)

c. Spatial distribution of temperature profiles

d. Profiles of temperature departure from average (mm)

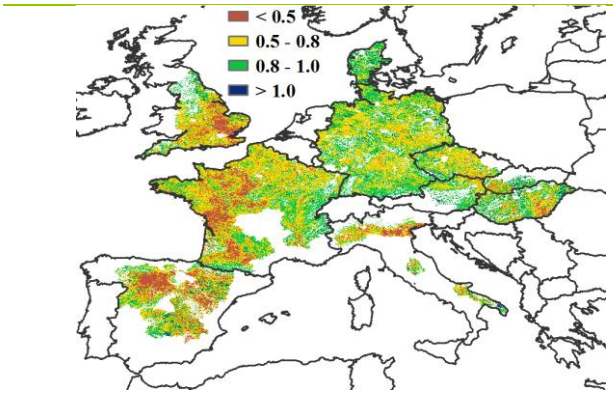

e. Maximum VCI

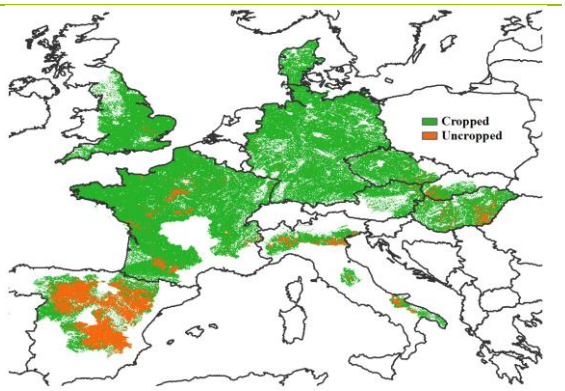

f. Cropped arable land

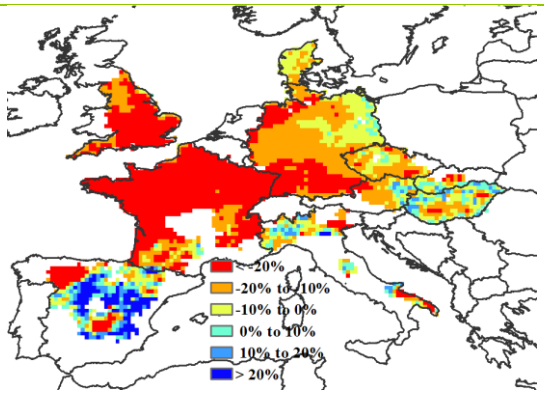

g. Biomass accumulation potential departure

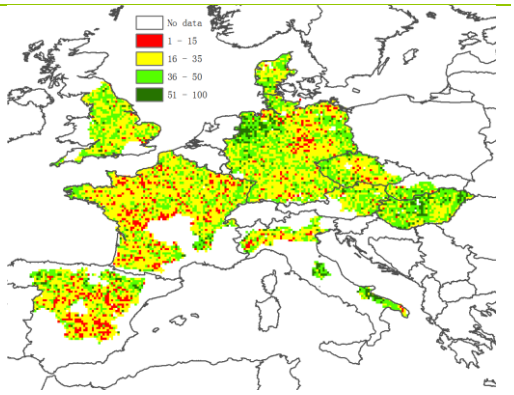

h. VHI minimum

Note: For more information about the indicators, see Annex C.

2.7 Central Europe to Western Russia

Over the monitoring period, the harvest of summer crops was completed, and winter crops were in their early vegetative stages under generally favorable weather conditions in most parts of the MPZ. The region experienced below normal thermal conditions, with a 1.7°C drop in temperature compared to average, while rainfall increased 9% and radiation dropped 6%.

According to the rainfall profiles, favorable rainfall affected the MPZ's western part (almost 39.2% of the MPZ) during October and November, especially in Romania (RAIN, +11%), Poland (+31%), and western Ukraine. The maximum precipitation occurred in January when it was 60% above average in Romania and southern Ukraine. Unfavorable rainfall was recorded in southern Russia (from the kray of Krasnodar to the Kabardino Balkariya republic), with the largest deficit occurring in the kray of Krasnodar, which experienced relative deficits of rain exceeding 20% in January. Much of the rain fell as snow, which started early (October), covering much of the MPZ (with fluctuations) from early December (covering only the Carpathian basin in Romania) and then the whole MPZ uninterruptedly from early January to the end of the reporting period.

Almost all areas of Central Europe to Western Russia enjoyed a below average temperature from October to December, which had negative effects on the development of winter crops. The coldest area included the oblasts of Kirovskaya and Nizhegorodskaya, along with Tatarstan republic, with two low periods in November and December. Due to the low temperatures during the monitoring period, the biomass production potential (BIOMSS) for the MPZ as a whole decreased by 10% compared to average. This results from BIOMSS drops in northern Ukraine (-7%), Belarus (-9%), and adjacent areas in Russia where this drop reaches 10% or even 20% and more. The maximum VCI (0.79) is lower compared with other MPZs. According to the maximum VCI map of this monitoring period, most pixels were below 0.5 in the central part of Ukraine and the oblasts of Krasnodar and Chelyabinsk, resulting from poor crop condition.

Uncropped arable land occurs mostly in Ukraine and southwestern Russia, which is also characterized by clusters of unfavorable VHIn and low VCIx. CALF, however, increased by 29 percentage points over the reference period. In general, mixed conditions are estimated to prevail in this MPZ; the output of current winter crops will depend on the agrometeorological conditions in the next key vegetative stage.

Figure 2.6. Central Europe-Western Russia MPZ: Agroclimatic and agronomic indicators, October 2016-January 2017

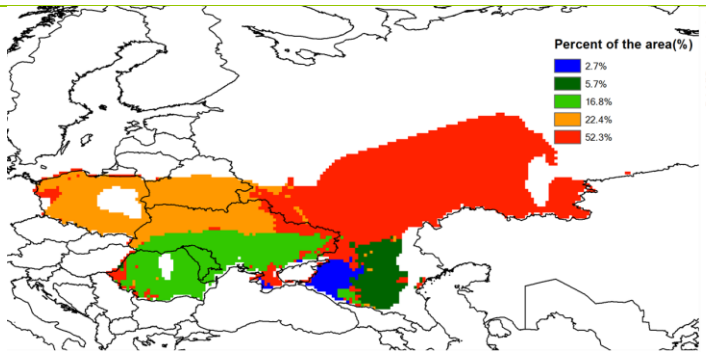

a. Spatial distribution of rainfall profiles

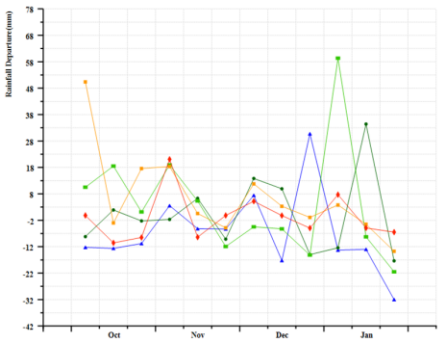

b. Profiles of rainfall departure from average (mm)

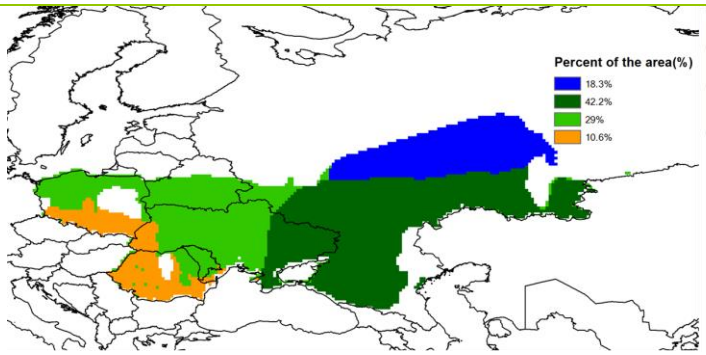

c. Spatial distribution of temperature profiles

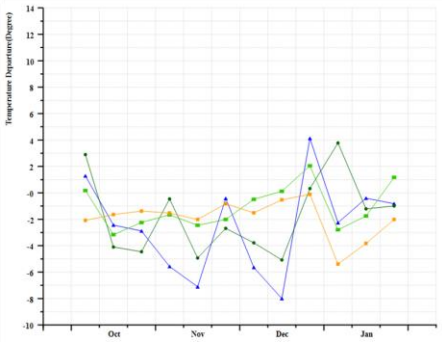

d. Profiles of temperature departure from average (mm)

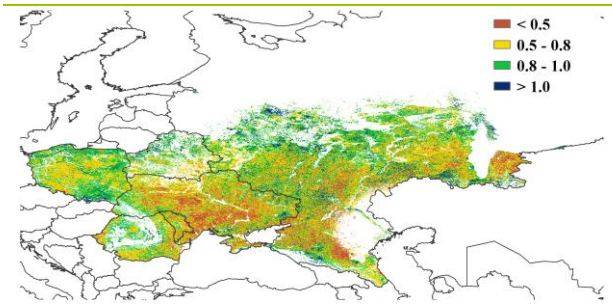

e. Maximum VCI

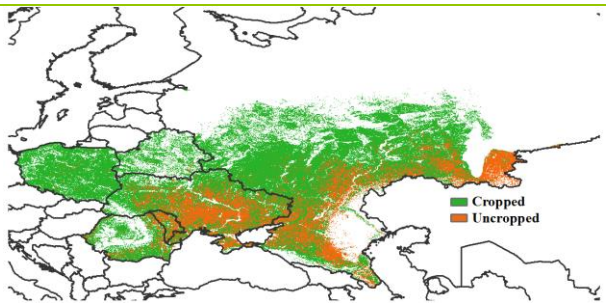

f. Cropped arable land

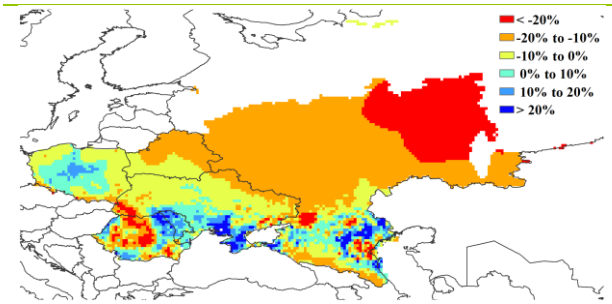

g. Biomass accumulation potential departure

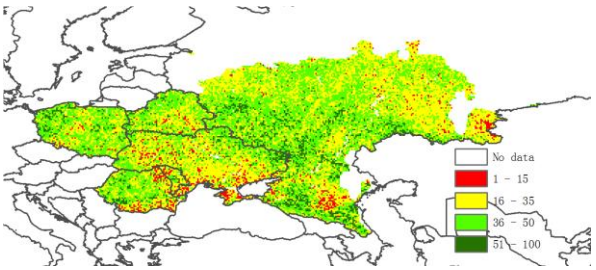

h. VHI minimum

Note: For more information about the indicators, see Annex C.

Chapter 3. Main producing and exporting countries

Building on the global patterns presented in previous chapters, this chapter assesses the situation of crops in 30 key countries that represent the global major producers and exporters or otherwise are of global or CropWatch relevance. In addition, the overview section (3.1) pays attention to all countries worldwide, to provide some spatial and thematic detail to the overall features described in section 1.1. In section 3.2, the CropWatch monitored countries are presented, and for each country maps are included illustrating NDVI-based crop condition development graphs, maximum VCI, and spatial NDVI patterns with associated NDVI profiles. Additional detail on the agroclimatic and BIOMSS indicators, in particular for some of the larger countries, is included in Annex A, tables A.2-A.11. Annex B includes 2016 wheat production estimates for Argentina, Australia, and Brazil.

3.1 Overview

Table 3.1 presents the agroclimatic and agronomic indicators for October 2016-January 2017, showing their departure from the five and fifteen-year averages as applicable; the underlying CWAI indicators are presented in figures 3.2-3.5. Many of the global rainfall patterns that characterize the current reporting period (October 2016 to November 2017, or "ONDJ") were already present in the previous CropWatch bulletin that covered the July-October 2016 (JASO) period. In some cases, the patterns are remarkably similar and can be summarized, as done in the section below, with descriptions based essentially on rainfall. This part of the report presents an overview of areas with extreme weather events, followed by brief descriptions of five areas (W01-W05) with wet conditions and ten areas (D01-D10) with dry conditions, as shown in figure 3.1.

Extreme weather

At the global scale, the largest rainfall deficits (RAIN more than 60% below average) occurred in five areas located in (i) India (Andhra Pradesh, Goa, Karnataka, Kerala, Puducherry, Sikkim and the western coastal agro-ecological region), (ii) the Brazilian nordeste (Sergipe, Alagoas and Pernambuco), (iii) the east of Africa (Somalia), (iv) Yemen, and (v) an agro-ecological region of France known as the "mixed maize, barley and rapeseed zone," which approximately coincides with the regions of Poitou-Charentes, Centre, and Pays de Loire. Although this is not maize and rapeseed season, the deficit is likely to affect winter wheat and barley, as well as rain-fed summer crops if abundant rain does not set in during the next reporting period. Some of the listed extremes (the mentioned areas in India, Africa, and France) are part of larger coherent areas defined below as D09, D05, and D03, respectively.

Most areas with very high rainfall excesses (RAIN departures larger than +120%) occur in the areas identified below as W04 and W05. The only exception is the province of Santa Cruz in southern Argentina where 33 mm represent almost a triplication (RAIN, +197%) of the expected rainfall. Since the area is semi-arid, however, this rainfall can have a significant effect on biomass production (BIOMSS, +258%). The second largest rainfall departure belongs to other areas that normally expect little rainfall during winter: Gujarat (RAIN, +473%) and Rajastan (+292%); both part of the W04 western and central Asia area, as shown in figure 3.1.

Table 3.1. CropWatch agroclimatic and agronomic indicators for October 2016-January 2017, departure from 5YA and 15YA

Country	Agroclimatic Indicators			Agronomic Indicators		
	Departure from 15YA (2002-2016)				Departure from 5YA (2012-2016)	Current
	RAIN (%)	TEMP (°C)	RADPAR (%)	BIOMSS (%)	CALF (%)	Maximum VCI
Argentina	23	-1.0	2	8	8	0.86
Australia	-15	-0.5	1	-8	40	0.70
Bangladesh	5	-0.3	0	16	1	0.92
Brazil	5	-0.4	2	-2	-4	0.81
Cambodia	120	-0.3	-10	62	-4	0.87
Canada	12	1.5	-9	17	2	0.92
China	12	0.8	-12	25	1	0.67
Egypt	-35	-0.6	0	-3	1	0.89
Ethiopia	-26	0.2	8	-20	7	0.90
France	-36	-3.5	3	-35	1	0.73
Germany	-24	-1.4	-8	-11	0	0.83
India	-30	0.1	3	-21	-1	0.96
Indonesia	13	-0.6	-5	6	0	0.87
Iran	-1	-0.3	1	-15	n.a.	0.42
Kazakhstan	41	-1.3	-8	-7	n.a.	0.87
Mexico	-24	0.6	1	-8	8	0.88
Myanmar	7	0.2	-3	10	0	0.94
Nigeria	-5	0.0	0	-9	2	0.90
Pakistan	30	0.4	-1	20	5	0.82
Philippines	50	-0.5	-6	20	0	0.90
Poland	31	-1.0	-14	-2	0	0.88
Romania	11	-2.2	-6	-2	2	0.73
Russia	-1	-1.8	-2	-18	16	0.87
S. Africa	9	-0.2	1	-1	7	0.79
Thailand	82	0.0	-7	38	0	0.94
Turkey	-15	-1.3	2	-16	-20	0.55
United Kingdom	-31	-2.3	-1	-18	0	0.87
Ukraine	33	-1.7	-7	-4	-12	0.67
United States	5	1.1	-3	12	10	0.97
Uzbekistan	100	-0.8	-2	51	n.a.	0.84
Vietnam	74	0.7	-11	38	-2	0.88

Note: n.a. = not applicable. Over the monitoring period, no crops are in the field in Iran, Kazakhstan and Uzbekistan.

Figure 3.1. Major wet (shades of green) and dry (shades of yellow and red) areas of global importance

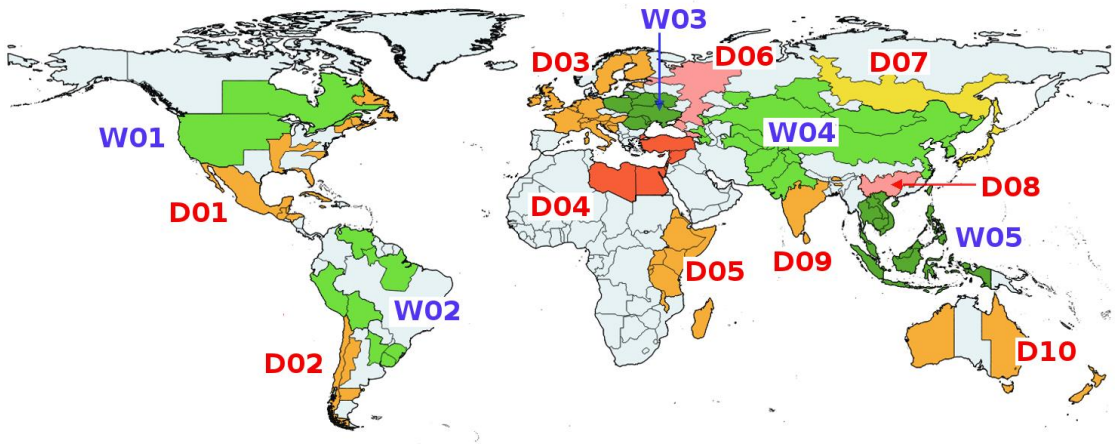

Note: W01-W05 (in blue) indicate wet areas, while areas D01-D10 (in red) are dry.

All large temperature drops (in excess of 3.0°C) occurred in France (in area D03) and Russia (D06) where negative departures close to -4.0°C were common, in terms of cold spell intensity. This is followed by an area between D06 and D07 where temperature was about 3.5°C below average in the Oblasts of Kurgan,

Perm, Sverdlovsk, and Tyumen. The largest positive departures occurred in American Boreal areas of little agricultural relevance.

Lowest relative sunshine (RADPAR departure below -15%) occurred almost all in D08, especially in the southeast (including China's Jiangsu, -22%; Henan -18%; and Shaanxi, -15%) and northwest in Russia and Kazakhstan with values about -10% to -15%. The highest RADPAR departures (+10% to +13%) do not follow a well-defined spatial pattern and occur in Ethiopia, boreal Canada, and the Democratic Republic of the Congo, Belize, and Uganda, among others.

The analysis of the combined anomalies highlights cold and dry Western Europe (D03), warm and wet areas in China (part of eastern W04), dry and warm India (parts of D09), as well as wet and cold southwest D09.

Wet conditions

W01, northern America

Wet conditions occurred over central-western North America, including Ontario and Quebec (RAIN, +24% and +29%, respectively), extending to Kansas (+11%) and California (+45%). In the Canadian Prairies, the average rainfall excess was +30%, while temperature remained negative but nevertheless 1-3°C above average. In the United States, the largest rainfall excesses (about double the average) were recorded around Wyoming, North Dakota, and Montana, with close to average temperature in most places.

W02, northern half of South America

Dry conditions in the Southern Cone of Latin America during the July-October recently improved in the southeast (southern Brazil, Uruguay, and northern Argentina) during the current reporting period. Overall, a large area with favorable precipitation now occupies much of the Andean and Amazonian areas of the continent. The precipitation excess reaches 33% on average, with the largest values in some important production areas such as Entre Rios and Santa Fe (both +48%) in Argentina and 53% in Amapa (Brazil). Temperature was slightly below average with average RADPAR and a potential biomass production increase (BIOMSS) at 12%.

W03, northern-central Europe

The area covers 12 CropWatch polygons in eastern and central European countries, from Poland and the Russian Oblast of Tula in the north and Ukraine and Romania in the south. Rainfall exceeds the average by 20%, with negative anomalies in temperature (TEMP, -1.3°C) and RADPAR (-9%), resulting in below average biomass production potential (BIOMSS, -9%). The most abundant precipitation fell in Poland (RAIN, +31%), Belarus (+41%), and Ukraine (+33%), with Ukraine also experiencing the largest drop in temperature (-1.7°C). Poland and neighboring Lithuania had the largest sunshine deficit, as expressed by a drop in RADPAR of -14% and -13%, respectively.

W04, western and central Asia

This area covers a large region in Asia and includes as much as 60 CropWatch polygons in an area centered around Kashmir, the north Kazakhstan region (Severo Kazakhsatanskaya) to eastern Asia (Primorsky Krai in eastern Russia), and Qinghai province of China. In the west, it reaches as far as the Caspian Sea, while its east-west extension is close to 7,000 km. In the eastern part of the area (for example on the Korean peninsula with RAIN departures of +31% to +44% from south to north), rainfall improved compared to the previous reporting period; this improvement, however, did not reach Japan, which remained dry (RAIN, -36%). Overall, the area experienced about the double of the average

precipitation (+84%), accompanied by about average temperature (TEMP, -0.4°C) but low solar radiation (RADPAR, -5%). The biomass production potential (BIOMSSS) increased 38% over average. Rainfall increased more than 200% in Haryana and Delhi (+240%) in India, +251% in Qinghai province in China, and as much as +292% and +473% in Rajastan and Gujarat (India), respectively, two areas that are normally relatively dry during this season. More than double the expected amounts occurred in Uzbekistan (+100%); the Chinese provinces of Shaanxi, Jilin, Gansu, Heilongjiang, Shandong, Xinjiang, Inner Mongolia, and Ningxia, as well as in Beijing (from about 100% to +180%); Tajikistan (+115%) and Kyrgyzstan (+148%); and the Kyzylorda region in Kazakhstan (+145%). Temperature varied spatially, while RADPAR stayed below the reference values and locally dropped well below (-11% in Shandong and -15% in Shaanxi, both in China).

W05, Southeast Asia

Wet conditions prevailed over most of continental and maritime Southeast Asia and adjacent areas in southern East Asia, although departures from average (RAIN, +49%) were in general lower than those just described for the western and central Asia (W04) area. The largest anomalies were recorded in Vietnam (+74%), Thailand (+82%), and Cambodia (+120%, reaching 784 mm). Similar to the W04 area, however, temperature was average and RADPAR -7% below reference values.

Dry conditions

D01, Southern North and Central America

Dry conditions prevailed over the southeastern United States, basically east of Arkansas, Illinois, Louisiana and Missouri, extending into the Caribbean (Cuba) and Central America. In the United States, the rainfall deficit was 10-20%, with temperature (TEMP) 1-2°C above average with a shortage of sunshine (RADPAR) and generally average biomass production potentials (BIOMSS). For the region as a whole, the average rainfall deficit reached 21%, with temperature above average (+1°C), RADPAR below (-1%), and BIOMSS down 6%. The largest deficits occurred in Cuba (RAIN, -45%) and Jamaica (-40%), followed by parts of Mexico and Florida (-30%). The deficit was mildest in West Virginia, New Hampshire, and Illinois (about 10%).

D02, Western Cono Sul

Dry conditions already affected eastern South America during the previous reporting period (July-October), but recently moved towards the west and south, to affect Chile and several areas in Argentina. The average precipitation deficit (RAIN, -35%), combined with cool temperature (-0.6°C) and RADPAR of 4% above reference values, is projected to result in a 28% drop in potential biomass production (BIOMSS).

D03, Western Europe

Dry conditions over western and north-western Europe started during the summer and currently cover sixteen countries, with a rather homogeneous RAIN deficit of 30% on average (from 14% in Switzerland to 48% in Ireland), with consistently below average temperature (TEMP, -1.8°C on average, ranging from -0.1°C in Estonia to -3.5°C in France) with low radiation departures (RADPAR, -2% on average, but -8% in Germany and Sweden; -5% in Austria). The BIOMSS index departure is -2%.

D04, Eastern Mediterranean

Dry conditions prevailed over the southern and eastern Mediterranean during July to October 2016, but improved thereafter in northwest Africa (west of and including Tunisia). Currently, dry conditions affect eight countries, with an average rainfall (RAIN) deficit of 39%: -15% in Turkey, the main agricultural

country in the area, to -54% in both Libya and Cyprus, of which only the latter expects agriculturally useful winter rains. Temperature (TEMP) was -0.7°C below average, while radiation (RADPAR) was up 1%. The drop in biomass production potential (BIOMSS) is significant with -28% on average.

D05, Eastern Africa

Dry conditions prevailed over eastern and southern Africa during the previous reporting period. This situation has now undergone a marked improvement, especially in the south where three countries—currently in their main growing season—report above average rainfall with values of +41% (reaching 418 mm) for Botswana, +31% or 577 mm for Zimbabwe, and +15% or 355 mm for Namibia. Dry conditions continue between Eritrea and Malawi, the East African Highlands, and Madagascar, all in their main agricultural season. The average precipitation deficit is 40%, from -11% in Malawi to -26% in Ethiopia and -76% in Somalia; in Somalia, however, irrigation plays a larger part in food production than in the other countries. Temperature for the area was average and radiation high (RADPAR, +5% over average), with a generally decreased biomass production potential (BIOMSS, -31%).

D06, western Russia

In this area, which extends from north to south from the Komi republic and the oblast of Arkhangelsk to the Adygeya autonomous oblast and the northern Black Sea, only radiation (RADPAR) was average.Rainfall and temperature were below average (RAIN, -21% and TEMP, -2.1 ° C), which resulted in a drop as well for the BIOMSS index (-17%). Both the largest precipitation deficit and the largest negative temperature anomaly occurred in the Komi-Permyak Okrug (RAIN, -34% and -3.5 ° C). The cold wave, however, was not associated with the precipitation deficit everywhere; it was most intense (-3.0 to -3.4 ° C) in the oblasts of Kirov and Perm and in the Udmurt republic. On the Black Sea, Georgia recorded a 12% RAIN deficit and a -2.2 ° C drop in TEMP.

D07, Southern Siberia to Japan

The area encompasses a west-to-east stretch from Siberia to Japan, starting at the Krai of Krasnoyarsk (the largest Krai in the Russian Federation) to the Krai of Khabarovsk in the Russian Far East, bordering the Atlantic Ocean and Japan. The average rainfall deficit in the region is -28%, with a temperature anomaly of -1.2°C, a slightly positive radiation, and a production potential drop (BIOMSS) of 25%. The largest anomaly for RAIN occurred in Ust-Orda Buryatia (-33%), an autonomous Okrug of Irkutsk Oblast, and Japan (-36%). Temperature anomalies vary from average (Japan) to -2.1°C in the Krai of Khabarovsk. RADPAR departures are mostly average and vary between -2% in Japan to +6% in the Amur oblast.

D08, Southern area of China

This rainfall deficit area (RAIN, -28%) includes the provinces of Guangxi, Guizhou, Hunan, Jiangxi, Yunnan, and Zhejiang, with average winter temperatures varying between 10 and 15°C. During the previous reporting period the same area was mostly wet, and the current relative drought has been developing since October, affecting most severely Guangxi (RAIN, -36%) and Hunan (-32%). On average, temperature in the region was 1.1°C above seasonal values, with a large deficit of solar radiation (RADPAR, -16%), which most typically defines the whole area: with the exception of Yunnan (where RADPAR was average), very large negative RADPAR departures in excess of 11% occur everywhere, reaching -22% in Jiangxi and Zhejiang and as much as -24% in Hunan, which is the absolute record—globally—for the current reporting period. The biomass production potential (BIOMSS) is down -12%.

D09, southern area of Asia

Dry conditions were confined to south-western India during the previous reporting period. From October, they expanded to enclose the northern center (Madhya Pradesh), the east, and northeast of the country, resulting in an almost generalized drought situation avoiding mostly the northwest. The area also includes Bhutan and Sri Lanka. The average rainfall deficit is as large as -46%, with close to average TEMP and positive RADPAR departure (+4%). Logically, the potential biomass production dropped sharply by 36% compared with average. The most severe deficits occur in Karnataka (RAIN, -74%, resulting in 53 mm of precipitation), Andhra Pradesh (-71% or 67 mm), Goa (-69% or 63 mm), Kerala (-62% or 205 mm), Tamil Nadu (-60% or 216 mm), and Jharkhand (-58% or 48 mm). The lowest deficits are those of Chhattisgarh (-25%) and Bihar (-23%). The positive average RADPAR value results from values between 0% in Meghalaya, +8% for Sri Lanka, and +9% in Tami Nadu. Temperature departures are small, in the range of 0.0°C to -0.4°C, with only one positive departure for the 14 CropWatch polygons, namely +1.5°C in Meghalaya, the wettest region in India, where "drought" is more of a blessing than a disaster. Meghalaya is also the only region with positive BIOMSS expectation, while BIOMSS for other parts drops by as much as 64% in Karnataka and the other states with large precipitation shortfalls.

D10, Oceania

The dry area in Oceania currently involves 6 CropWatch polygons, with an average RAIN deficit of 28%, mostly affecting New-Zealand (a decrease in RAIN of 52% compared to average, to 145 mm) as well as Tasmania (-50% to 107 mm) and Victoria (-25% to 148 mm) both in Australia. All three areas had slightly negative RADPAR departures in the range of -2%. The below average temperature (TEMP, -0.5°C on average) results from values between -0.3°C (New Zealand) and -0.9°C in Western Australia, where (in the case of Western Australia) RADPAR departure was positive (+2%). Altogether, the BIOMSS potential dropped -22%.

Figure 3.2. Global map of October 2016-January 2017 rainfall (RAIN) by country and sub-national areas, departure from 15YA (percentage)

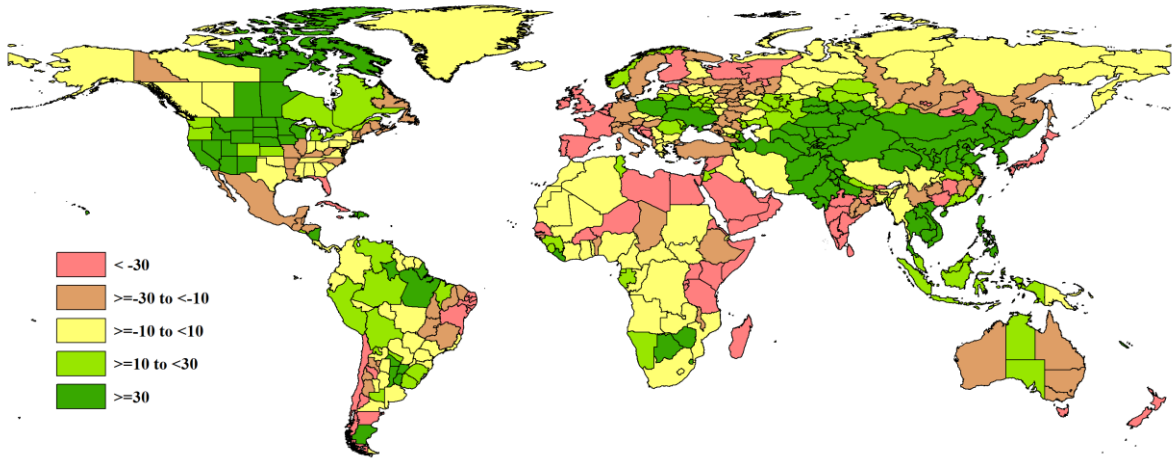

Figure 3.3. Global map of October 2016-January 2017 temperature (TEMP) by country and sub-national areas, departure from 15YA (degrees)

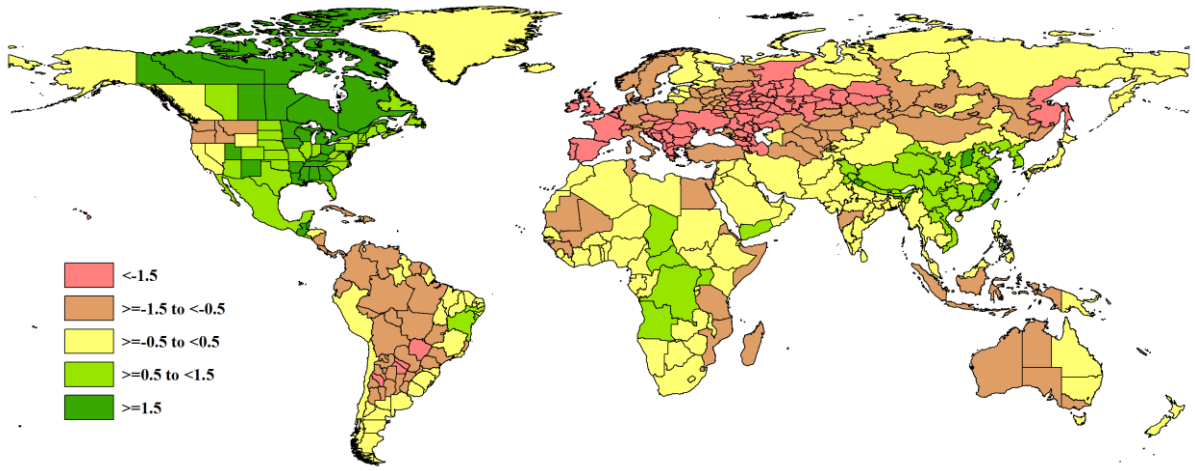

Figure 3.4. Global map of October 2016-January 2017 PAR (RADPAR) by country and sub-national areas, departure from 15YA (percentage)

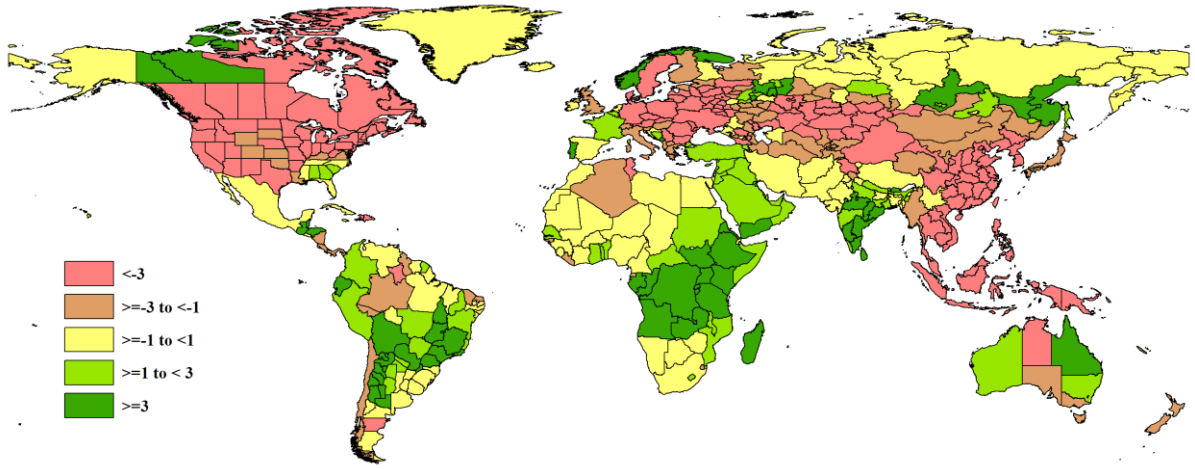

Figure 3.5. Global map of October 2016-January 2017 biomass (BIOMSS) by country and sub-national areas, departure from 15YA (percentage)

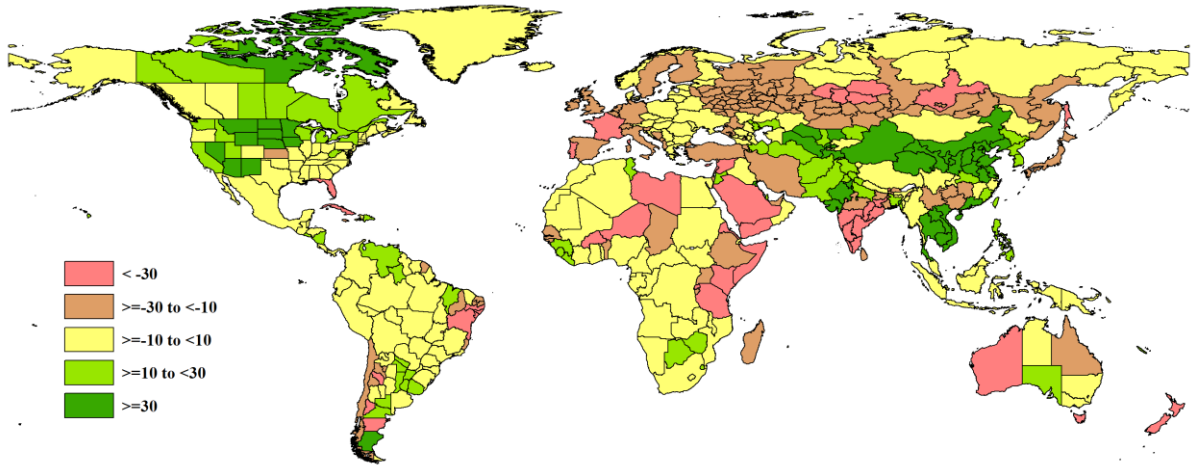

3.2 Country analysis

This section presents CropWatch analyses for each of thirty key countries (China is addressed in Chapter 4). The maps refer to crop growing areas only and include (a) Crop condition development graph based on NDVI average over crop areas, comparing the October 2016-January 2017 period to the previous season and the five-year average (5YA) and maximum. (b) Maximum VCI (over arable land mask) for October 2016-January 2017 by pixel; (c) Spatial NDVI patterns up to January 2017 according to local cropping patterns and compared to the 5YA; and (d) NDVI profiles associated with the spatial pattern under(c). See also Annex A, tables A.1-A.11, and Annex B, tables B.1-B.3, for additional information about indicator values and production estimates by country. Country agricultural profiles are posted on **www.cropwatch.com.cn**. Snow cover information for the country analyses was derived from NOAA Snow Cover Maps.[2]

Figures 3.6-3.35. Crop condition for individual countries ([ARG] Argentina- [ZAF] South Africa) October 2016-January 2017

[2] https://www.ncdc.noaa.gov/snow-and-ice/snow-cover/.

[ARG] Argentina

The current monitoring period covers the harvesting of wheat as well as the planting and main growing stages for maize and soybean. Problems were reported in part of the Pampas during this period, with flooding in Cordoba, Santa Fé, and northwest Buenos Aires, and drought in southern Buenos Aires province. Some of CropWatch indicators reflect variations in these areas too. Also reported are changes in crop proportion related to changes in the country's export policies, reducing the planted area of soybean and increasing that of wheat and maize compared to recent years. For the whole country, a large increment of rainfall above average was observed (RAIN, +23%), while temperature (TEMP) dropped 0.7°C and radiation (RADPAR) underwent a small increase (2%), resulting in BIOMSS increasing about 8% over average. Positive temperature anomalies were recorded for December and January, the warmest months of the year, mainly in the major production areas of central and southern Pampas. For the whole country, negative NDVI anomalies have been observed since November 2016.

High positive rainfall departures from average occurred in eastern Argentina including the provinces of Santa Fé (RAIN, +48%), Entre Ríos (+47%), Corrientes (+42%), and Chaco (+37%). The low positive departures observed in Buenos Aires (+7%) and Córdoba (+3%) could be the result of a combination of flooding and drought situations. On the contrary, arid and semi-arid regions of Argentina showed strong negative anomalies: Catamarca (-30%), La Rioja (-37%), and Patagonia (-27%). In general, lower RADPAR values were observed in provinces with the highest RAIN values. Negative NDVI anomalies were observed in the already mentioned "problem areas" of south and northwest Buenos Aires province and part of the province of Córdoba. NDVI anomalies could also be explained by early ripening of winter crops, with crops maturing in December (reflecting more area with reductions in NDVI compared to recent years). The VCI map shows low values in the mentioned problem areas.

Overall, although this monitoring period recorded above average rainfall, the negative impact of floods and drought in part of the Pampas (confirmed by NDVI and VCI indicators) could result in reduced grain production in Argentina. Wheat production estimates for the country are listed in table B.1 in Annex B.

Figure 3.6. Argentina crop condition, October 2016-January 2017

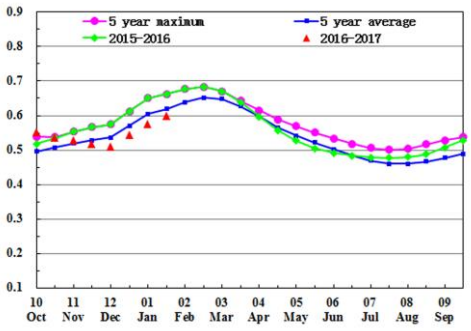

(a) Crop condition development graph based on NDVI

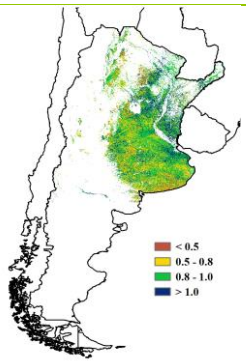

(b) Maximum VCI

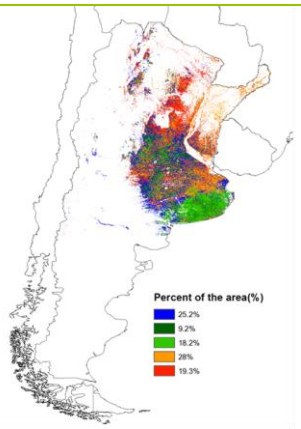

(c) Spatial NDVI patterns compared to 5YA

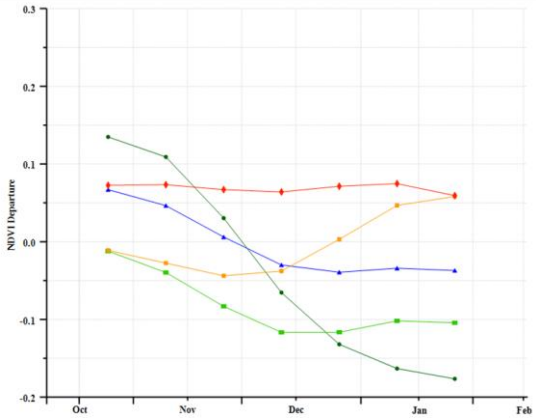

(d) NDVI profiles

[AUS] Australia

Australian crops show generally above average condition during the monitored period from October to January. This period covers the harvesting of winter crops and planting of summer crops. Although rainfall dropped below average (New South Wales: RAIN, -19%; Victoria, -25%; Western Australia, -10%) irrigation makes up for the inadequacy of precipitation. The NDVI profiles also reflect the above average conditions in almost all cropped regions in the country from October to November, with only 11.1% of the cropped land, covering central and northeastern New South Wales, showing below average values in December and January. The maximum VCI reaches an overall value of 0.7 for Australia's cropped lands.

With the fraction of cropped arable land up 40 percentage points compared to the average of the previous five years, CropWatch estimates that the production of wheat in 2016-17 will increase 24.3% over 2015-16. Table B.2 in Annex B shows CropWatch wheat production estimates for Australia.

Figure 3.7. Australia crop condition, October 2016-January 2017

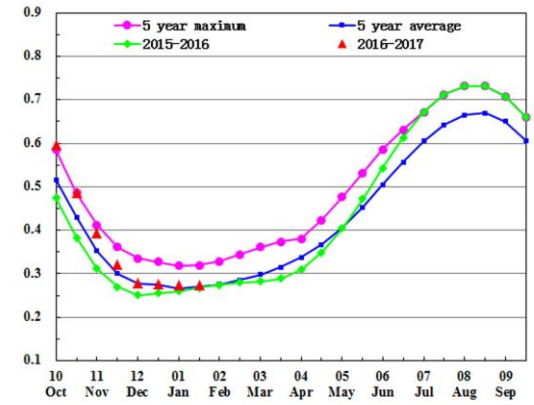

(a) Crop condition development graph based on NDVI

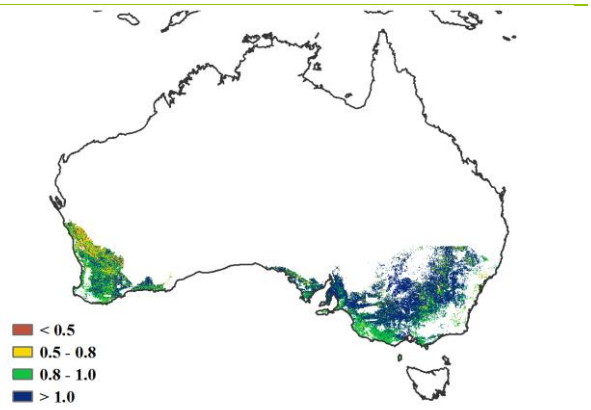

(b) Maximum VCI

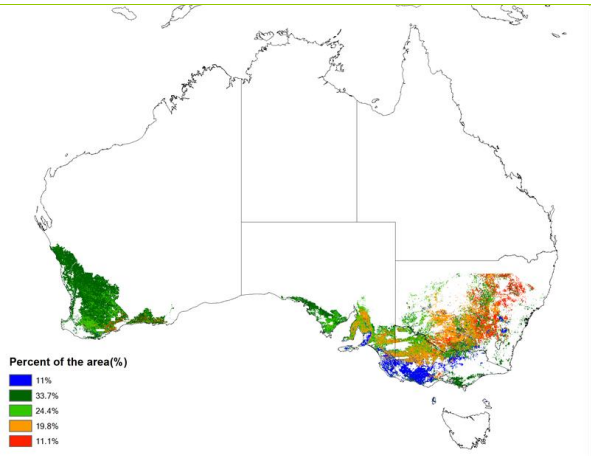

(c) Spatial NDVI patterns compared to 5YA

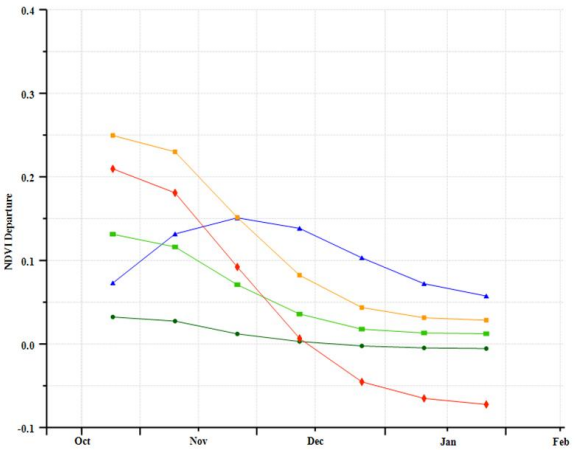

(d) NDVI profiles

[BGD] Bangladesh

The monitoring period covers the harvesting of late-monsoon Aman and planting of the dry season irrigated Boro rice. Overall, the CropWatch indicators show favorable conditions for the country. Although the previous season monsoon flood damaged the standing Aman rice (as reported in the November 2016 CropWatch bulletin), it also had positive impact on the planting of Boro.

Nationwide, both the fraction of cropped arable land (CALF) and accumulated biomass (BIOMSS) increased, by 1.3 percentage points and 16%, respectively. Temperature (TEMP) and photosynthetically active radiation (RADPAR) were average in the monitoring period. The crop condition development was below average in November and December; however, it turned average from January on forward. The national NDVI profiles and patterns were average, except for Rangpur, Sylhet, and Chittagong, where they (in the case of Chittagong) increased to average after December. The maximum VCI values over the country were above 0.5, pointing to favorable crop condition. Overall, the current increase of cultivated land and biomass as well as good rainfall (RAIN, +5%) contributed to the favorable crop condition for the country.

Figure 3.8. Bangladesh crop condition, October 2016-January 2017

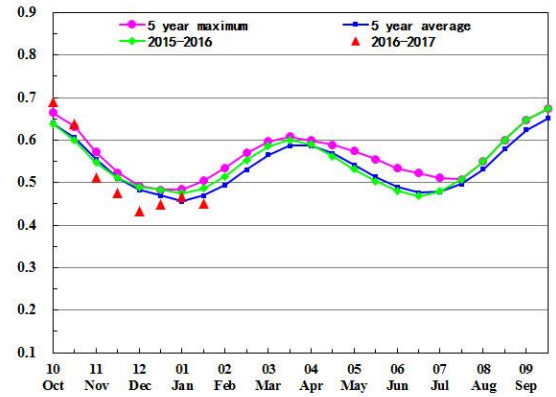

(a) Crop condition development graph based on NDVI

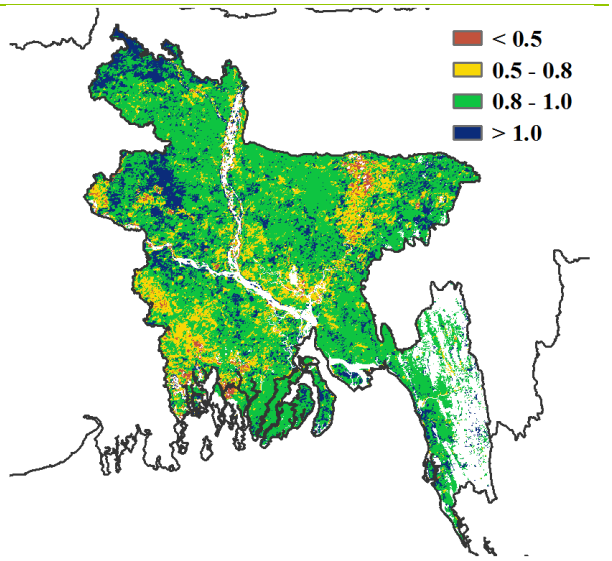

(b) Maximum VCI

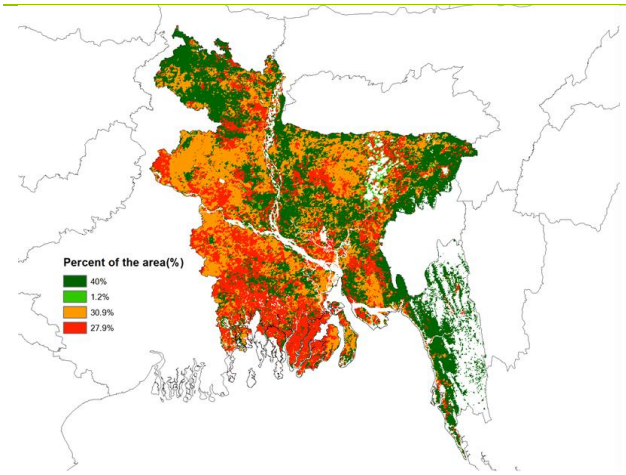

(c) Spatial NDVI patterns compared to 5YA

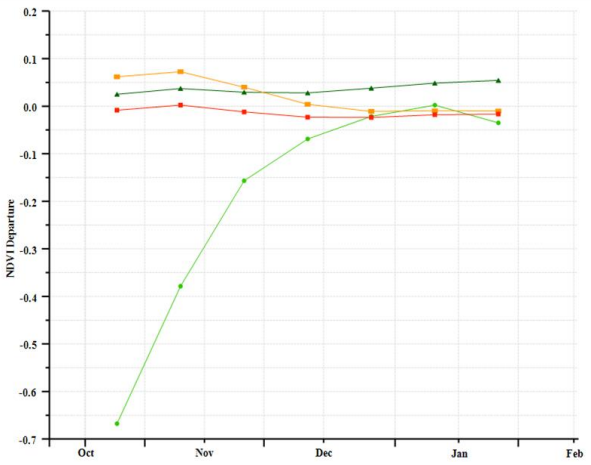

(d) NDVI profiles

[BRA] Brazil

Generally, crop condition in Brazil was slightly above the average of the previous five years. Harvest of winter wheat was concluded by the end of 2016. The planting of first maize as well as soybean are almost completed by January, while sowing of the second maize is just starting. Overall agroclimatic conditions were "normal" at the national level, with RAIN at 5% above average, TEMP at -0.4°C below, RADPAR 2% above, and BIOMSS 2% below average. As a result of the size of the country, however, agroclimatic conditions vary a lot from state to state. Sufficient rainfall was recorded in the major wheat producing states, as well as in the soybeans and maize producers, especially Rio Grande do Sul (+30% rainfall compared with average). Well below average rainfall occurred in the Nordeste, including Rio Grande do Norte (RAIN, -33%), Paraiba (-49%), Pernambuco (-64%), and Sergipe (-76%). In the states of Mato Grosso do Sul and Mato Grosso, 6% above average rainfall will benefit soybean fields, as well as the second maize to be planted in the coming season. Temperature and radiation were close to average in almost all states.

Agronomic indicators consistently show slightly above average crop condition. According to the NDVI-based crop condition development graph, national NDVI was slightly above average and the previous year but decreased to below average by the end of January. The maximum VCI map presents overall favorable condition with the only exception in the Nordeste where VCIx was below 0.5 due to drought. Spatial NDVI patterns and the corresponding NDVI departure profiles also confirm that continuously below average NDVI during the monitoring period mainly occurred in the Nordeste. Above average NDVI mostly occurs in central and southern Brazil and coincides with high VCIx areas. Altogether, CropWatch revised the wheat production to 7,747 ktons, 10% up from the previous harvest season (table B.3 in Annex B).

Figure 3.9. Brazil crop condition, October 2016-January 2017

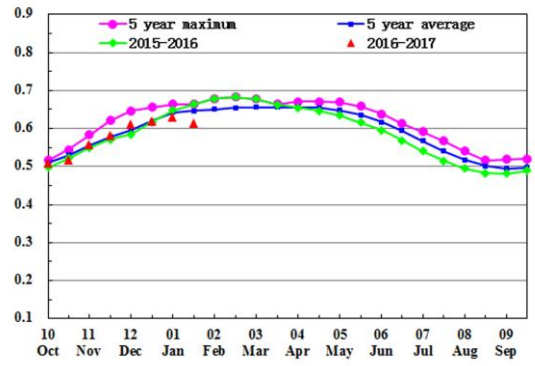

(a) Crop condition development graph based on NDVI

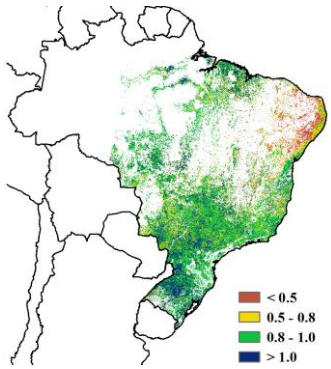

(b) Maximum VCI

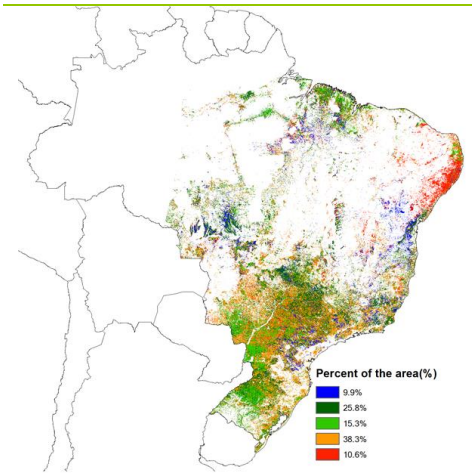

(c) Spatial NDVI patterns compared to 5YA

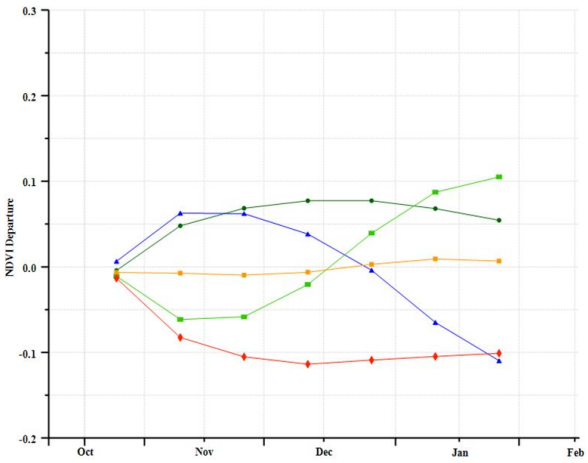

(d) NDVI profiles

[CAN] Canada

In Canada, only winter crops are grown during the reporting period, during which rainfall was 12% above average, temperature exceeded seasonal values by 1.5°C, and RADPAR was very significantly below average (-9%). Saskatchewan, Manitoba, Alberta, and Ontario together account for 98% of Canadian wheat production, and abundant rain fell in Manitoba (+63%), Saskatchewan (+50%), and Ontario (+24%), while Alberta recorded 5% below average rainfall. As last summer Ontario suffered a serious drought, the current above average rainfall will help avoid future water stress by replenishing soil water, benefitting both winter crops after over-wintering and future summer crops. Contrary to Ontario (TEMP, -0.9°C), other main grain provinces observed above average temperature, including Alberta (+0.9°C), Manitoba (+2.6°C), and Saskatchewan (+1.7°C). The growth of winter crops will be favored by warm weather.

Compared to the five-year average, the cropped arable land fraction (CALF) appeared to have increased by 2.2 percentage points, which may result from the delay in the harvesting period. Overall, crop prospects are currently favorable in Canada.

Figure 3.10. Canada crop condition, October 2016-January 2017

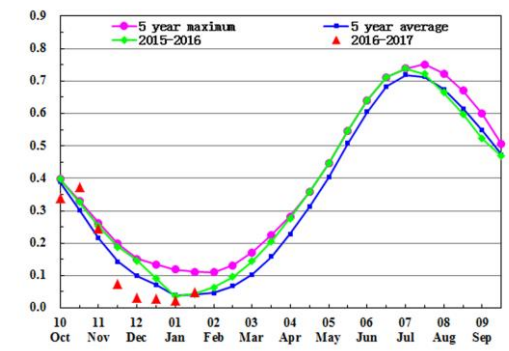

(a) Crop condition development graph based on NDVI

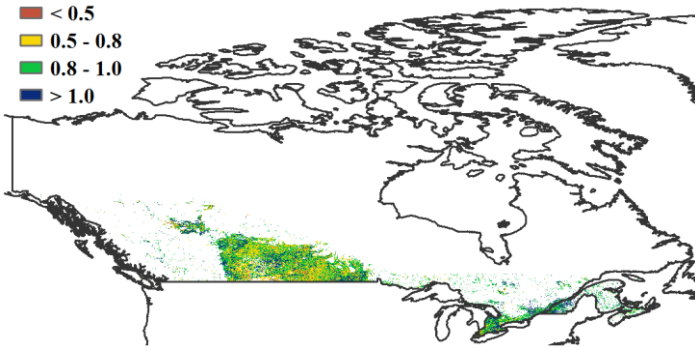

(b) Maximum VCI

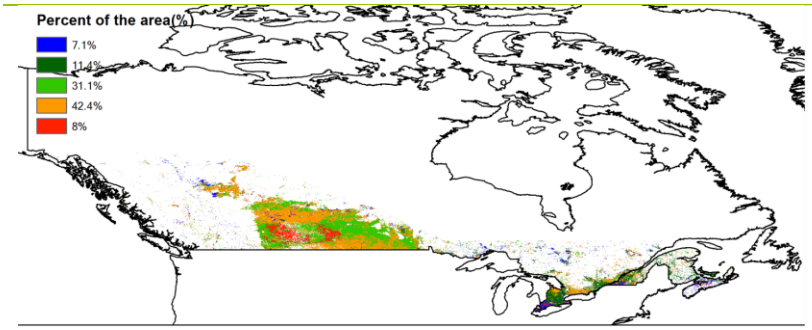

(c) Spatial NDVI patterns compared to 5YA

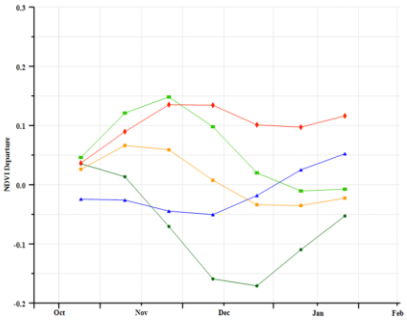

(d) NDVI profiles

[DEU] Germany

Over the reporting period, the nationwide crop condition, as illustrated by the NDVI development graph, was first below average until early December, close to average until the end of that month, and then very significantly below average. The period (October 2016-January 2017) covers the late stages of sugar beets (October harvest) and early vegetative stages of winter wheat and winter barley (planted in October). Cold and dry agroclimatic conditions prevailed, with indicators showing significant negative departures at the national level for rainfall and temperature (RAIN, -24% and TEMP, -1.4°C), and an 8% decrease in radiation (RADPAR). As a result, the biomass production potential BIOMSS dropped 11% nationwide compared to the five-year average.

As shown by the spatial NDVI profiles, values were below average from October to early November due to a lack of rainfall in the north, west, and south of Germany. Substantially drier-than-usual conditions in early October in western Germany hampered the sowing of winter crops. In mid-November, most parts of the country enjoyed favorable temperature and precipitation. This then developed into water stress from early November to January, with cold weather and heavy snow sweeping across the country in January. The spatial NDVI patterns also indicate that NDVI was below average from early December to January in 90% of arable land. This spatial pattern is also reflected by the maximum VCI, with a VCIx of 0.83 for Germany overall.

Generally, due to the cold temperature and water stress after early November, and the fact that NDVI plunged before the lasting snow set in in January, CropWatch assesses the current situation of most winter crop areas of Germany as unfavorable.

Figure 3.11. Germany crop condition, October 2016-January 2017

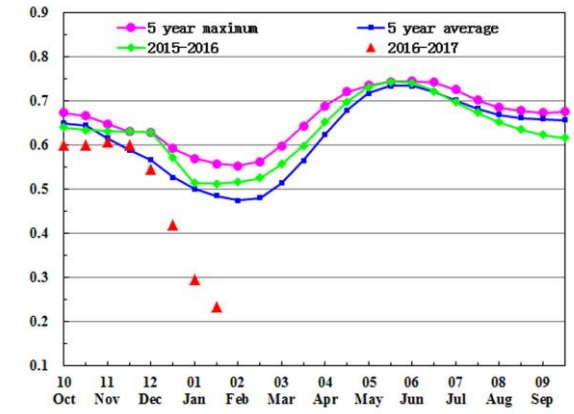

(a) Crop condition development graph based on NDVI

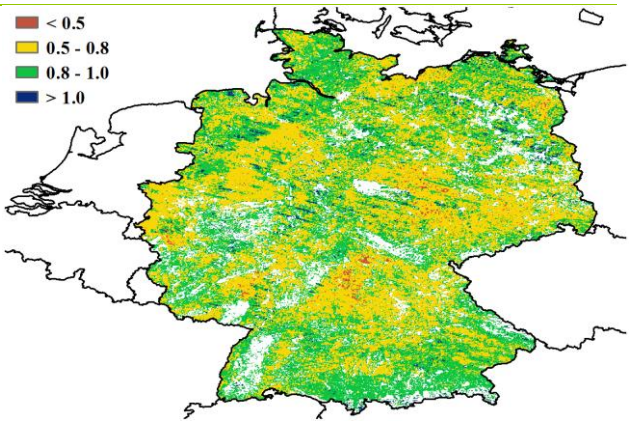

(b) Maximum VCI

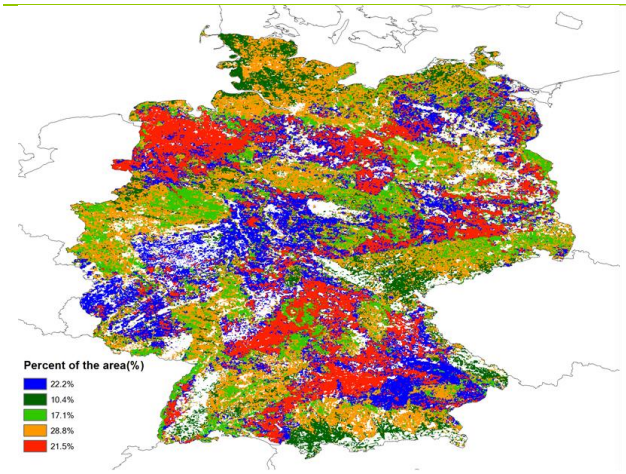

(c) Spatial NDVI patterns compared to 5YA

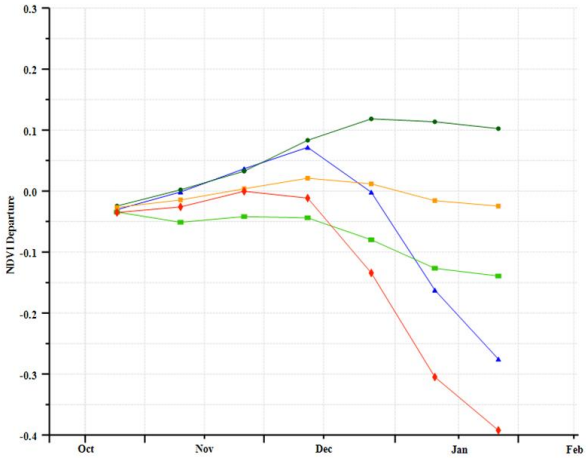

(d) NDVI profiles

[EGY] Egypt

In Egypt, the monitoring period covers the harvesting season of maize and rice, as well as the growing season of winter wheat and barley. The CropWatch agroclimatic indicators show that the period was characterized by a decrease of rainfall below average (RAIN, -35%) and a slight reduction in biomass production potential (BIOMASS, -3%), while temperature and RADPAR were about average (-0.6°C and 0% departures, respectively).

Apart from the sunshine, however, weather plays a minor part in a country where almost all crops are irrigated. The national crop condition development graph based on NDVI shows that crops were significantly below the average of the past five years and below that of the similar monitoring period (October-January) in 2015-2016. The maximum VCI and the spatial NDVI profiles show relatively good crop condition in the delta, while conditions are mixed in the Nile valley, especially in the south, together covering about 50% of the arable land. In general, for this monitoring period, winter crops in Egypt are assessed as below average.

Figure 3.12. Egypt crop condition, October 2016-January 2017

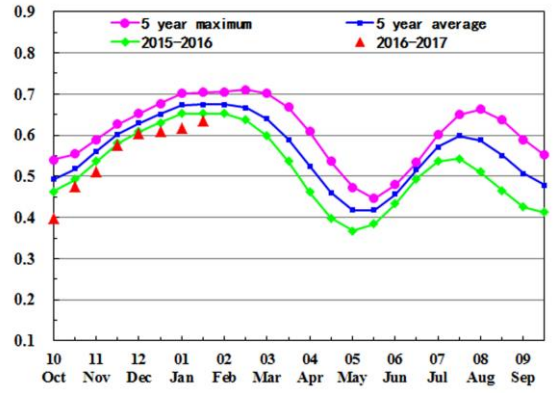

(a) Crop condition development graph based on NDVI

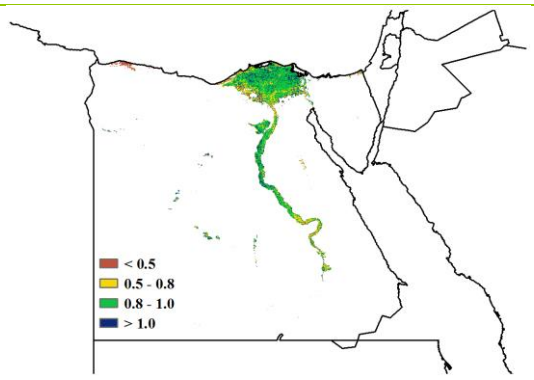

(b) Maximum VCI

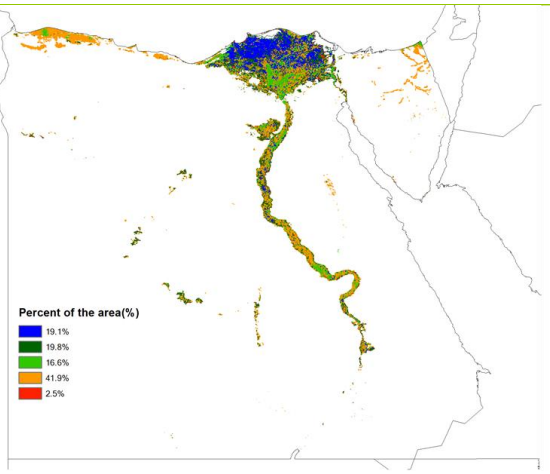

(c) Spatial NDVI patterns compared to 5YA

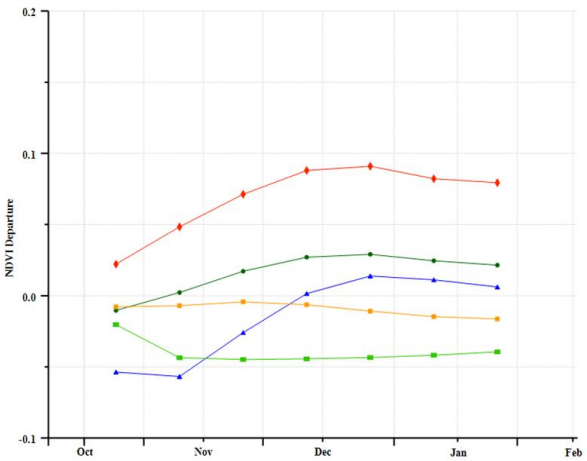

(d) NDVI profiles

[ETH] Ethiopia

Crop condition was below average during the reporting period for most parts of the country. Rainfall (RAIN) was reduced by about 25% compared to average and only a marginal 116 mm was recorded, whereas radiation (RADPAR) increased by 8%. The southeastern maize belt was the most devastated with about a 44% reduction in rainfall compared to the average. Temperature only increased by a slight 0.2°C, which combined with the prevailing water deficit resulted in a 20% reduction of the biomass production potential (BIOMSS). This affects most crops, such as teff, maize, and barley, that are harvested around December. The maximum VCI was highest (0.9) in the central and northern parts of the country, which include Amhara, Oromia, and North Wollo, as well as parts of northeast SNPP and the far east of Oromia.

The spatial NDVI clusters and profiles revealed trends comparable to those of the previous growing season. Additionally, the fraction of cropped arable land (CALF) increased by 6.8 percentage points, while throughout the monitoring period crop development was below average. Central Amhara, the main teff and wheat producing area, shows high NDVI values of more than 0.8, depicting a generally favorable situation and good production output. About 2% of the country experienced poor conditions, especially in southern parts of SNPP and Oromia. Overall, up to December, below average crop conditions occurred in about 20% of the country, which is likely to affect the Meher harvest. This is particularly true if water shortage occurred at critical phenological stages of the crops. In addition, the current shortage of rain, except in the northwest, will unfavorably affect Belg crops.

Figure 3.13. Ethiopia crop condition, October 2016-January 2017

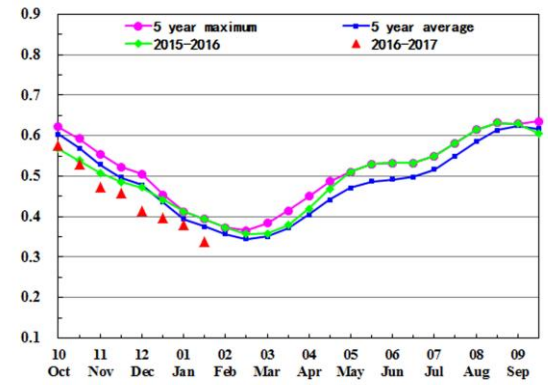

(a) Crop condition development graph based on NDVI

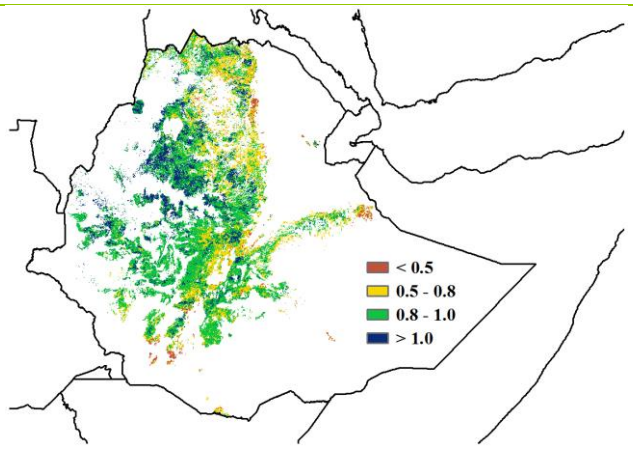

(b) Maximum VCI

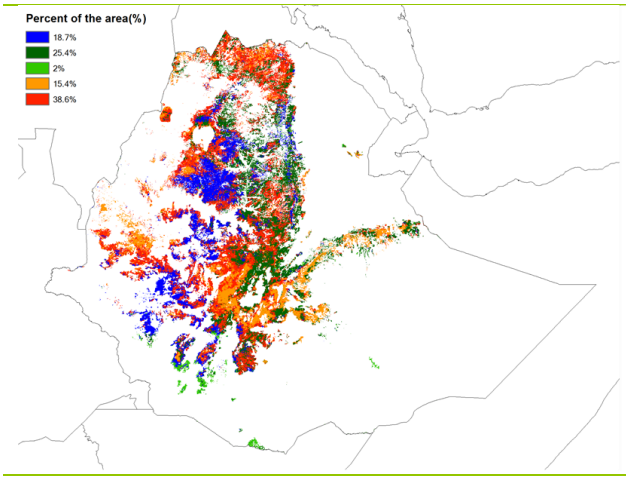

(c) Spatial NDVI patterns compared to 5YA

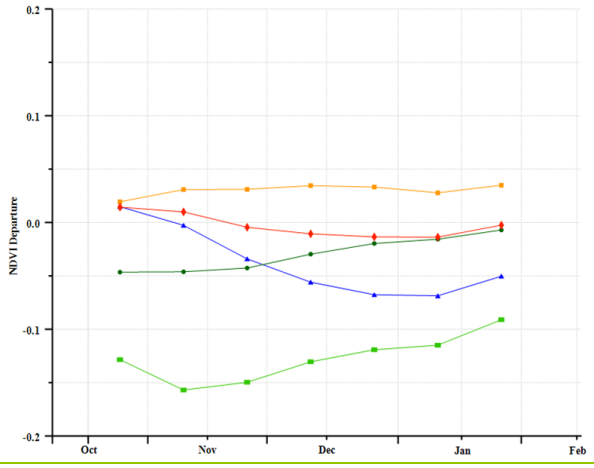

(d) NDVI profiles

[FRA] France

This monitoring period includes the late stages of sugar beets (October harvest) and the early vegetative stages of soft wheat and winter barley (planted in October). At the national scale, the CropWatch RADPAR indicator for radiation was slightly above average (+3%), but rainfall (RAIN) and temperature (TEMP) were 36% and -3.5°C below average, resulting in a biomass production potential (BIOMSS) drop of 35% below the recent five-year average.

As shown by the crop condition development graph, national NDVI values were basically below average during the whole monitoring period due to drier-than-usual and colder-than-usual conditions, consistent with a maximum VCI of 0.73 for France overall. Maximum VCI in the west, southwest, and southeast of France was low compared to other regions. The country's spatial NDVI patterns indicate a situation that on the whole is worse than the five-year average (especially in the northeast of the country (3.9% of the area) after December), with the exception of 2.7% of agricultural areas, which includes the southern Midi-Pyrénées, southeast of Languedoc-Roussillon, northeast of Rhone-Alpes, and northeast of Riviera. Generally, the CropWatch indicators point at unfavorable condition for most winter crop areas of France, especially in the north-east (Bourgogne to Lorraine and Alsace).

Figure 3.14. France crop condition, October 2016-January 2017

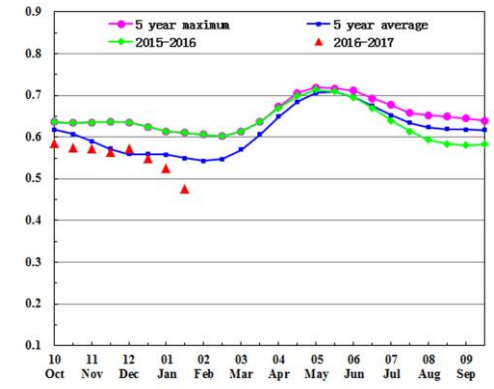

(a) Crop condition development graph based on NDVI

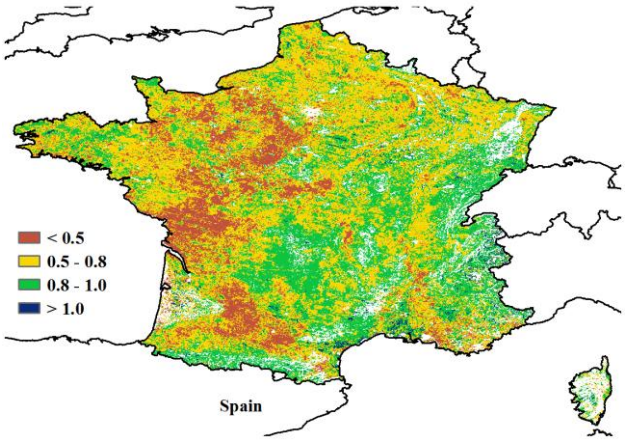

(b) Maximum VCI

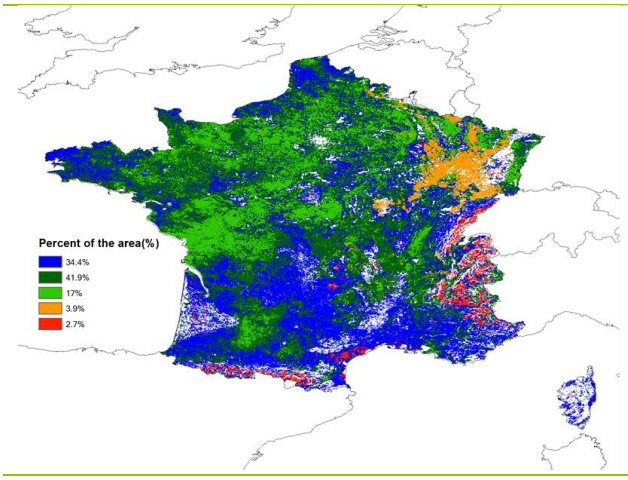

(c) Spatial NDVI patterns compared to 5YA

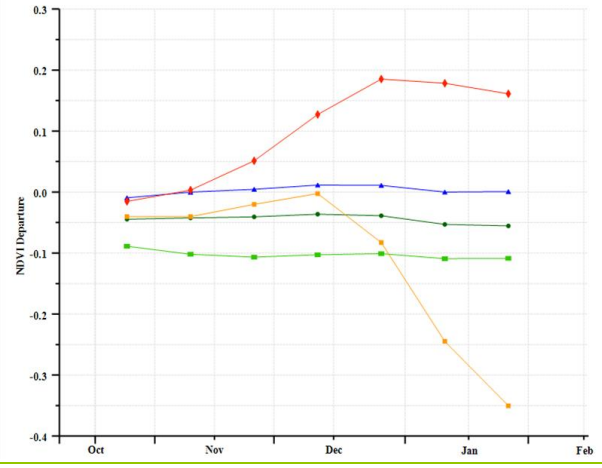

(d) NDVI profiles

[GBR] United Kingdom

Summer crops (sugar beets) in the United Kingdom have been harvested, and winter crops (winter wheat, winter barley, and rapeseed) have been planted. In the monitoring period, negative departures from average were recorded for both agroclimatic and the agronomic indicators. As shown by the NDVI profiles, national NDVI values were lower than average from November to early January, but above to average by late January. According to the crop condition map based on NDVI, close to 62.1% of the country recorded lower than average NDVI from October to January, while for the remainder (37.9% of the region) crop condition was higher than average, including Norfolk, Suffolk, Yorkshire, Durham, Northumberland, Berwickshire, East Lothian, Midlothian, Fife, Kinross-shire, and Perthshire). This spatial pattern is also reflected by the maximum VCI in the different areas, with a VCIx of 0.87 for the country overall. At the national scale, precipitation totals were 31% below average, and temperature (TEMP, -2.3°C) and radiation (RADPAR, -1.2%) were below the average. Prospects for winter crops are currently unfavorable.

Figure 3.15. United Kingdom crop condition, October 2016-January 2017

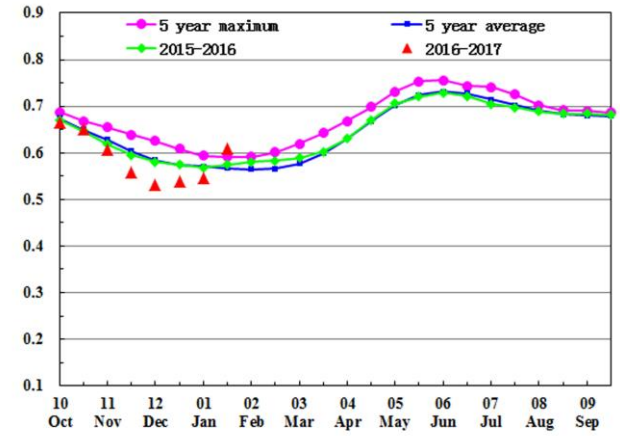

(a) Crop condition development graph based on NDVI

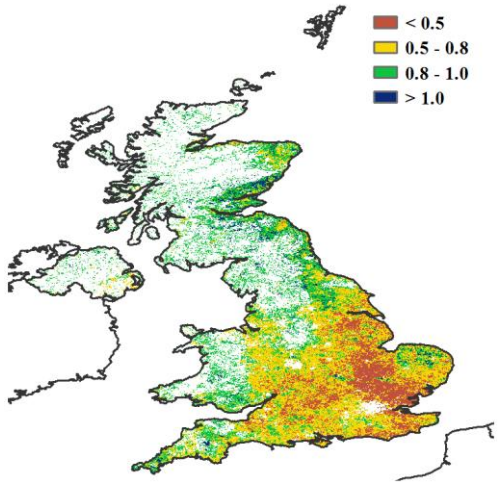

(b) Maximum VCI

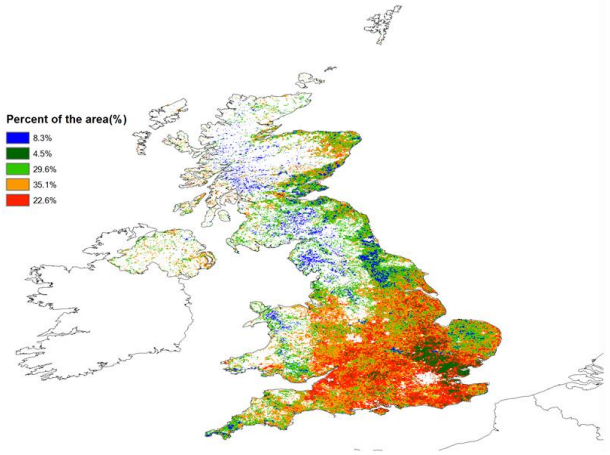

(c) Spatial NDVI patterns compared to 5YA

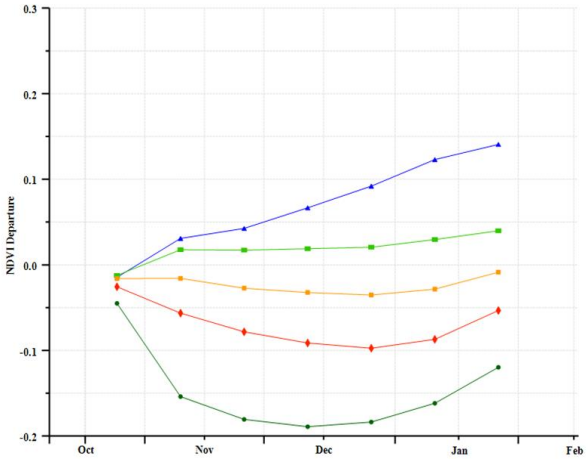

(d) NDVI profiles

[IDN] Indonesia

The crops in Indonesia generally showed poor condition between November and January. The period covers the harvesting stage of the dry season maize and rice, while wet season crops are currently in the field. Compared with the recent average, precipitation was significantly above average (RAIN, +13%), while temperature was below average (TEMP, -0.6°C) with cloudiness causing a significant drop in sunshine (RADPAR, -7%). BIOMSS increased by 6% compared to the recent five-year average. The area of cropped arable land (CALF) was comparable to the five-year average; VCIx was moderate.

Nationwide, the NDVI development curve was below both normal and last year's values from November. In November and December, crops in over 25% of the country were in poor condition, especially on the island of Sumatra. According to the spatial patterns of NDVI profiles, in the southern and eastern part of Kalimantan, rice was below average condition from mid-December to January.

Altogether, although the NDVI profiles showed poor crop growth condition, the abundant rainfall during the reporting period benefited the wet season crops and fair production can be expected.

Figure 3.16. Indonesia crop condition, October 2016-January 2017

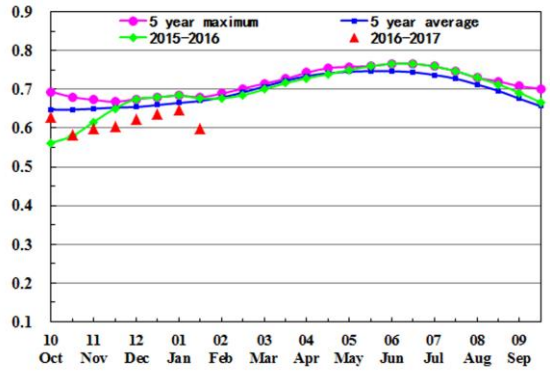

(a) Crop condition development graph based on NDVI

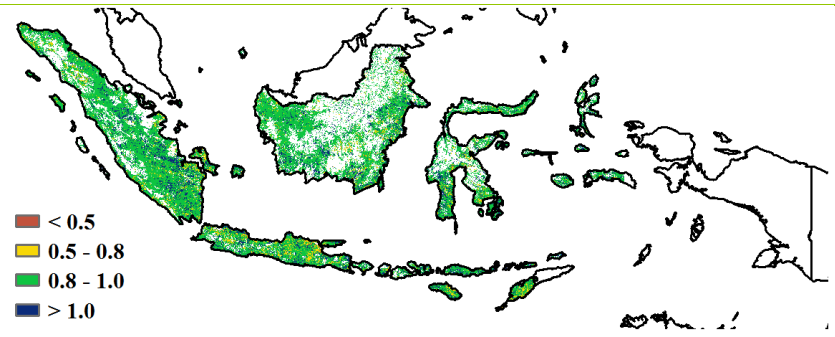

(b) Maximum VCI

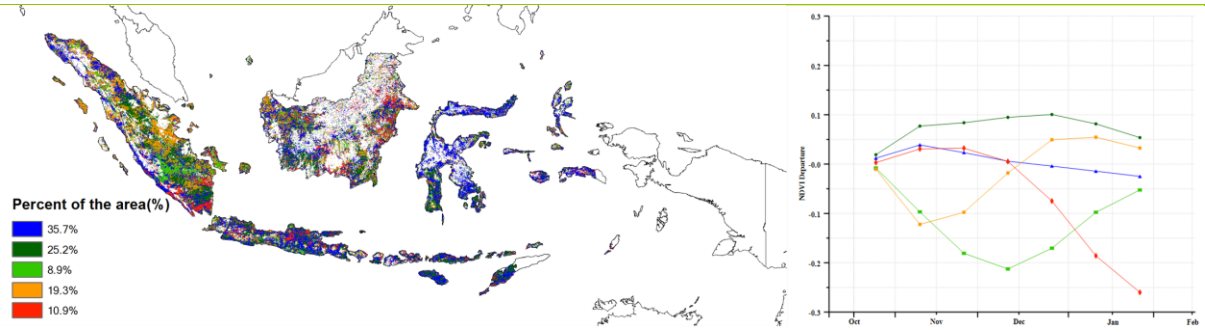

(c) Spatial NDVI patterns compared to 5YA

(d) NDVI profiles

[IND] India

The monitoring period corresponds to the harvest of Kharif crops. The assessed crop condition is poor, and reduced output is expected primarily due to the below average rainfall and decreased area of cultivated land. Noticeably, crops in the south Indian states are in poor condition. During the monitoring period the country experienced 30% less rainfall (RAIN) than expected, including Andhra Pradesh (RAIN, -71%), Assam (-7%), Bihar (-23%), Chhattisgarh (-25%), Goa (-69), Jharkhand (-58%), Kerala (-62%), Karnataka (-74%), Maharashtra (-42%), Madhya Pradesh (-34%), Nagaland (-15%), Odisha (-28%), Tamil Nadu (-60%), and West Bengal (-18%). The national biomass accumulation potential (BIOMSS) is -20% below the previous five-year average and linked to the poor performance of rainfall. All of the mentioned rainfall deficit states experienced low BIOMSS ranging between -17% and -64%. Crop condition development was below average during October to November, but turned average starting in early December. The NDVI values and spatial NDVI patterns were average over the country except in the south Indian regions. Again, the maximum VCI values were below 0.5 in south Indian regions, confirming poor crop condition. The crop arable land fraction (CALF) dropped by -0.56 percentage points compared to the previous five-year average. Temperature (TEMP) was average, while photosynthetically active radiation (RADPAR) was +3% above average. Damage caused by floods in previous months (reported in the November 2016 bulletin) along with the present condition of deficit rainfall altogether result in poor crop condition for the country. Reduced output is expected.

Figure 3.17. India crop condition, October 2016-January 2017

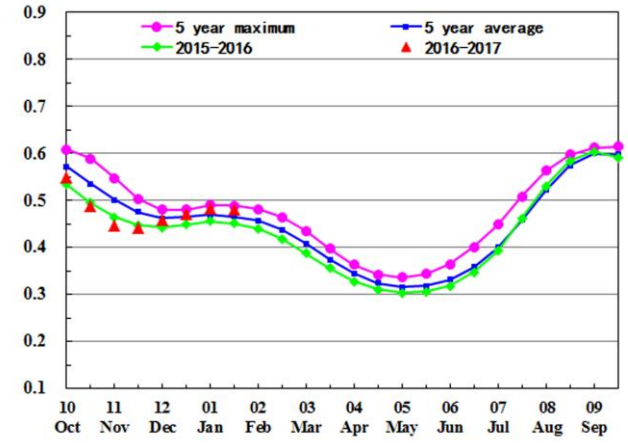

(a) Crop condition development graph based on NDVI

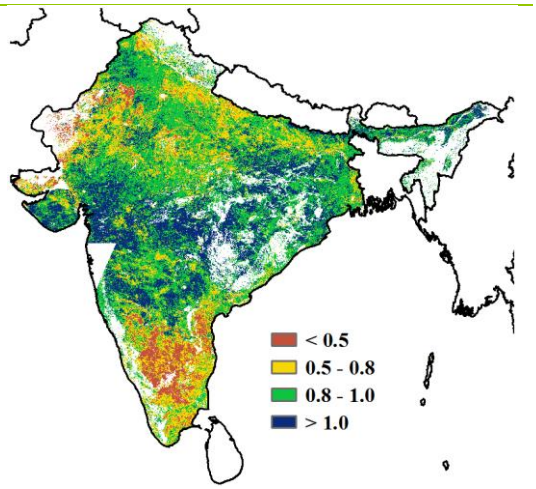

(b) Maximum VCI

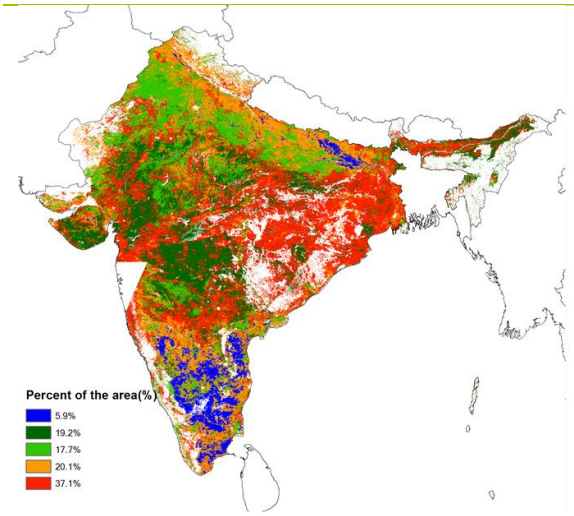

(c) Spatial NDVI patterns compared to 5YA

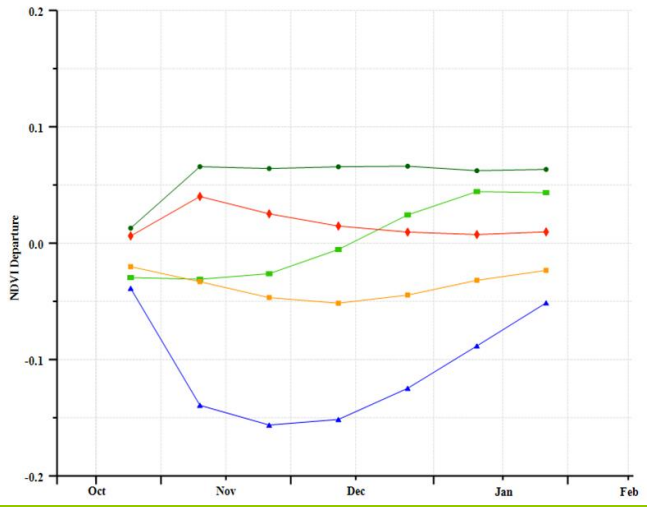

(d) NDVI profiles

[IRN] Iran

Crop condition was generally below average from October 2016 to January 2017 in Iran. The planting of winter wheat has been completed, while it was still underway for barley in late January. Accumulated rainfall (RAIN, -1%) and temperature (TEMP, -0.3°C) were below average during the monitoring period, while radiation (RADPAR, +1%) was close to average. The unfavorable weather conditions resulted in the decrease of the potential biomass indicator (BIOMSS) by 15%. The national average of VCIx (0.42) was below average and rather low for a national value.

According to the national NDVI development graphs, crop condition was below average for the entire monitoring period in most of Iran. Above average crop condition from October to early December was mainly distributed in the Ardabil province of the northwest region. Some areas of Mazandaran and Golestan provinces of the central-north region, and Fars province of the southwest region, experienced favorable crop conditions over the reporting period.

Overall, the outcome for the winter crop season is estimated to be unfavorable.

Figure 3.18. Iran crop condition, October 2016-January 2017

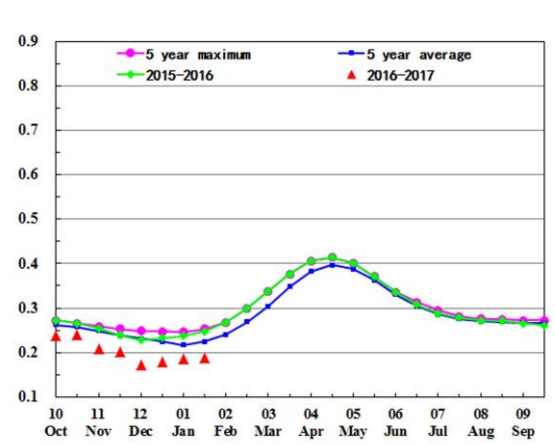

(a) Crop condition development graph based on NDVI

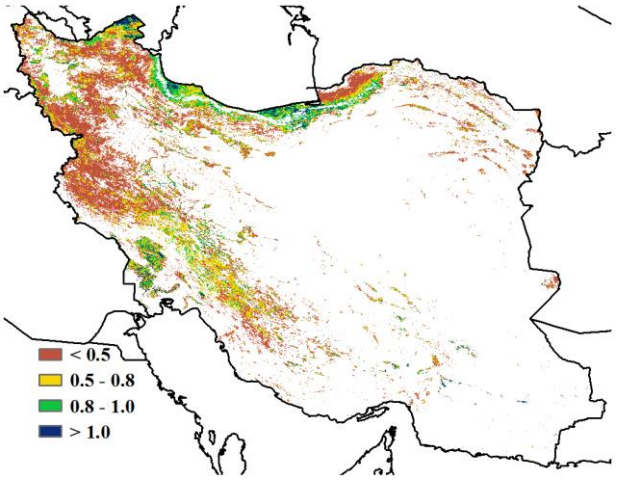

(b) Maximum VCI

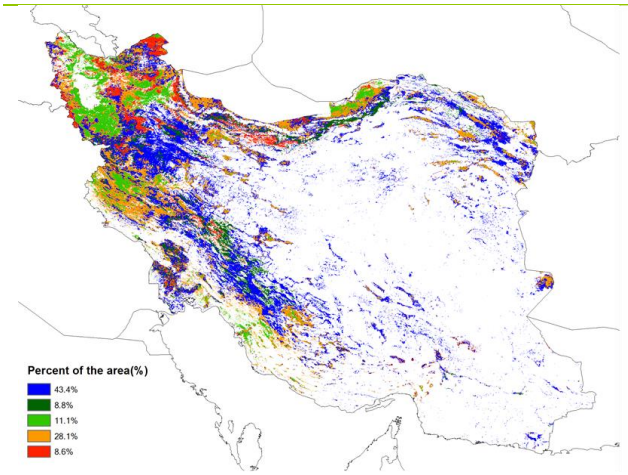

(c) Spatial NDVI patterns compared to 5YA

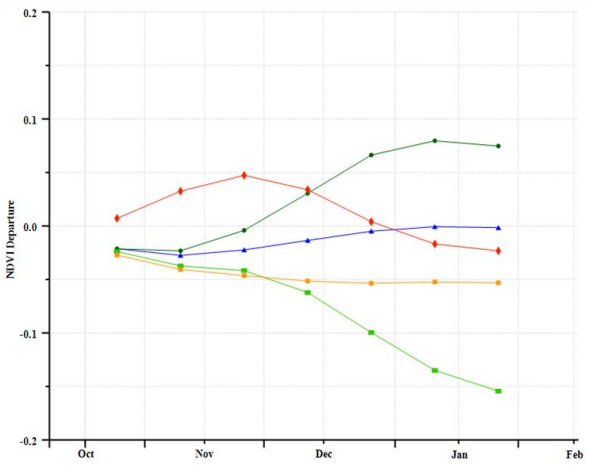

(d) NDVI profiles

[KAZ] Kazakhstan

This analysis covers the harvesting period of last year's summer crops (cereals, spring barley, and wheat) from October 2016 to late January of this year. Among the nationwide CropWatch agroclimatic indicators, compared with average, rainfall showed and increase (RAIN, +40.8%), temperature a decrease (TEMP, -1.3°C), and RADPAR a sharp decrease (RADPAR, -8.4%); the biomass production potential (BIOMSS) is expected to drop by 6.8%. The only region where rainfall decreased (RAIN, -2%) is the northeastern Zapadno-Kazakhstanskaya Oblast. NDVI clusters indicate that crops were in poor condition from October to December in the Oblasts of Severo-Kazakhstanskaya (north Kazakhstan) and Akmolinskaya (central region of Akmola). No crop was planted since November, and from December the NDVI index has been close to zero. The crop condition development graph also showed that crops were worse off than last year and the average of the last five years, but favorable rainfall has provided the appropriate soil moisture for the initial stages of the forthcoming crops.

Figure 3.19. Kazakhstan crop condition, October 2016-January 2017

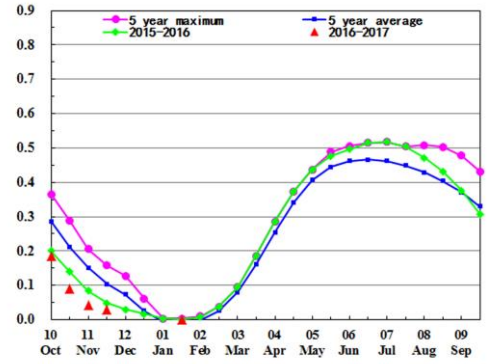

(a) Crop condition development graph based on NDVI

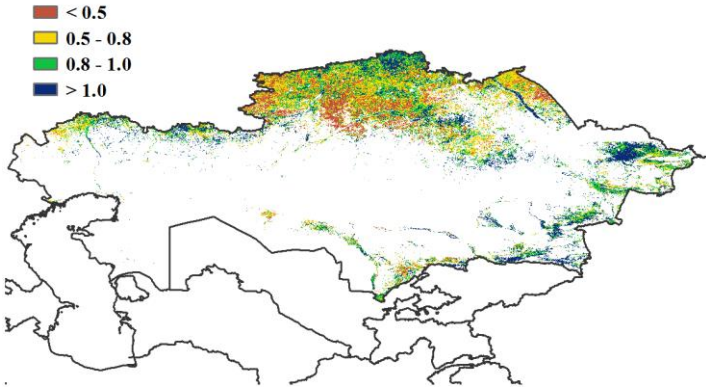

(b) Maximum VCI

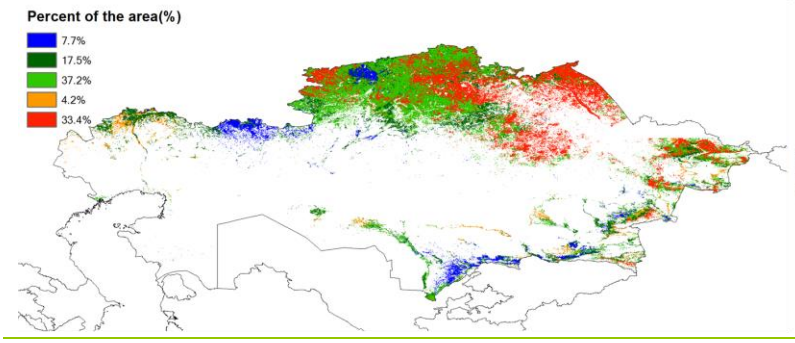

(c) Spatial NDVI patterns compared to 5YA

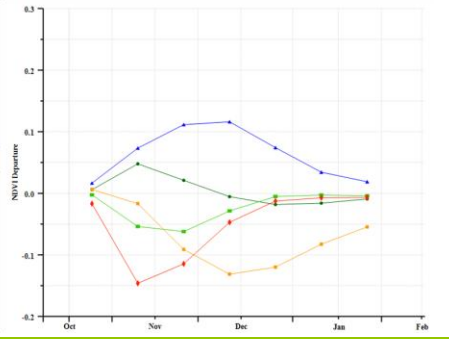

(d) NDVI profiles

[KHM] Cambodia

October to January covers the growing period of the main (wet season) rice crop, and the early stage of the second (dry season) rice in Cambodia. The fraction of cropped arable land was a little lower than the average of the previous five years (-4 percentage points). Compared to average, the CropWatch agroclimatic indicators show a sharp decrease in radiation (RADPAR, -10%) and a slight temperature decrease (TEMP, -0.3°C) with a more than doubling of rainfall (RAIN, +120%), causing a 62% increase in the biomass production potential (BIOMSS).

Favorable conditions resulted in NDVI exceeding the five-year average in over 90 percent of cropland in the country. Sufficient rainfall was beneficial for the sowing and emergence of second rice. Vegetation condition indices (VCIx) are high (>0.8) in most parts of the country. The condition of crops in the country is better than average.

Figure 3.20. Cambodia crop condition, October 2016-January 2017

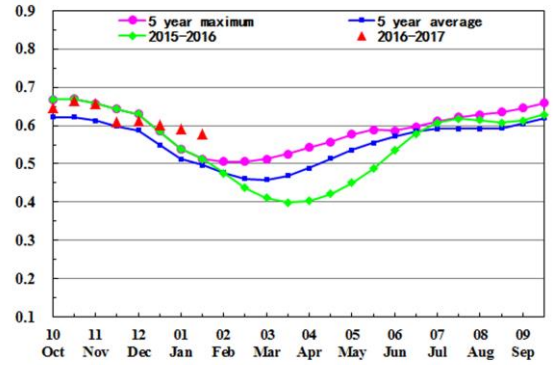

(a) Crop condition development graph based on NDVI

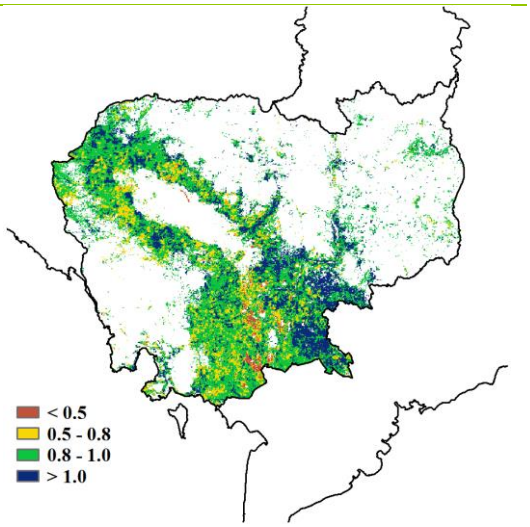

(b) Maximum VCI

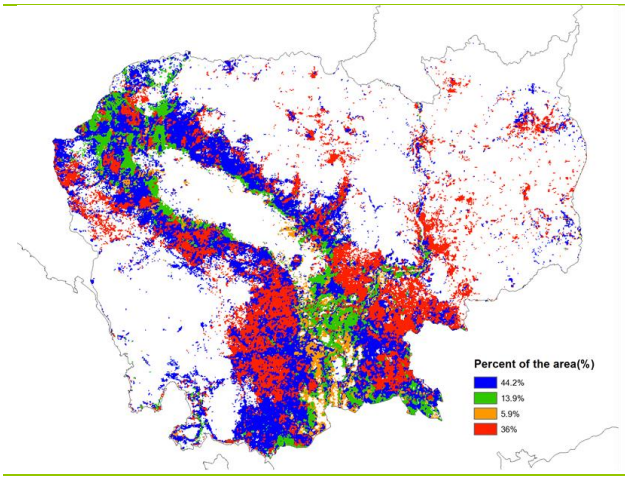

(c) Spatial NDVI patterns compared to 5YA

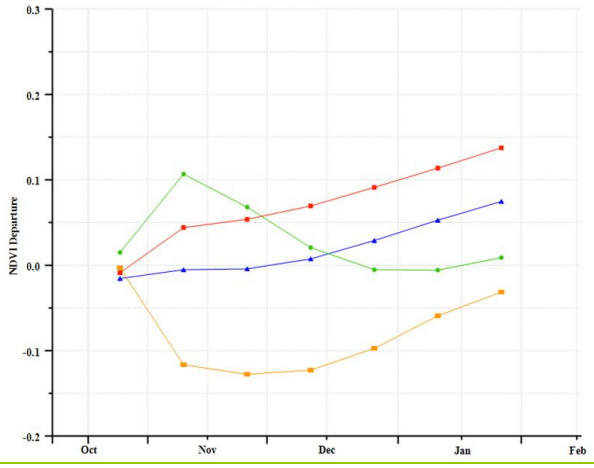

(d) NDVI profiles

[MEX] Mexico

During the monitoring period, maize, sorghum and rice grown during the spring through summer period had been already been harvested, while autumn maize, sorghum and wheat were being planted. Overall, the condition of crops was average, as shown by the national NDVI development graph.

The CropWatch agroclimatic indicators show that rainfall significantly decreased by 24% compared to average, whereas temperature and RADPAR rose respectively by 0.6°C and 1%. Consequently, the biomass production potential (BIOMSS) was below average, with a decrease of 9%. The maximum VCI at the national level was 0.88, with high values being located in Sinaloa, Durango, Nayarit, Zacatecas, Jalisco, and Guerrero, while low values appear in Tamaulipas, Sonora, and Chihuahua. According to the map of spatial NDVI patterns compared to the five-year average and the corresponding NDVI departure profiles, 31% of crop areas in Mexico were continuously below average, mainly situated in Sonora, Sinaloa, Yucatan, Quintana Roo, Oaxaca, and Chiapas. Crops in favorable condition are widely distributed throughout the country: with crops above average in 25.7% of planted areas and average in 43.3% of cropland.

Considering the cropped arable land fraction (CALF) was 8.48 percentage points over average, the crop yields of the current season are estimated to be above average.

Figure 3.21. Mexico crop condition, October 2016-January 2017

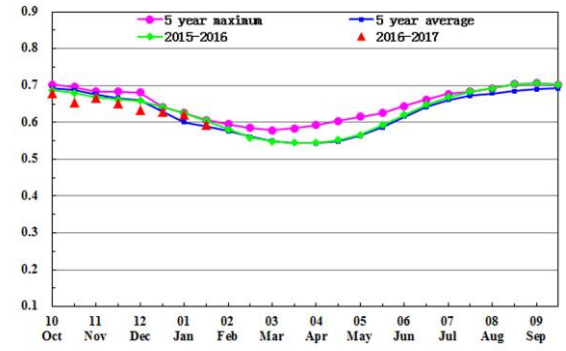

(a) Crop condition development graph based on NDVI

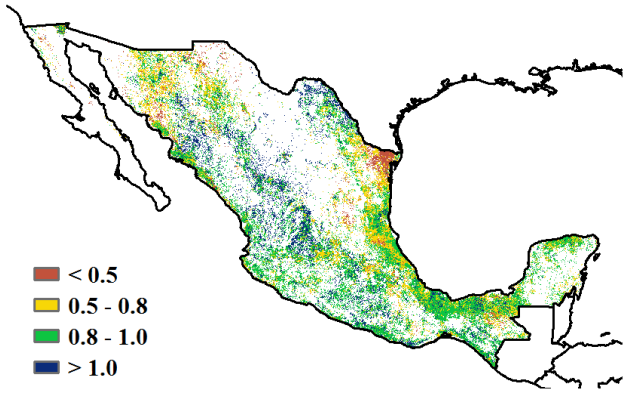

(b) Maximum VCI

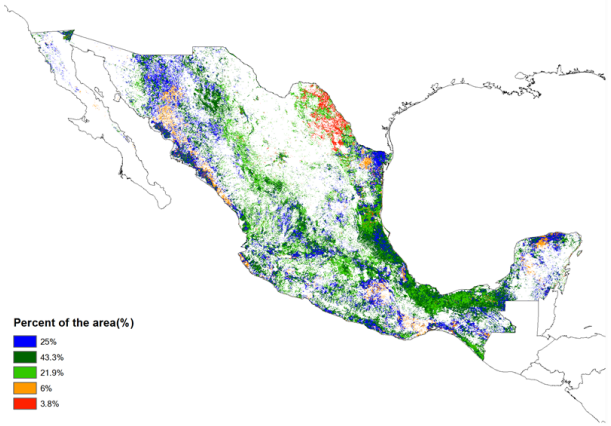

(c) Spatial NDVI patterns compared to 5YA

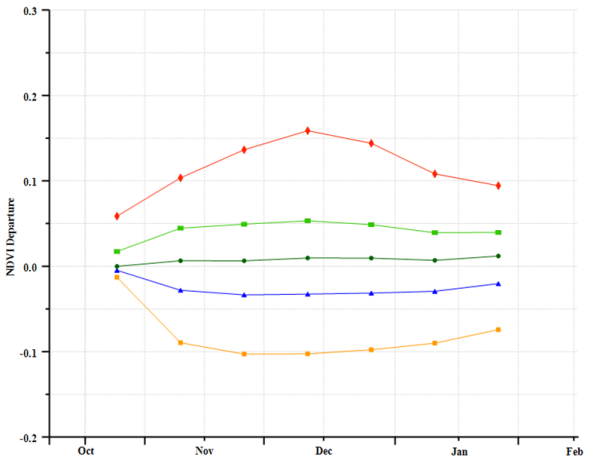

(d) NDVI profiles

[MMR] Myanmar

The reporting period corresponds to the harvesting season of rice and the planting season of maize and wheat in Myanmar. As shown by the CropWatch agro-climatic, rainfall increased by 9%; temperature remained almost average (TEMP, +0.2°C), while radiation showed a slight decrease (RADPAR, -3%). The fraction of cropped arable land (CALF) showed no change and the biomass accumulation potential (BIOMSS) increased by 10% compared to its five-year average value. The indicators suggest that sufficient precipitation promoted crop condition, while the area of cultivated farmland remained average.

National crop condition development profiles were above the five-year maximum and exceeded the previous five-year average during the whole period. The spatial NDVI profile values were below average from October to January in some scattered areas of Yangon, while the rest of the country performed well, which is consistent with the maximum VCI map. According to CropWatch indicators and a high maximum VCI value, overall crop condition in Myanmar is good.

Figure 3.22. Myanmar crop condition, October 2016-January 2017

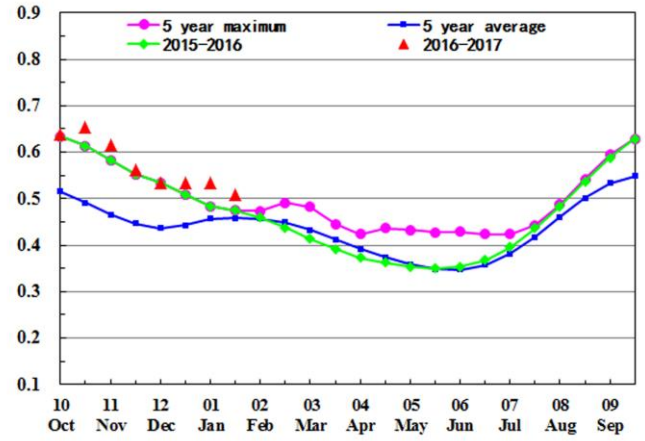

(a) Crop condition development graph based on NDVI

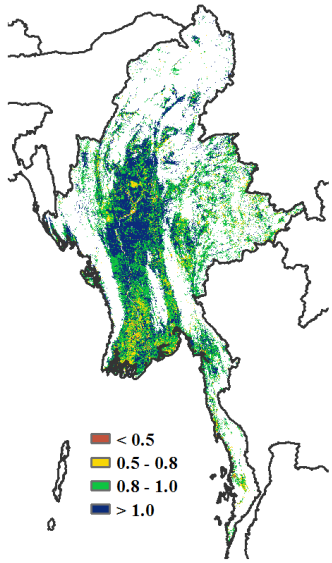

(b) Maximum VCI

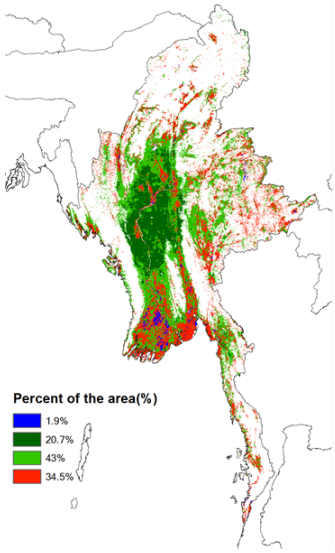

(c) Spatial NDVI patterns compared to 5YA

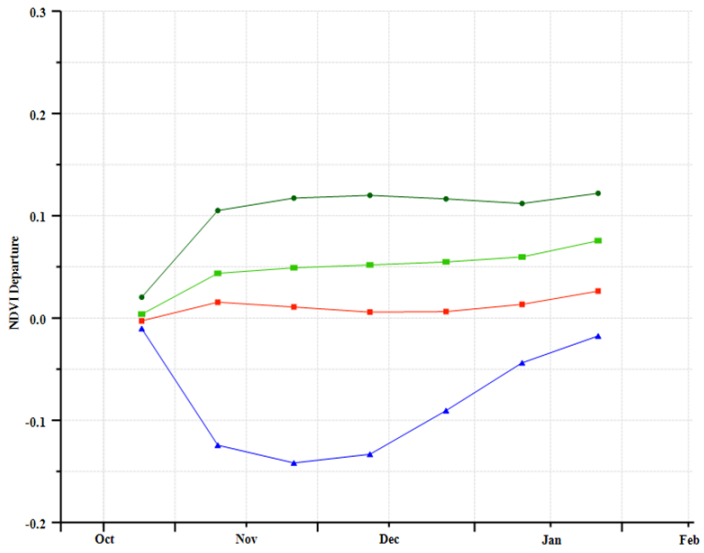

(d) NDVI profiles

[NGA] Nigeria

During the monitoring period, Nigeria has been harvesting the second maize crop, rice, cotton, peanuts, and potatoes, while it was the sowing period for rice (the second crop for the north and south regions). Furthermore, according to the crop calendar, cassava has been planted. Compared to average, the agroclimatic indicators show a slight reduction in precipitation (RAIN, -5%), which results in a reduction of 9% of biomass production potential (BIOMSS). The Soudano-sahelian region experiences the worst rainfall decrease (RAIN, -51%) linked to a 50% decrease in BIOMSS. Temperature and radiation were generally average. Nationwide, an increase occurred in the fraction of cropped arable land (CALF, +2.40 percentage points) compared to the five-year average.

The NDVI development profiles indicate that crop condition generally was less favorable than the five-year average and also less favorable than conditions for the same monitoring period last year (November 2015-January 2016). Maximum VCI reveals a poor crop condition in the Borno region in the north of the country. Better crop condition occurs in a broad strip from Kebbi state in the west to Yobe state in the east, with VCIx values from 0.8 to 1 and values higher than 1. The spatial NDVI patterns and clusters indicate that crop condition was generally above average over the northern region of the country (8.6% of the total agricultural area) and poor in some patches in the southern regions (2.0% of area).

Figure 3.23. Nigeria crop condition, October 2016-January 2017

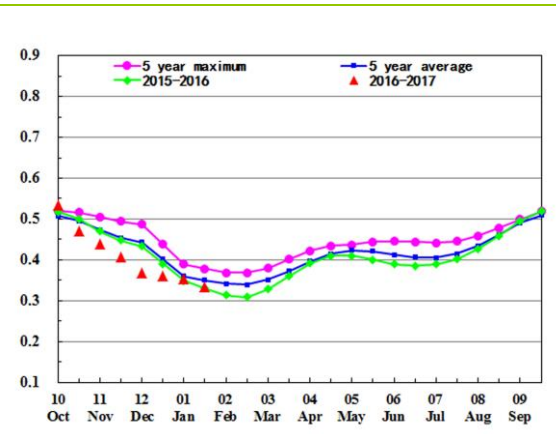

(a) Crop condition development graph based on NDVI

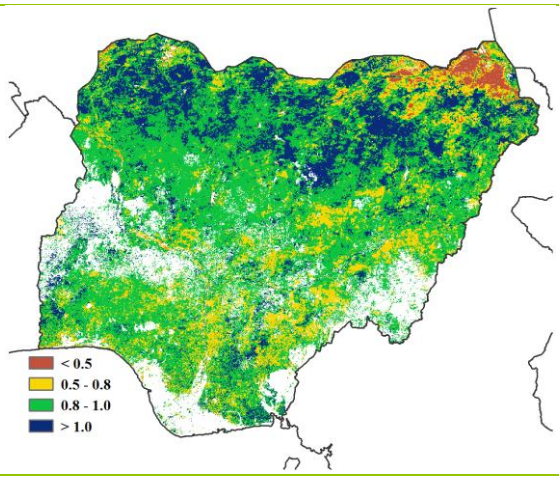

(b) Maximum VCI

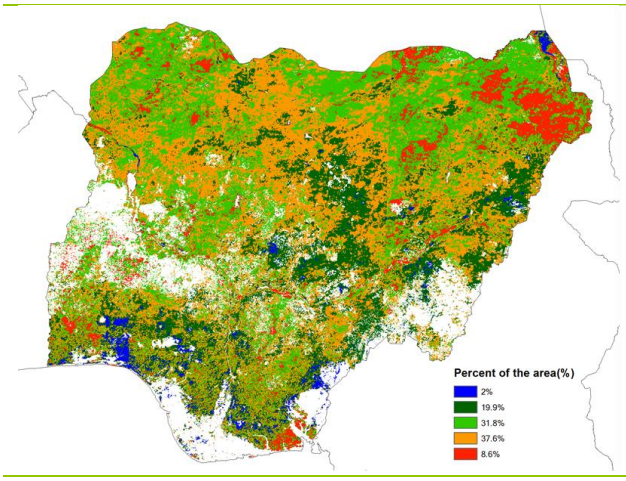

(c) Spatial NDVI patterns compared to 5YA

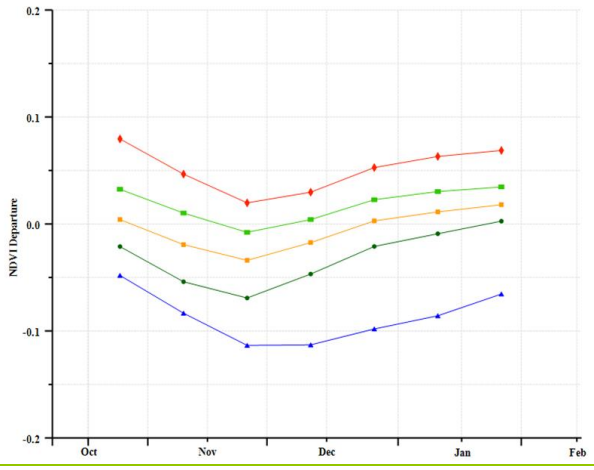

(d) NDVI profiles

[PAK] Pakistan

The main crops in the field during the reporting period are winter wheat and winter barley, as well as maize and some patches of rice nearing maturity. Agroclimatic and agronomic conditions for the reporting period were about average or above: RAIN, +30%; RADPAR, -1%; TEMP, +0.4°C; and CALF, +5%. For the different sub-zones in the country, the most variable factor was rainfall (RAIN), noting: (i) +6% in the northern highlands of FATA and NWFP, with VCIx values mostly below 0.5; (ii) +16% in North Punjab, with VCIx usually above 0.5 and no low values; (iii) +60% in the main irrigated areas of the Lower Indus Basin, where most of the above-average NDVI values and high VCIx occur; and (iv) +127% in Baluchistan where the supplementary water will no doubt boost irrigated crops.

At the national level maximum VCI was 0.82 on average, while the biomass production potential (BIOMSS) increased 20%, with spatial variations from -1% in the northernmost areas, due to above-average temperature (+0.8°C) to 48% in the lower Indus basin. Most positive values are probably exaggerated, as rainfall mostly supplements irrigation in many areas. Even considering that the cropped arable land fraction (CALF) did not change significantly compared with previous years, crop prospects are at least average in Pakistan.

Figure 3.24. Pakistan crop condition, October 2016-January 2017

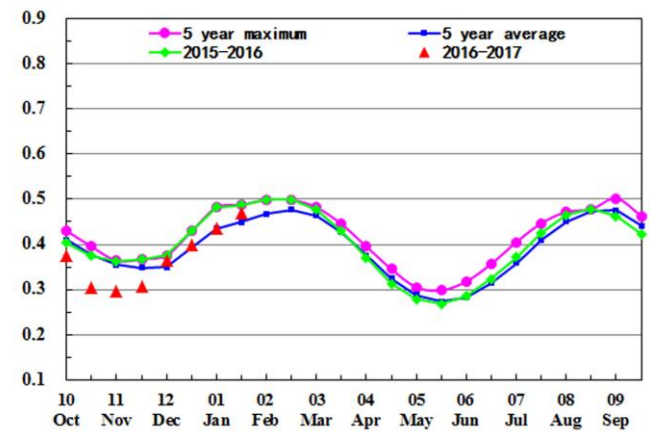

(a) Crop condition development graph based on NDVI

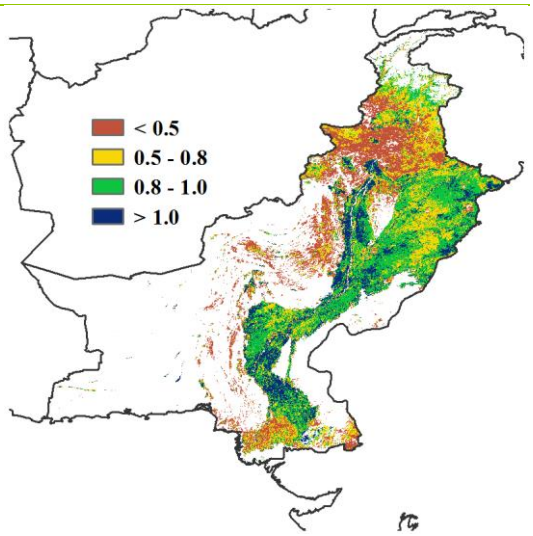

(b) Maximum VCI

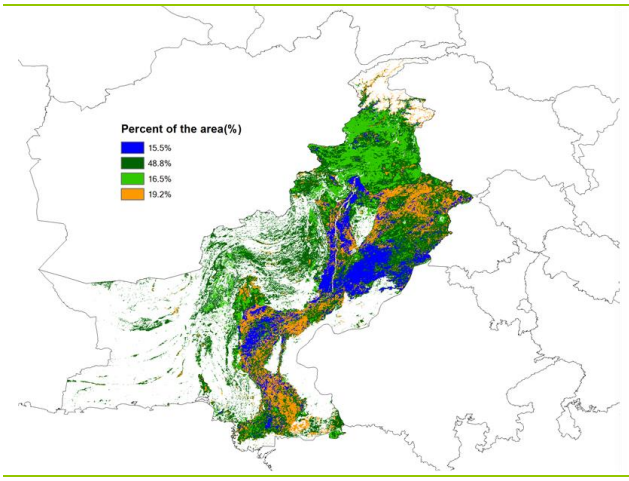

(c) Spatial NDVI patterns compared to 5YA

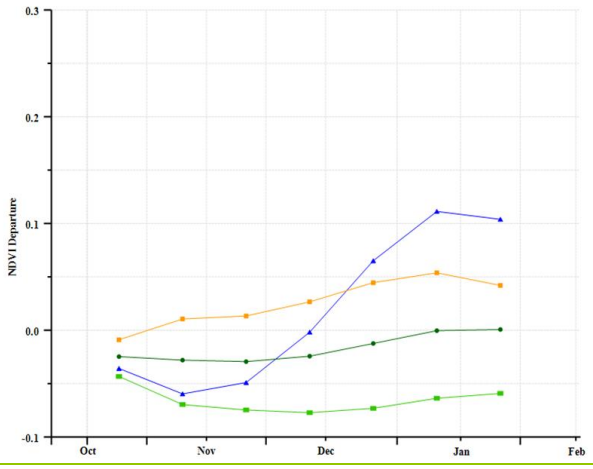

(d) NDVI profiles

[PHL] The Philippines

The monitoring period covers the harvesting stage of last year's main rice, as well as the sowing and growing stage of secondary rice and maize. Nationwide, precipitation (RAIN) presents a positive departure of 50% over average, accompanied by decreased temperature (TEMP, -0.5°C) and below average radiation (RADPAR, -6%). The biomass accumulation potential (BIOMSS) shows an increase of 20%. The fraction of cropped arable land (CALF) for the Philippines is comparable to the five-year average, while the VCIx during the monitoring period is 0.9.

As shown in the NDVI condition development graph, the NDVI curve was below both the five-year average and last year's values from December. In January, storms brought some heavy and short duration rain (see section 5.2 on disasters), causing flash floods in northern Mindanao and the Visayas; secondary rice suffered badly in some areas, which is confirmed in the spatial patterns of NDVI profiles. Crop condition in Calabarzon and Western Visayas (accounting for about 17% of the country's area), dropped below average from January. The adverse weather was subscribed to limited areas and lasted only a short time. As a result, the nationwide output of crops can be expected to be fair.

Figure 3.25. Philippines crop condition, October 2016-January 2017

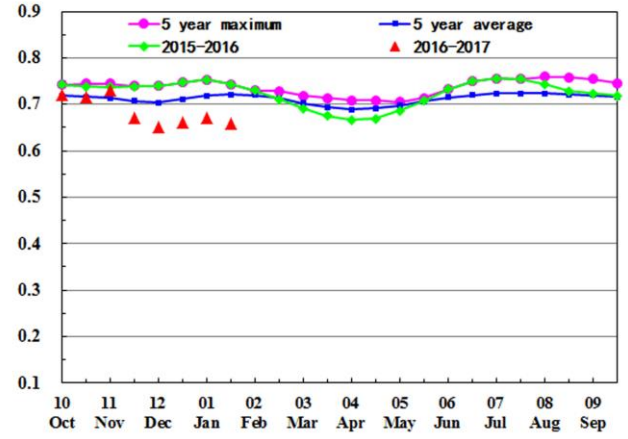

(a) Crop condition development graph based on NDVI

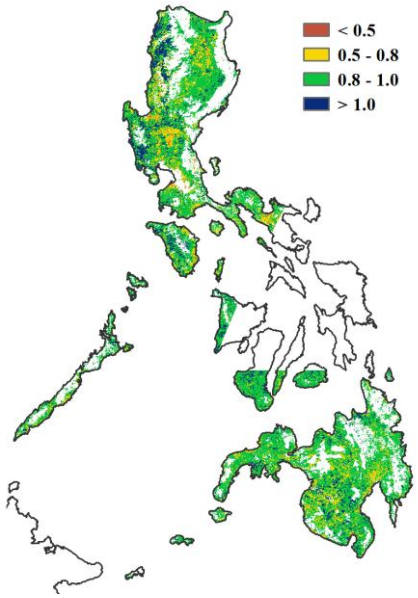

(b) Maximum VCI

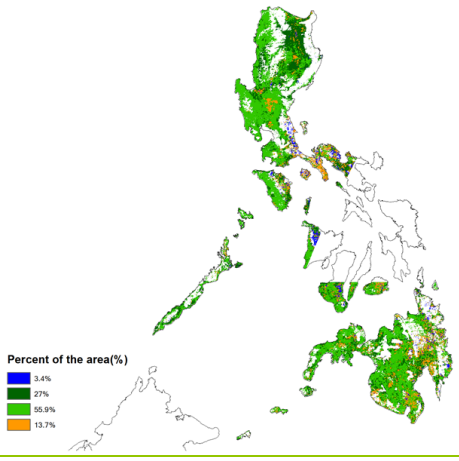

(c) Spatial NDVI patterns compared to 5YA

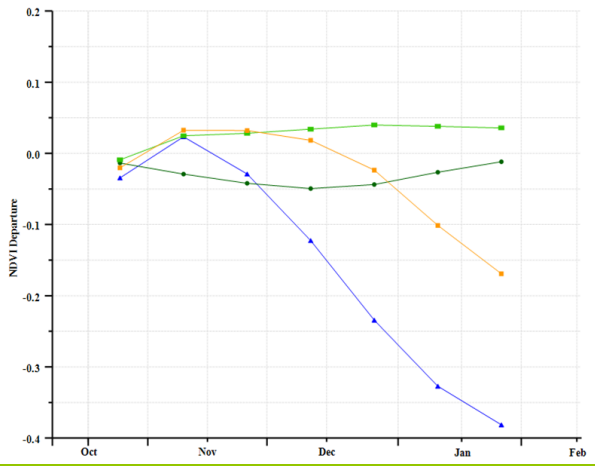

(d) NDVI profiles

[POL] Poland

In Poland, this monitoring period witnessed the harvest of maize (before October) and the sowing of winter wheat. The cropped arable land fraction (CALF) was close to average. From October to January, weather conditions were wetter and colder than average: rainfall departure was +31%, while temperature decreased 1.0°C. RADPAR decreased 14%, and the potential biomass production potential (BIOMSS) was below average due to the cold weather conditions.

As shown in the national crop condition development graph and the NDVI profiles, NDVI values were below average at the end of January in all but 20% of the croplands, which are located in the south around the Lesser Poland Voivedeship, the area with the warmest climate in Poland (Malopolske, Slaskie, and Opolskie). It is not clear to what extent this is due to snow, which covered the country from January 5 on forward: NDVI started dropping in November, when there was limited and only transient snow cover.

The VCIx in Poland during this monitoring period was 0.88. The snow has probably protected crops from cold weather and will provide enough soil moisture. The outlook of winter crops is mixed to average.

Figure 3.26. Poland crop condition, October 2016-January 2017

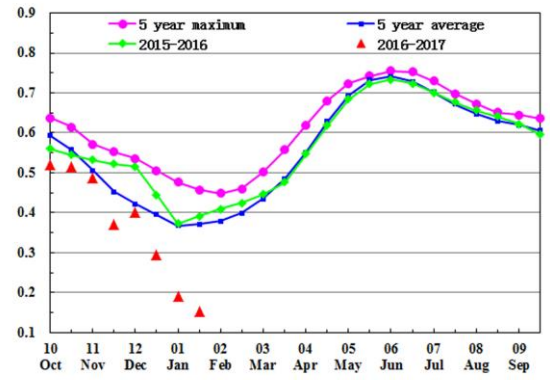

(a) Crop condition development graph based on NDVI

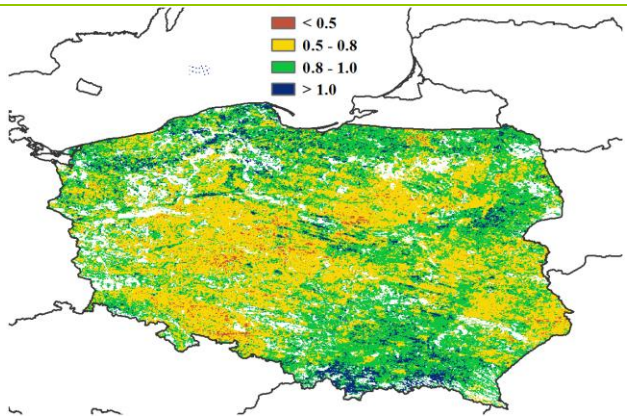

(b) Maximum VCI

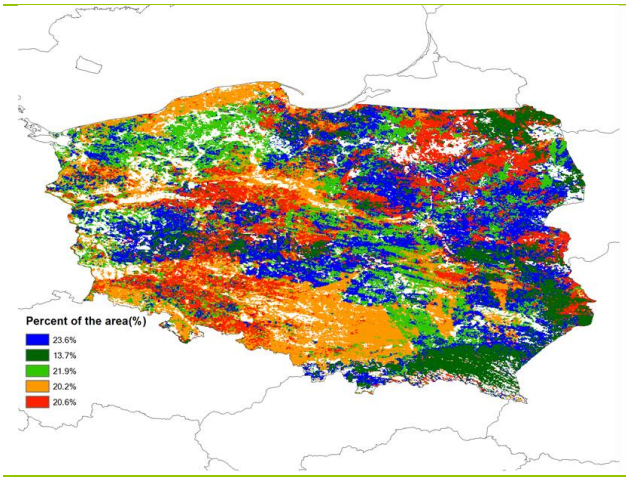

(c) Spatial NDVI patterns compared to 5YA

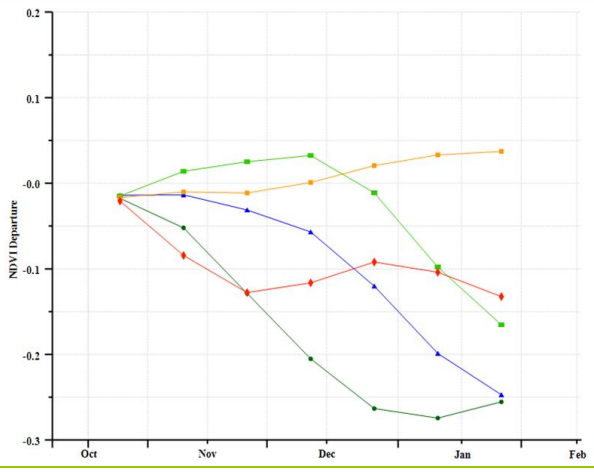

(d) NDVI profiles

[ROU] Romania

Over the reporting period, the main crops in Romania are maize (harvested in 2016) and early stages of winter wheat. Nationwide, rainfall exceeded average by 11% and CALF increased 2.19%, with other indicators mostly below average (RADPAR, -6%; TEMP, -2.2°C; and maximum VCI, 0.73, with a lot of spatial variability). The spatial distribution of NDVI profiles clearly shows the effect of snow that typically depresses NDVI: Early snow was sporadically recorded over the Transylvanian plateau (and the neighboring highlands) from mid-November, in an area that makes up about 16.5% of arable land and where NDVI decreased throughout the reporting period. This is, nevertheless, the area where most high VCIx values are concentrated.

Snow eventually spread to the northern half of the country in December, which is when NDVI started dropping in the eastern Danube valley and the Delta (12.2% of arable lands). The Delta is also where most low VCIx values occur. From early January, the whole country was covered with snow, up until the end of the month and beyond. Most areas retained about average NDVI (53.5% of the territory), with moderate negative anomalies in the area west of Carpathians, as well as the Getic plateau in the west and the Budjak steppe in the east. Moderate positive departures, which varied during the season between 0 and 0.1 NDVI units, occur in 17.9% of the country, mostly concentrated between the eastern Carpathian and the Moldavian border.

Due to the presence of snow, the interpretation of NDVI can be problematic. However, considering that temperature was not excessively low and that crops were protected by snow, there is no specific reason to consider that crops will not be fair.

Figure 3.27. Romania crop condition, October 2016-January 2017

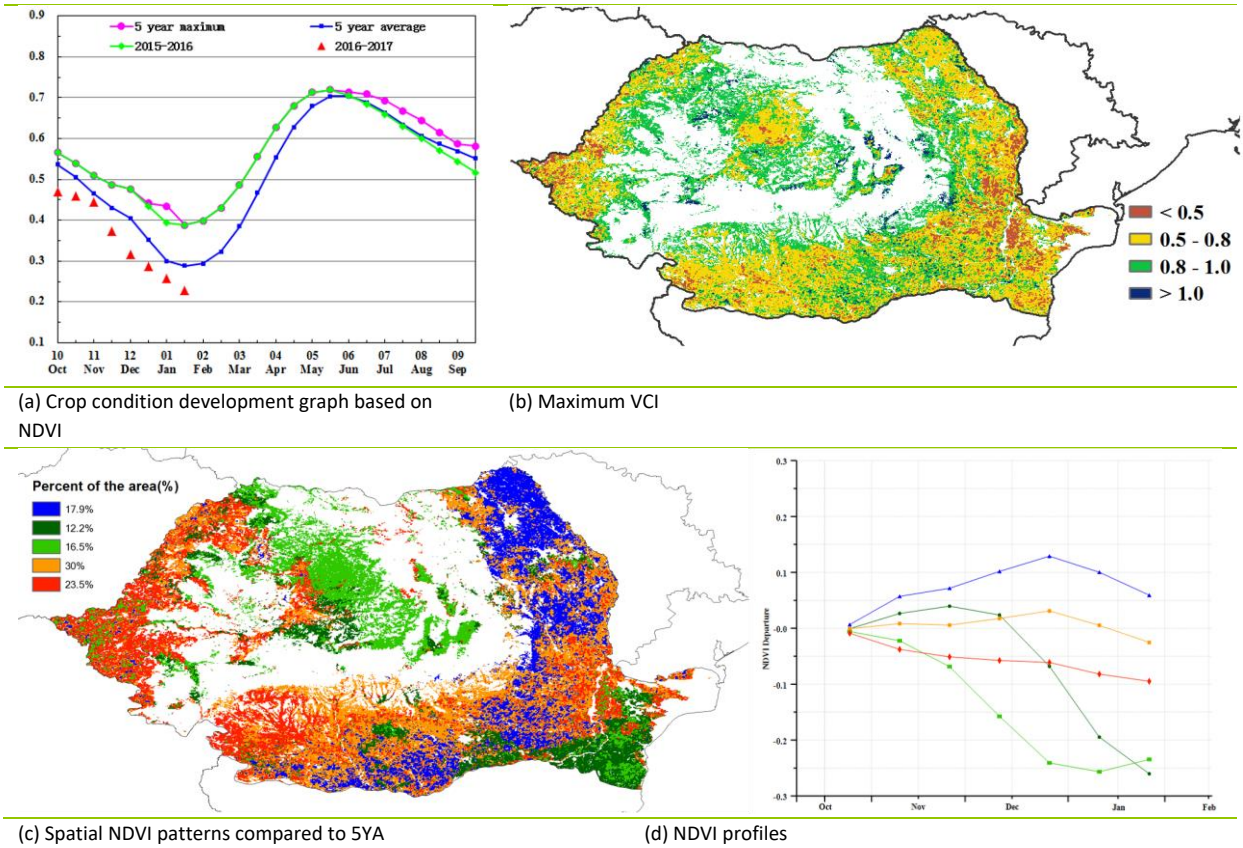

(a) Crop condition development graph based on NDVI

(b) Maximum VCI

(c) Spatial NDVI patterns compared to 5YA

(d) NDVI profiles

[RUS] Russia

During the monitoring period, the sowing of winter wheat was delayed but nevertheless completed before November, while maize and spring wheat were harvested up to October. Cropped arable land (CALF) increased by a spectacular 16 percentage points compared to the five-year average. Like parts of the Central Europe to Western Russia MPZ, the weather in Russia was colder than average. Rainfall was average (RAIN, -0.7%), but temperature decreased 1.8°C below seasonal values. The biomass production potential indicator (BIOMSS) also decreased 18.3% due to the poor weather condition. Specifically, in Kostromskaya oblast, rainfall and temperature were well below average (RAIN, -21% and TEMP, -2.0°C). The largest precipitation deficit and the largest negative temperature anomaly occurred in the Komi-Permyak okrug (-32% and -3.5°C).

NDVI is normally low during the Russian winter (0.05 in January, see NDVI development graph) due to the snow. This year, however, NDVI was even below average as snow started early. The whole country, with the exception of the western Caspian area (the least continental part of Russia), was snow covered from mid-November until even the western Caspian was affected starting in early January. At the time of reporting, the western Caspian is the only area with below average NDVI (11.3% of croplands), while remaining areas recovered from about 0.2 units below average. As shown in the spatial NDVI cluster pattern graph, NDVI was slightly above average in November in the Volga Federal District, while in parts of the Ural and Siberia NDVI is close to average. In the Caucasus Federal District and Southern Federal District, NDVI is below average.

The VCIx in Russia during this monitoring period was 0.87. The outlook for Russian winter crops remains average to above average.

Figure 3.28. Russia crop condition, October 2016-January 2017

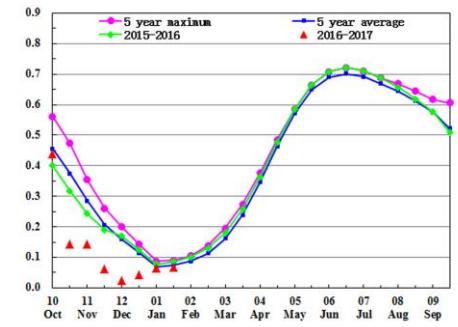

(a) Crop condition development graph based on NDVI

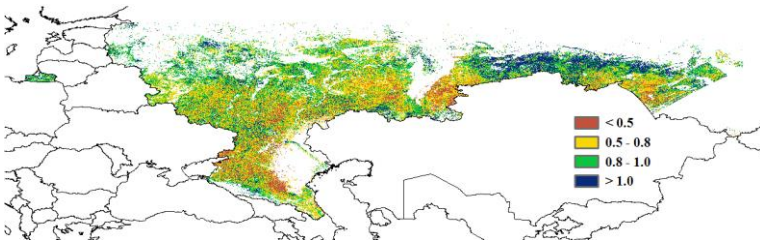

(b) Maximum VCI

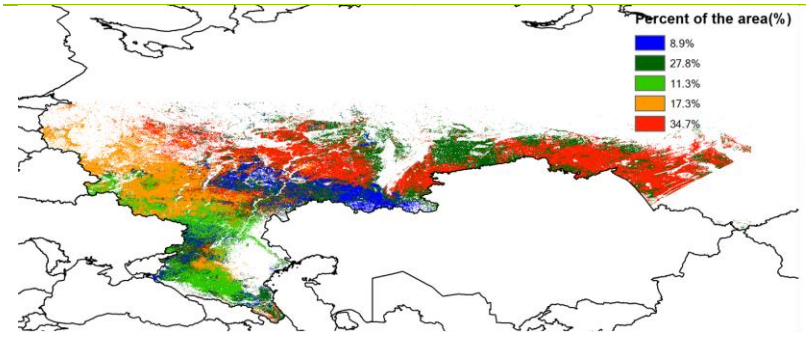

(c) Spatial NDVI patterns compared to 5YA

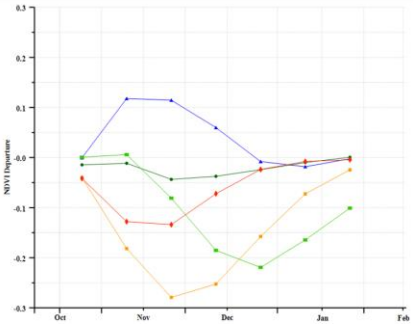

(d) NDVI profiles

[THA] Thailand

During the monitoring period, the harvest of the main rice crop in Thailand was completed, while the planting of the second rice crop started in early January. According to CropWatch indicators, radiation was below average (RADPAR, -7%) and temperature was just average, while rainfall (RAIN, +82%) was significantly above the seasonal norm. On the national level, crop condition was above average, which is confirmed by an increase of BIOMSS by 38%. Similar to the agroclimatic indicators for the national level, RAIN and BIOMSS in the single as well as double and triple-cropped rice, horticulture, and mountain areas are above average, while radiation was below average.

Nationwide, from October to December, crop condition was close to the five-year average, while in January—according to NDVI—condition was above. As shown by the NDVI profiles, more than half the crop areas (blue and bright green) in Thailand (areas located in the northeast, center, west and east) experienced above average condition. Other areas, accounting for 28.4% of the total agricultural land and located mostly in the northeast, began with below average condition, which subsequently improved to above average crop condition in January. At the end of January, crop condition was below average (and thus unfavorable) in only 3.5% of croplands, situated mostly in the center-west, centered around Chainat, and in the south, in East Surat Thani and Nakhon Si Thammarat. Overall, crop condition in Thailand is favorable.

Figure 3.29. Thailand crop condition, October 2016-January 2017

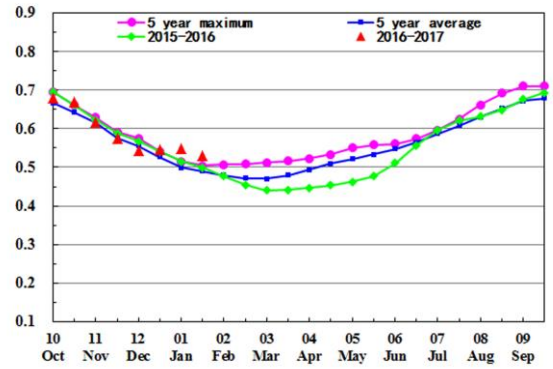

(a) Crop condition development graph based on NDVI

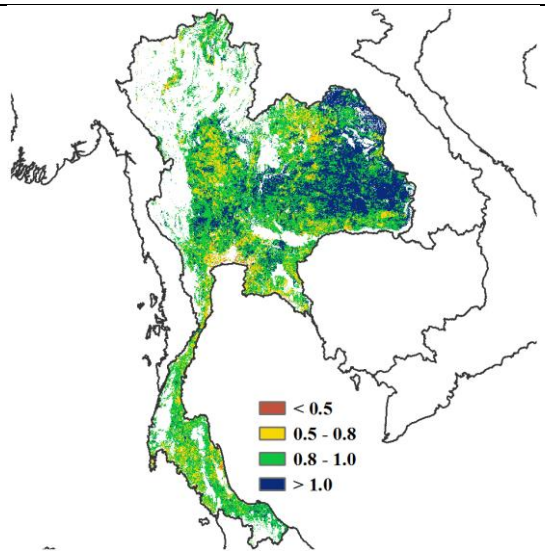

(b) Maximum VCI

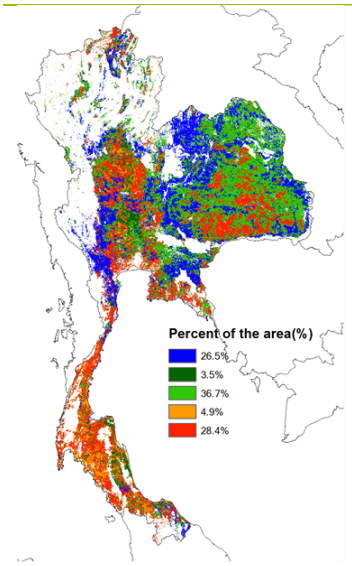

(c) Spatial NDVI patterns compared to 5YA

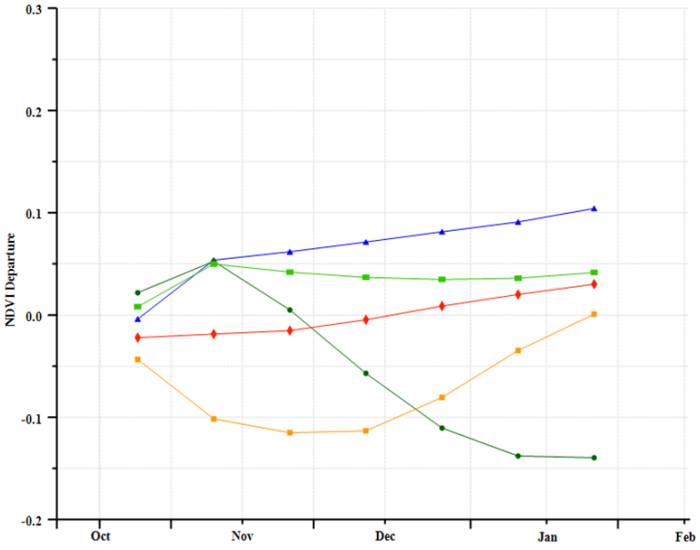

(d) NDVI profiles

[TUR] Turkey

Crop condition was generally below average in Turkey over the reporting period, during which the planting of winter grains was completed. Accumulated rainfall (RAIN, -15%) and temperature (TEMP, -1.3°C) were below average, while radiation (RADPAR, +2%) was above. The agroclimatic indices concur to indicate unfavorable conditions for crop growth, which is confirmed by the decrease of the biomass production potential (BIOMSS) by 16%. Compared to the five-year average, the national maximum VCI (VCIx=0.55) was average. The significant decrease in the fraction of cropped arable land (CALF, -20 percentage points) indicates low land utilization for winter crops.

According to the NDVI profiles, crop condition in Turkey was below average during the whole monitoring period. Compared to the recent five-year average, for three regions—the Central Anatolia, Black Sea, and Marmara regions—the NDVI departure value was below 0.2 from December 2016 to January 2017. This could, however, be largely attributed to the rainfall deficit and precipitation of mostly snow in the three regions, with BIOMSS decreases in the three regions of 31%, 15%, and 16%, respectively. The snow, however, will greatly improve soil moisture and benefit crop growth after the winter period.

Overall, the crop condition of winter crops for this season seems unfavorable due to the continual rainfall deficit from the last monitoring period, but the interpretation of the NDVI-based indicators is difficult due to snow. The final outcome of the season will be largely determined by the change in CALF and soil moisture from March to May.

Figure 3.30. Turkey crop condition, October 2016-January 2017

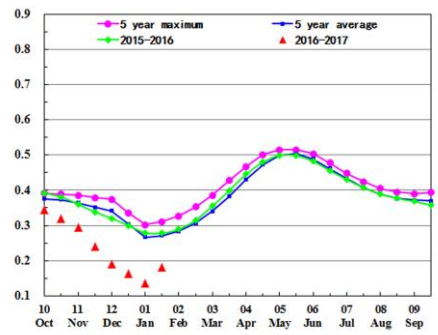

(a) Crop condition development graph based on NDVI

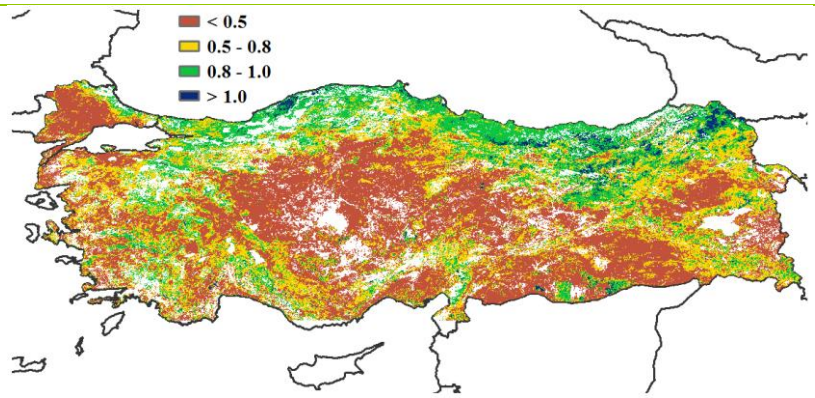

(b) Maximum VCI

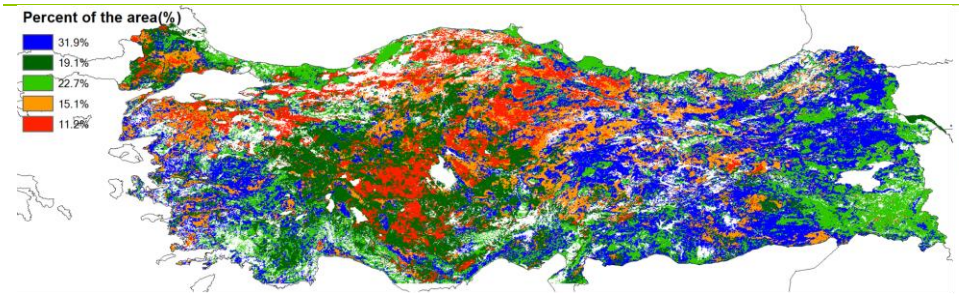

(c) Spatial NDVI patterns compared to 5YA

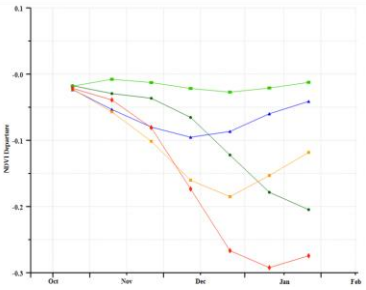

(d) NDVI profiles

[UKR] Ukraine

From October to January in Ukraine, the main crops in the field are maize, ready for harvest in October, and winter cereals in their early stages. On a national level, agroclimatic and agronomic conditions other than RAIN were below average over the reporting period (RAIN, +33.0%; RADPAR, -7%; TEMP, -1.7°C, CALF, -11.74 percentage points; and maximum VCI, 0.67). As illustrated in the section on the Central Europe to Western Russia MPZ (chapter 2.7), the increase in biomass production potential is large (BIOMSS >20%) in the southern part of the country. A major decrease in BIOMSS (up to 20%), however, is observed in the northern, eastern, and western parts of Ukraine, along the borders of Russia, Belarus, Poland, and Slovakia.

The NDVI departure trends show that over the reporting period, 17% of the country's agricultural land undergoes a decline in NDVI from October to December, with an increase starting after that. Another 58.9% show a decline from October to mid-December, and also an increase after. For another 9.7% of the country, the initial decrease in NDVI only happened up to mid-November, again followed by an increase. Finally, 14.4% of cropland experienced stable NDVI from October to mid-November, with also an increase after that. Maximum VCI varies widely over the reporting period. What looks like unfavorable crop conditions at the national level (BIOMSS down 4%) is misleading: the country experienced early snow from the end of October, followed by a short lasting snow cover in November and almost permanent and nationwide presence of snow throughout December and January. The snow cover accounts for low NDVI and, considering also abundant water supply in the form of rain and snow, it is likely that the crop prospects in Ukraine are at least average at the time of reporting.

Figure 3.31. Ukraine crop condition, October 2016-January 2017

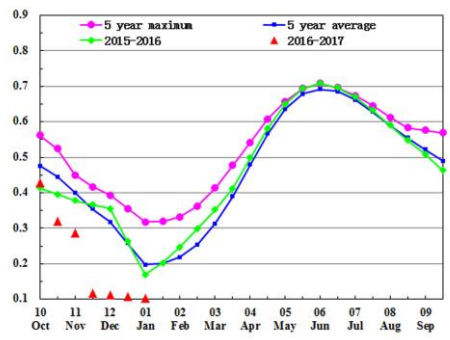

(a) Crop condition development graph based on NDVI

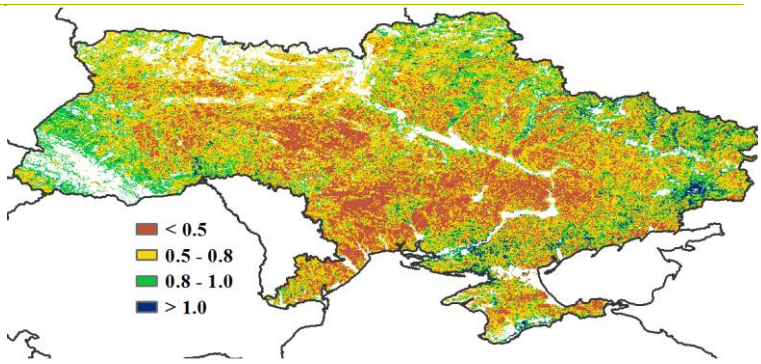

(b) Maximum VCI

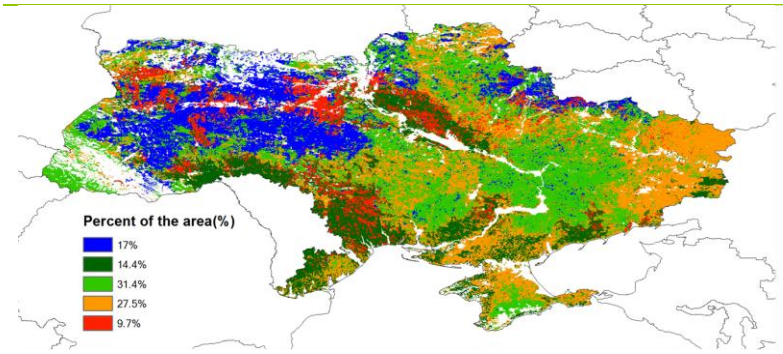

(c) Spatial NDVI patterns compared to 5YA

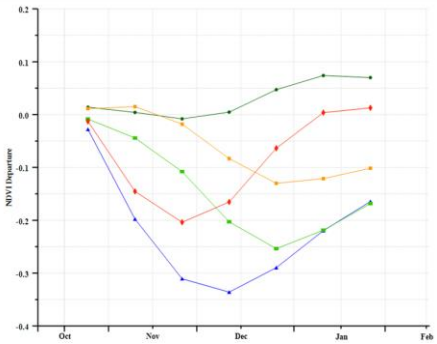

(d) NDVI profiles

[USA] United States

This monitoring period covers the planting and early growth of winter crops. The national NDVI development profile illustrates initially below average crop condition, which then grows closer to average in January. With 317 mm of rainfall, rainfall was 5% above average, temperature (6.7°C) was above average as well (+1.1°C), while radiation (RADPAR) was 3% below.

The Great Plains, Northwest, and lower Mississippi are the main winter wheat areas for the country. Among these, the lower Mississippi area experienced dry and warm weather in the important winter wheat production states of Arkansas (RAIN, -20% and TEMP, +1.6°C), Missouri and Louisiana (both -14% for rain but TEMP at +1.4°C and 1.8°C, respectively), and Mississippi (RAIN, -6% and TEMP +2.1°C). This resulted in unfavorable crop condition that is supported by low VCIx values and negative NDVI departure profiles. On the contrary, abundant rainfall was recorded in states of the Great Plains and Northwest, including Kansas (RAIN, +11%), South Dakota (+86%), Montana (+115%), Washington (+13%), Oregon (+22%), and California (+45%), which provides a needed soil water supply for winter wheat growth. The northwest and western states suffered from ice storms in December and January, including Washington (TEMP, -0.9°C), Oregon (-1.1°C), Idaho (-2.9°C), and California (-0.2°C). Above average rainfall also benefited the growth of winter wheat in the Great Plains; this is supported by positive NDVI anomalies in Kansas, South Dakota, and California. The cold wave in northwest states is well illustrated by the negative NDVI departures after December.

The warm and wet condition in winter wheat areas resulted in an increase of the fraction of cropped arable land (CALF) by as much as 10.15 percentage points compared with the five-year average. Crop condition in the United States is currently average, while conditions in the lower Mississippi area need continued close monitoring.

Figure 3.32. United States crop condition, October 2016-January 2017

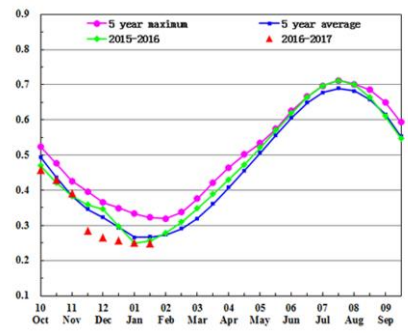

(a) Crop condition development graph based on NDVI

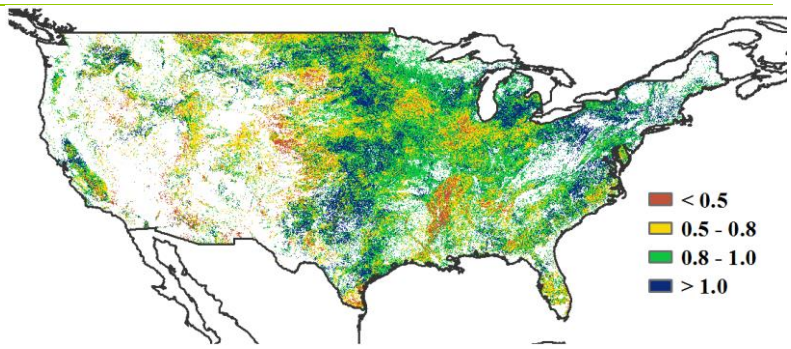

(b) Maximum VCI

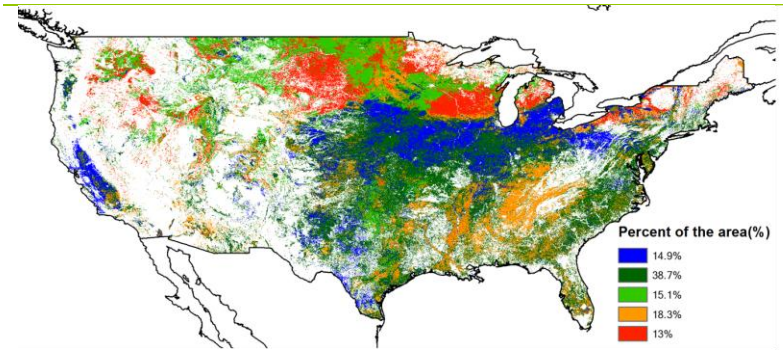

(c) Spatial NDVI patterns compared to 5YA

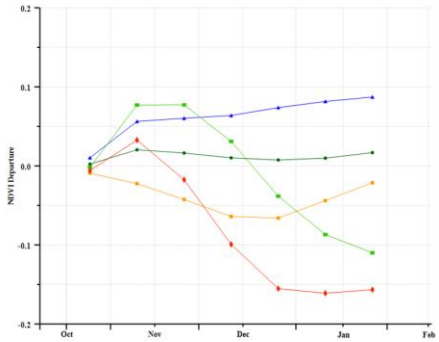

(d) NDVI profiles

[UZB] Uzbekistan

The reporting period covers the sowing and early growing stages of winter barley as well as wheat, the most important cereal crop in Uzbekistan. Crop condition was generally below average, but returned to normal in January. The national average VCIx was 0.84, and the arable land fraction (CALF) increased by 19.8 percentage points compared to the five-year average. Among the CropWatch agroclimatic indicators, RAIN was very significantly above average (almost double), and TEMP and RADPAR were below average by -0.8°C and 2% respectively. This combination of factors results in a high increase in biomass potential (BIOMSS, +51%) compared to the five-year average. At the end of January, NDVI was below average in 20% of croplands, mainly in parts of Qunghirot, Altynkul, Chimbay, and Takhtakupyr provinces, as well as part of Bukhoro and Gazli provinces. NDVI was below average in parts of Quqon, Farghoma, and Namangan. Conditions were normal or above average in other regions, especially in parts of Almalyk, Angren, Samargand, Qarshi, Andijon, Namangan, and Termiz, which make up about 80% of croplands. Altogether, CropWatch assessment is that the current crop prospects for the country are optimistic.

Figure 3.33. Uzbekistan crop condition, October 2016-January 2017

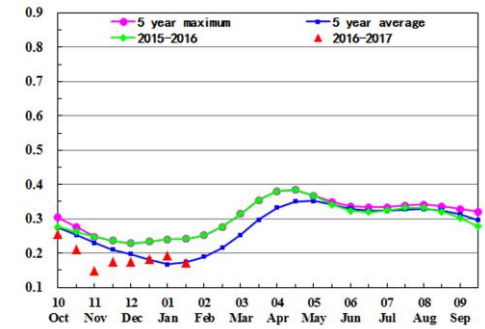

(a) Crop condition development graph based on NDVI

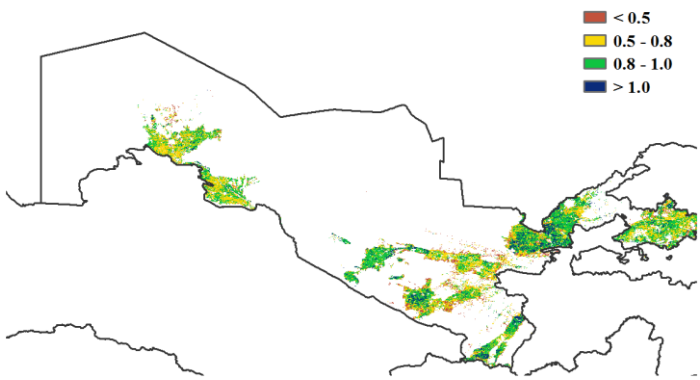

(b) Maximum VCI

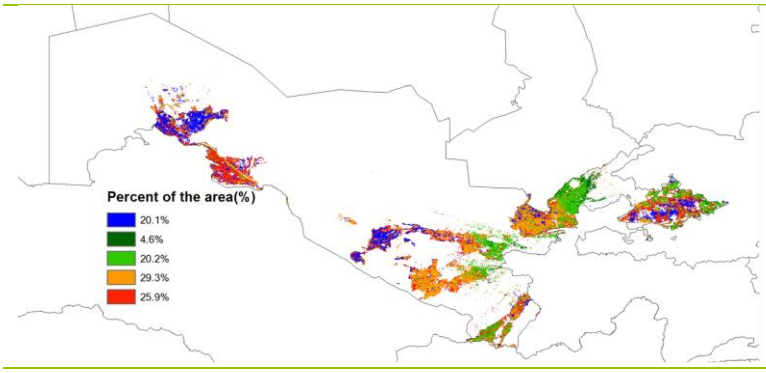

(c) Spatial NDVI patterns compared to 5YA

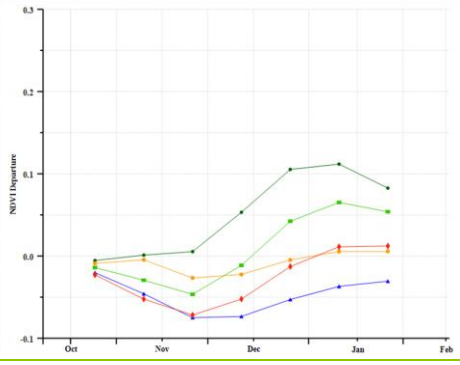

(d) NDVI profiles

[VNM] Vietnam

This monitoring period from October 2016 to January 2017 covers the growing stages of the 10th month rice, as well as the sowing of winter and spring rice in Vietnam. Most of the rice cultivation regions are distributed in the northern Red River delta and the Mekong River delta in the south.

The fraction of cropped arable land (CALF) for the reporting period is similar to the five-year average (-2.29 percentage points). Vegetation condition indices (maximum VCI) are favorable (>0.8), accompanied by an increase in BIOMSS (+37.5%) because of the good water condition (RAIN, +74%) along with a decrease in radiation (RADPAR, -10.77%) and average temperature (TEMP, +0.70°C). Crop condition is below the five-year average, but above starting in 2017.

Over 70% of the crop lands show average or better than average crop condition, with unfavorable crops in the middle mountain area such as Ha Nam, Hoang Mai, and Hung Yen. Overall, crop condition is assessed as average or better than average.

Figure 3.34. Vietnam crop condition, October 2016-January 2017

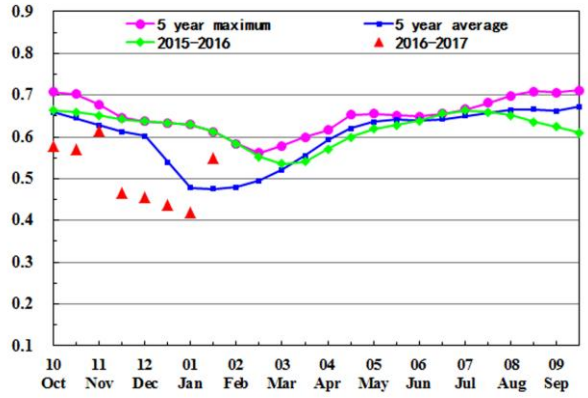

(a) Crop condition development graph based on NDVI

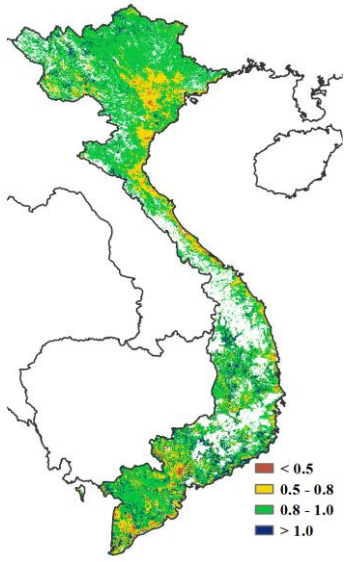

(b) Maximum VCI

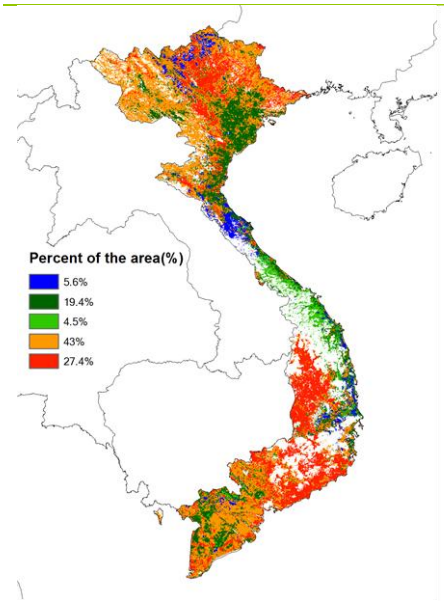

(c) Spatial NDVI patterns compared to 5YA

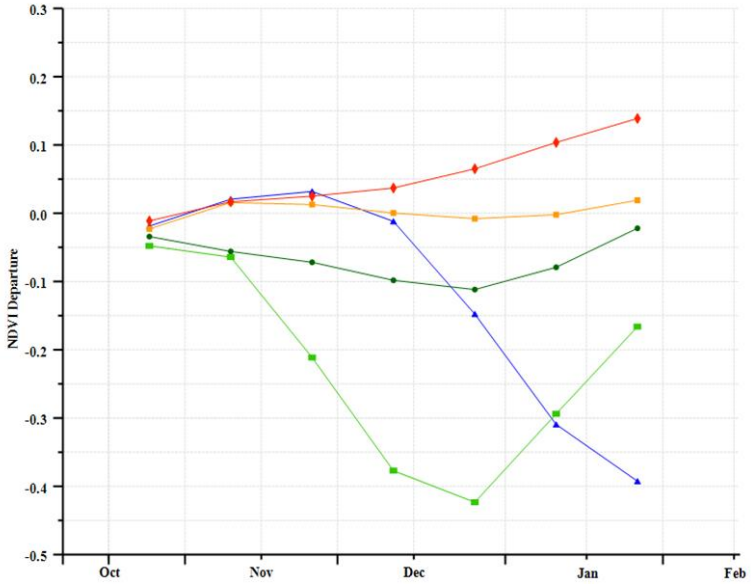

(d) NDVI profiles

[ZAF] South Africa

The reporting period coincides with the planting and vegetative stages of the main crop in South-Africa: maize. The crop is grown from October over most of the eastern half of the country, together with other coarse grains. November and December is also the planting season for vegetables, fruits, and herbs in the southwestern Mediterranean Cape, as well as the harvesting period for barley and wheat, crops that have been consistently declining in the country over the last decade. Overall, the nationwide condition of crops was better than last year's for the same reporting period. In the Mediterranean area, rainfall was well below average (RAIN, -61%) but largely compensated by irrigation. Nevertheless, the most unfavorable conditions were observed in the southwestern cape, covering about 11% of cropped areas. The overall rainfall increase for the country (RAIN, +9%) is mostly relevant for the main rainfed maize growing areas where temperature was also very slightly below average and radiation showed an increase of 1%, altogether yielding an average biomass production potential.

Nationwide (thus including the southwest), VCIx reaches a fair value of 0.79, but generally favorable values (up to 1 and above) occur in most of Orange Free State and North West Province. For more than 75% of cropped areas, NDVI was average or above at the end of January. High NDVI values also occur in the irrigated citrus producing areas of southern Kwa-Zulu Natal. Altogether, the condition of cereals harvested at the end of 2016 in the Mediterranean areas was below average. For the current maize crop in the east and north, prospects are favorable. The final outcome of the season will depend on February rainfall, which is a crucial variable at the time when maize flowers throughout the southern-African region.

Figure 3.35. South Africa crop condition, October 2016-January 2017

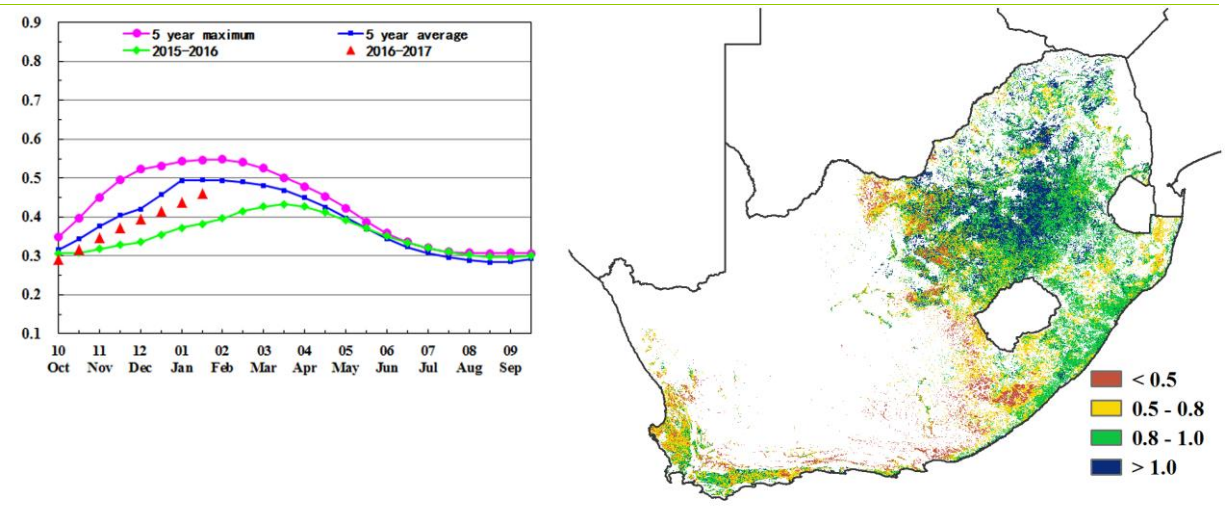

(a) Crop condition development graph based on NDVI (b) Maximum VCI

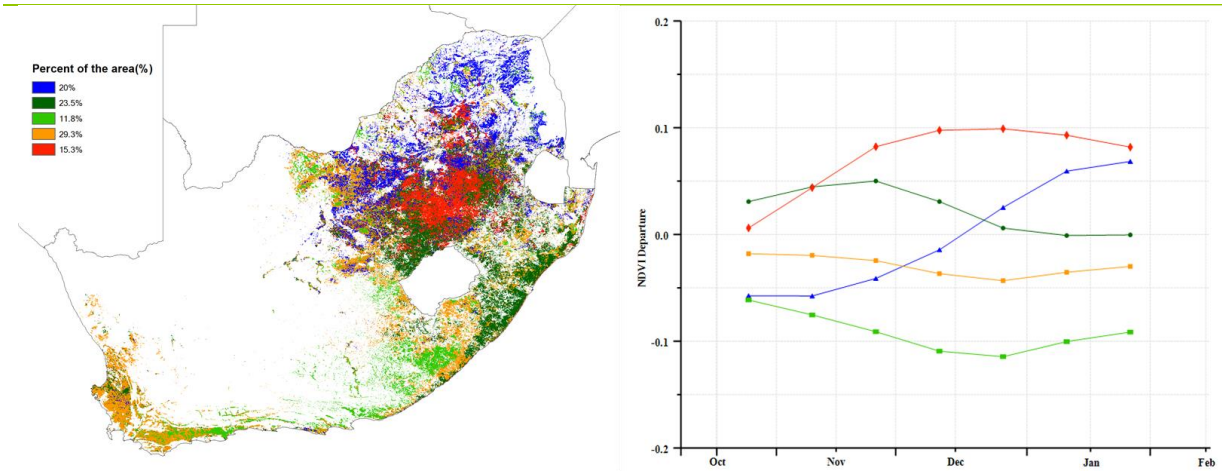

(c) Spatial NDVI patterns compared to 5YA (d) NDVI profiles

Chapter 4. China

Chapter 4 presents a detailed analysis for China, focusing on the seven most productive agro-ecological regions of the east and south. After a brief overview of the agroclimatic and agronomic conditions over the monitoring period (section 4.1), sections 4.2 and 4.3 present an update on the 2017 import and export outlook for China (4.2) as well as the status of domestic prices for major crops (4.3). Section 4.4 presents CropWatch analysis for each of the seven individual regions. Additional information on the agroclimatic indicators for agriculturally important Chinese provinces are listed in table A.11 in Annex A.

4.1 Overview

Overall, China enjoyed crop conditions similar to last year's. At the national scale, the agrometeorological conditions that prevailed during the monitoring period (TEMP, +0.7°C and RADPAR, -12%) were quite close to the average. Together with favorable rainfall (RAIN, +12%), they resulted in above average potential biomass (BIOMSS, +25%). TEMP was quite close to average everywhere, with the largest—but still moderate—departures occurring in the Loess region (+1.3°C) and in Northeast China (-0.6°C). RAIN was much higher than expected in Inner Mongolia (+151%), while the Loess region and the Huanghuaihai region recorded increases of 121% and 107%, respectively. Abundant precipitation was also reported in several provinces, especially in Ningxia province (+182%). Some parts of the major agricultural areas of China suffered from relative low temperatures during early-November and mid-November, while some parts suffered from relative low rainfall during early-October, early-November, mid-December and late-January. Figures 4.1-4.4 and table 4.1 below illustrate the distribution of the various CropWatch indicators.

Table 4.1. CropWatch agroclimatic and agronomic indicators for China, October 2016-January 2017, departure from 5YA and 15YA

Region	Agroclimatic indicators			Agronomic indicators		
	Departure from 15YA (2002-2016)			Departure from 5YA (2012-2016)		Current
	RAIN (%)	TEMP (°C)	RADPAR (%)	BIOMSS (%)	CALF (%)	Maximum VCI
Huanghuaihai	107	0.6	-13	99	-6	0.73
Inner Mongolia	151	0.7	-4	91	n.a.	0.55
Loess region	121	1.3	-9	101	-5	0.70
Lower Yangtze	-12	1.0	-21	6	-8	0.67
Northeast China	90	-0.6	-3	7	n.a.	0.70
Southern China	-7	1.0	-9	4	0	0.55
Southwest China	-5	0.9	-12	0	0	0.73

Note: n.a. = not applicable. Over the monitoring period, no crops are in the field in Northeast China and Inner Mongolia.

High VCIx values occurred mostly in China's southwest and southern regions. Low VCIx values mainly affected the Loess region, central and northeast China, and particularly the southeast of Henan province and northwest of Anhui province. At the regional scale, BIOMSS was above average in the six regions except Southwest China, with especially high values in the Loess (+101%), Huanghuaihai (+99%), and Inner Mongolia (+91%) regions. At the provincial level, the highest BIOMSS values occurred in Ningxia (+171%), Guangdong (+115%), and Shandong (+115%) provinces. Low BIOMSS was mainly recorded in southern areas such as Guangxi (-19%), Guizhou (-16%), and Yunnan (-11%) provinces.

Figure 4.1. China spatial distribution of rainfall profiles, October 2016-January 2017

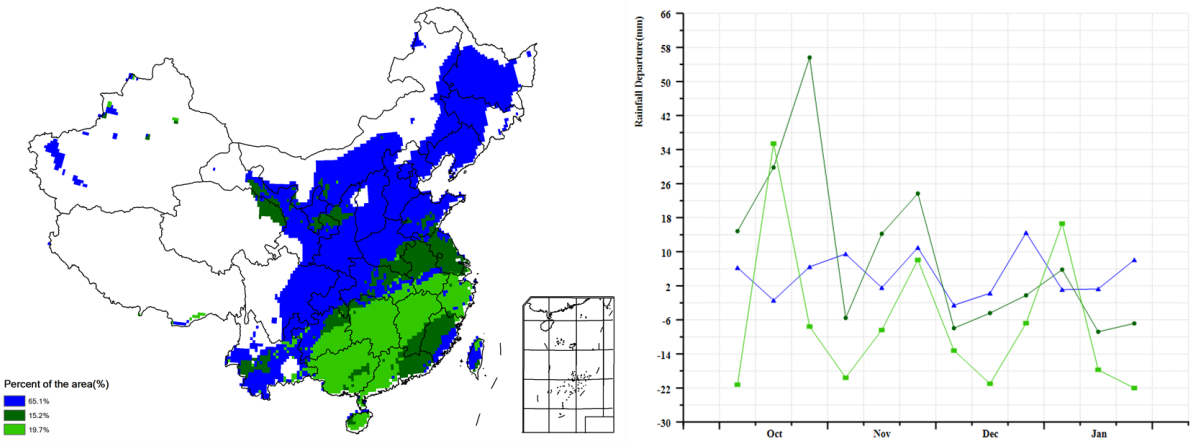

Figure 4.2. China spatial distribution of temperature profiles, October 2016-January 2017

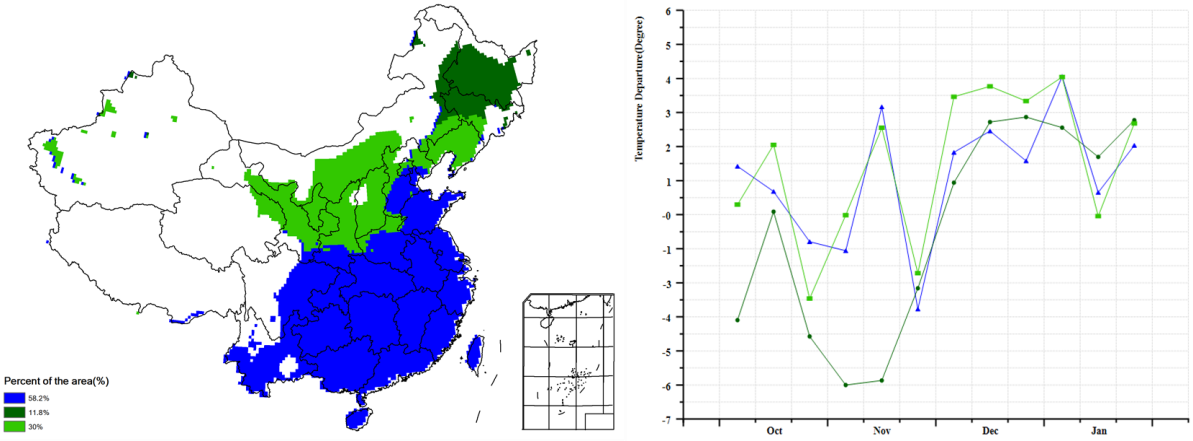

Figure 4.3. China cropped and uncropped arable land, by pixel, October 2016-January 2017

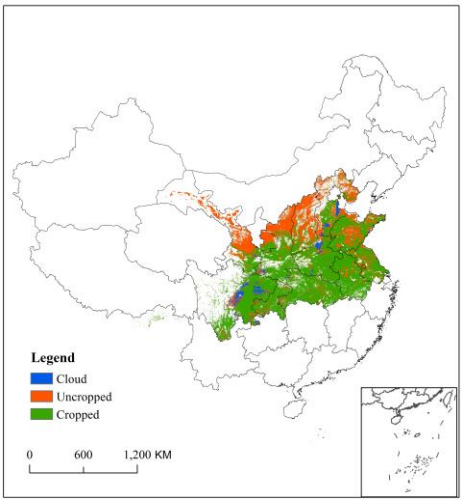

Figure 4.4. China maximum Vegetation Condition Index (VCIx), by pixel, October 2016-January 2017

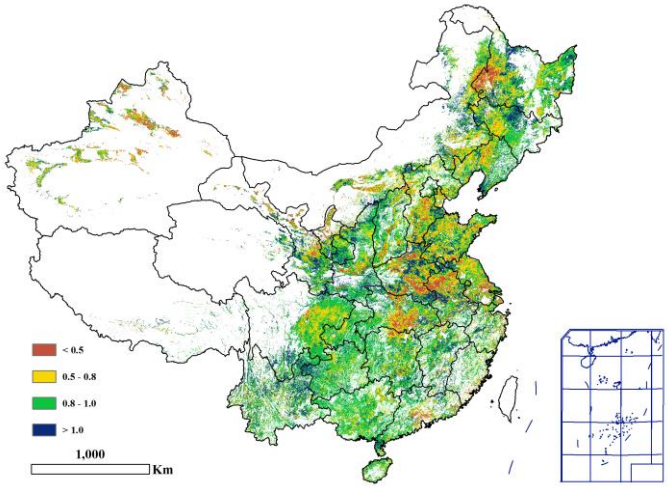

During the monitoring period, the cropped arable land fraction (CALF) overall had the tendency to a bit of decreasing in comparison with the previous five years' average. For two of the seven monitored regions, CALF was equal to the five-year average, while three relative negative values were recorded in the Huanghuaihai region (-6 percentage points), the Loess region (-5 percentage points), and the Lower Yangtze region (-8 percentage points). The uncropped land is mainly distributed in the north of Gansu, Shanxi, and Shaanxi, east of Ningxia, and central Shandong and Sichuan provinces.

4.2 China food imports in 2016 and export outlook for 2017

Previous year (2016)

Food

In 2016, China imported 21.997 million tons of cereals, 32.8% below the previous year's imports (Table 4.2). Main sources for imported grains were the United States, Australia, Ukraine, and Vietnam, accounting for, respectively, 31.6%, 25.4%, 13.7% and 7.4% of the total volume of imports. Their total value amounted to US$ 5.714 billion. Food exports were 636,000 tons, which was 19.5% more than the previous year. Exported grain mainly went to South Korea, Hong Kong, and Japan, respectively accounting for 29.8%, 16.4%, and 14.7% of the total exports. Exports amounted to US$ 505 million.

Wheat

Wheat imports in 2016 reached 3.412 million tons, an increase of 13.5% over the previous year. Main sources were Australia (40.8% of total imports), Canada (30.2%), and the United States (22.8%). Total wheat imports amounted to US$ 815 million. Exports (112,800 tons) went mainly to Hong Kong and the Democratic People's Republic of Korea, which received respectively 83.5% and 5.5% percent of the total, the value of which amounted to US$ 62 million.

Rice

In 2016, 3.563 million tons of rice were imported, up 5.5% over the previous year. The main sources of imports were Vietnam, Thailand, and Pakistan (45.4%, 26.9%, and 19.8% of the total, respectively), for a total value of US$ 1.614 billion. Rice exports (395,100 tons worth US$ 351 million) went mainly to the Republic of Korea, the Democratic People's Republic of Korea and Japan, respectively accounting for 44.4%, 10.6%, and 9.6%.

Maize

China imported 3.166 million tons of maize last year, 3.0% less than the year before. The main sources of imports were Ukraine, the United States, and Laos, respectively accounting for 84.0%, 7.0%and 4.4%ofthe total. Maize imports amounted to US$ 634 million. Exports were 3,457 tons, of which most went to the Democratic People's Republic of Korea (90.4% of total exports). Exports totaled $1.110 million.

Soybean

In 2016, soybean imports were 83.230 million tons, up 1.8%, mainly from Brazil, the United States, and Argentina (45.7%, 40.4%, and 9.6%). The value of imports amounted to US$ 34.018 billion. Soybean exports were 128,300 tons, down 4.2%.

2017 prospects for imported food staples in China

The projections below are based on 2016-2017 global crop monitoring of remote sensing data and a simulation model that takes into account major shocks and policies (based on the standard GTAP model).

In 2017, the imports of major crop types are expected to increase. Figure 4.5 compares projected imports and exports of the main commodities.

Wheat.

Wheat imports will grow 5.0% while wheat exports will fall 7.2%. Although the comparative benefit of wheat is low, the overwintering conditions of winter wheat in the north and south of China have generally been good. Wheat imports are stable with a slight increase in 2017.

Rice

In 2017, rice imports are expected to increase 6.0%, while exports will decrease 1.5%. At present, domestic and foreign price differentials are still expanding, and rice imports are predicted to keep increasing in 2017, but still within the quotas.

Maize

Imports are expected to drop 8.6% and exports 4.3%. At present, the situation of domestic maize supply and demand is still loose; prices are low, and maize imports are restricted. Maize imports are stable with decreasing trend in 2017.

Soybean

In 2017, soybean imports are expected to increase 0.6%, while exports decrease 3.5%. Under the influence of planting structure adjustment policies and low maize prices, the soybean hectarage will slightly increase, and imported soybean growth will be reduced.

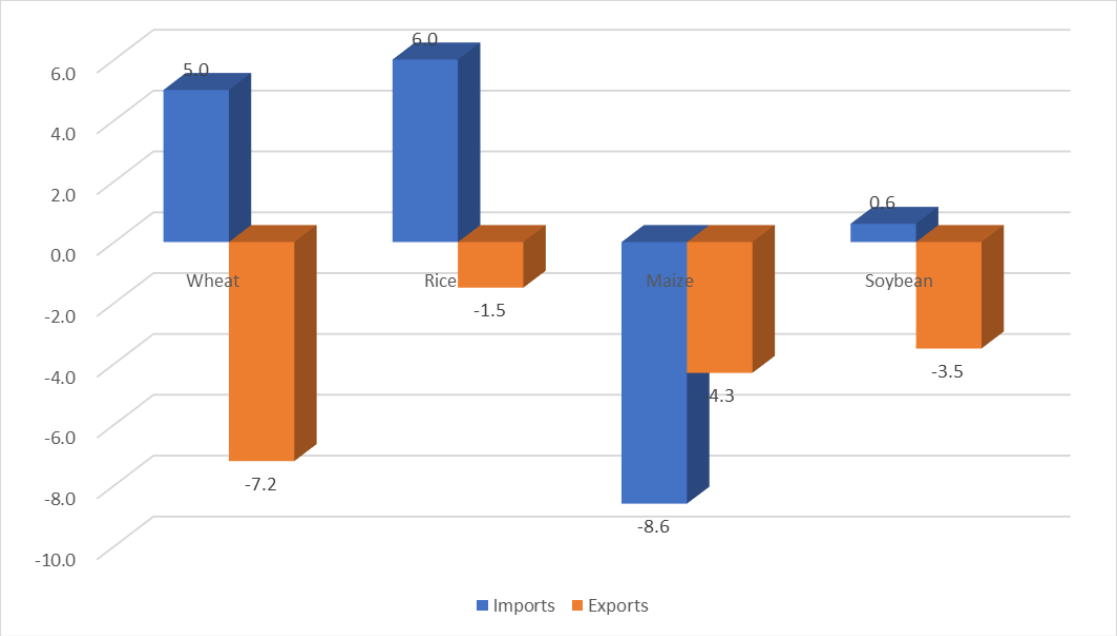

Figure 4.5. Change in import and export of four main crops in China, 2017 (percentage).

Table 4.2. Chinese imports and exports of main commodities in 2016 and 2017 (projections)

		2016		2017 projection	
		M tons	Δ%	M $	Δ%
Imports	Wheat	3.4119	+13.5	815	+5.0
	Rice	3.5628	+5.5	1614	+6.0
	Maize	3.1663	-33.0%	634	-8.6
	Cereals	21.9970	-32.8	5714	
	Soybean	83.2302	+1.8	34018	+0.6
Exports	Wheat	0.1128		62	-7.2
	Rice	0.3951		351	-1.5
	Maize	0.0035		1.1095	-4.3
	Cereals	0.6360	+19.5	505	
	Soybean	0.1283	-4.2		-3.5

Δ% indicates percentage difference with previous year. M tons indicates amount in million tons; M$ indicates value in million US$.

4.3 Outlook for the domestic price of four major crops

The following analysis of domestic prices for soybean, maize, japonica rice, and wheat in China is based on (i) nationwide monthly grain price data between December 2006 and December 2016 provided by the price information center of China's National Development and Reform Commission (NDRC) and (ii) price trend forecasts and early warning obtained by Fang Jingxin's price-spiral model, in addition to other national and international ancillary data sources. The outlook is as follows:

- *Soybean.* According to data for the last six months, the international consumption ratio for soybean is at equilibrium. Domestic soybean prices are also at equilibrium but fluctuate around the trend line; fluctuations are expected to amplify.
- *Paddy rice.* As a result of the changing relationship between supply and demand, the recent downward trend for the price of paddy rice in China will slow down. For now, the price has returned above the trend line; if it can keep this position for five months, it is assumed the upward price trend will continue. (See figure 4.6.)
- *Maize.* Maize prices have hit bottom, and the consumption rate has entered the non-equilibrium interval. This shows that the supply and demand situation is conducive to recovery. An early warning is made for the reversal of the declining price trend.
- *Wheat.* Current prices and consumption rates are at equilibrium. It is expected that the decline will gradually calm down to above the trend line. Similar to the situation for paddy, if the price position can be maintained for five months, an upward trend for the price of maize is assumed.

Figure 4.6. Fluctuations in the price of paddy rice, December 2006 to December 2016

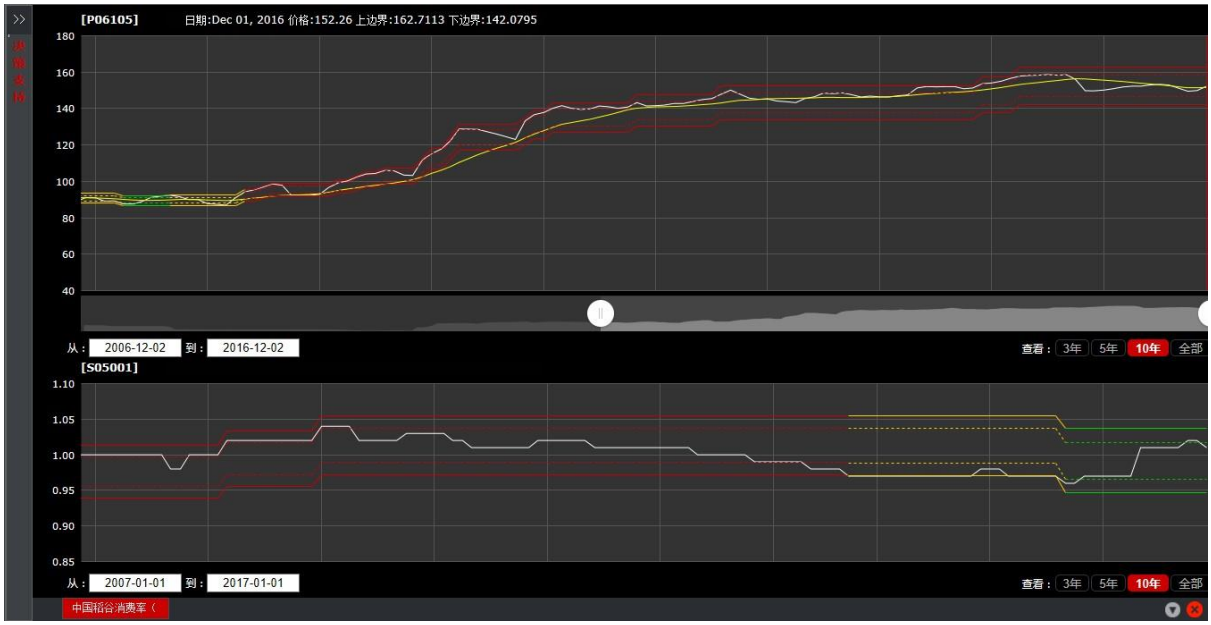

4.4 Regional analysis

Figures 4.7 through 4.13 present crop condition information for each of China's seven agricultural regions. The provided information is as follows: (a) Crop condition development graph based on NDVI, comparing the current season up to January 2017 to the previous season, to the five-year average (5YA), and to the five-year maximum; (b) Spatial NDVI patterns for October 2016 to January 2017 (compared to the (5YA); (c) NDVI profiles associated with the spatial patterns under (b); (d) maximum VCI (over arable land mask); and (e) biomass for October 2016-January 2017. Additional information about agroclimatic indicators and BIOMSS for China is provided in Annex A, table A.11.

Northeast region

No crops are grown between late October and January in Northeast China due to the low temperatures. For the period under consideration, however, agroclimatic conditions were favorable for crops to be planted in April. The CropWatch agroclimatic indicators show markedly above average rainfall (RAIN, +90%) and a slight decrease in radiation (RADPAR, -3%). Temperature (TEMP, -0.6°C) was generally about average. These favorable agroclimatic conditions resulted in a 7% above average potential biomass production (BIOMSS) in the region. The only exception to these generally good conditions is a region west of Heilongjiang province (Xiaoxingan ranges), which shows below average NDVI due to heavy snow and extreme low temperature during the previous monitoring period; VCIx also shows this spatial pattern (with a VCIx <0.5 in this area). In general, abundant snow will ensure good soil moisture, which will benefit spring crops in 2017.

Figure 4.7. Crop condition China Northeast region, October 2016-January 2017

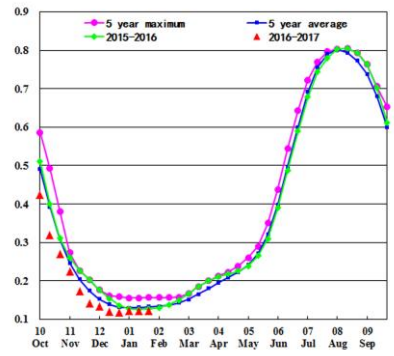

(a) Crop condition development graph based on NDVI

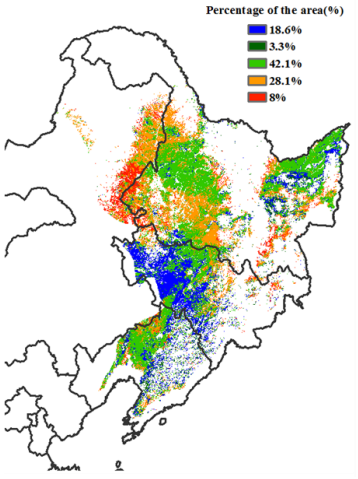

(b) Spatial NDVI patterns compared to 5YA

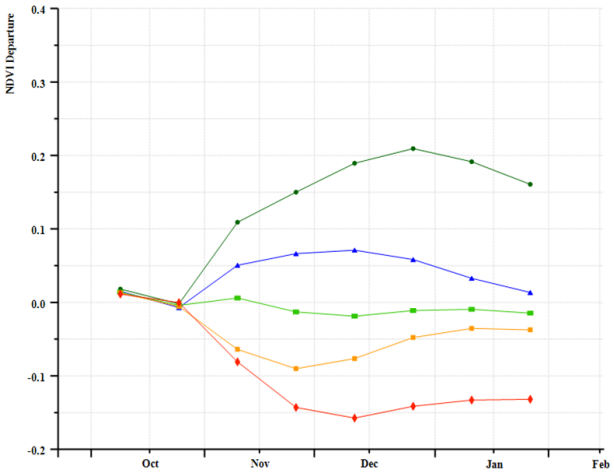

(c) NDVI profiles

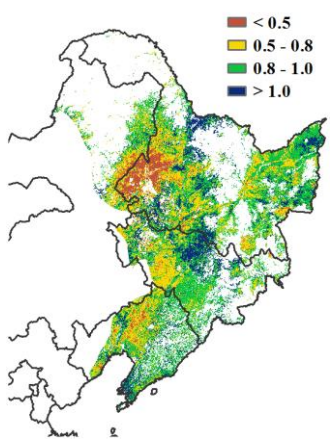

(d) Maximum VCI

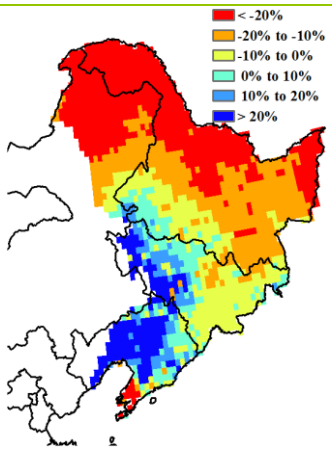

(e) Biomass

Inner Mongolia

Over the reporting period, winter crops in Inner Mongolia cannot survive due to very low temperatures. Prevailing conditions nevertheless will influence the forthcoming spring crop season. Compared with average conditions, the CropWatch agroclimatic indicators show a very significant increase of RAIN (+151%) and a decrease of RADPAR (-4%), while TEMP was about average (+0.7°C). BIOMSS, however, was significantly above the five-year average for the same period (+91%).

From October, below average conditions had little effect as the crops had reached maturity, even if excess rainfall locally hampered harvesting. Abundant snow since December will provide favorable soil moisture for the sowing of upcoming spring crops. Potential biomass during the monitoring period in most areas of Inner Mongolia was at least 20% above average, but 10% below average in the north. Some risk exists that higher than average temperature may have some influence on spring crops by prematurely depleting reserved soil moisture.

Figure 4.8. Crop condition China Inner Mongolia, October 2016-January 2017

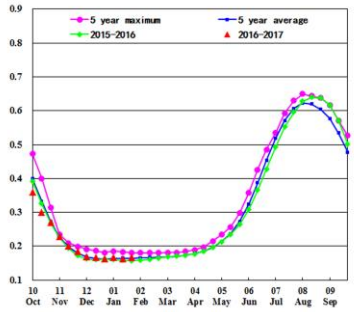

(a) Crop condition development graph based on NDVI

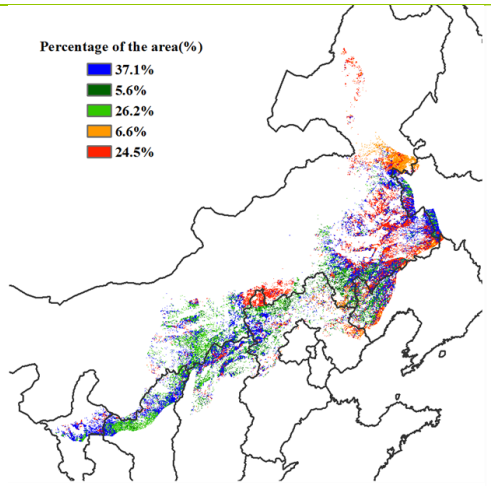

(b) Spatial NDVI patterns compared to 5YA

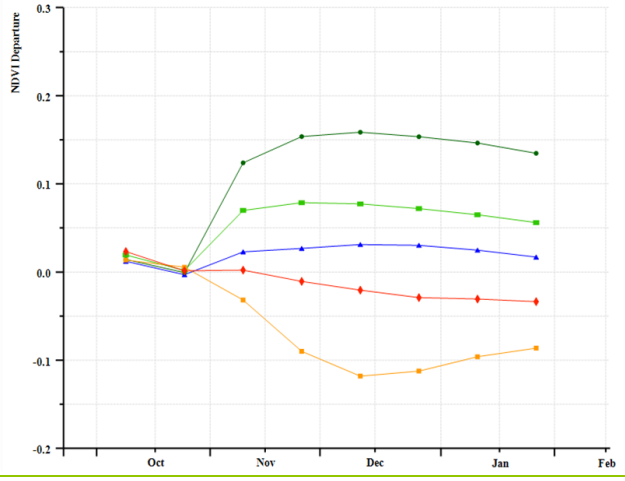

(c) NDVI profiles

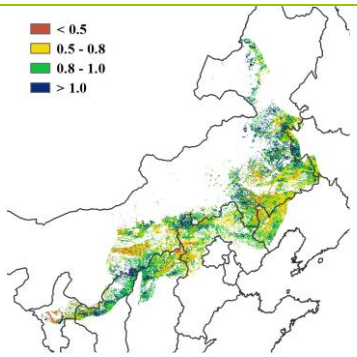

(d) Maximum VCI

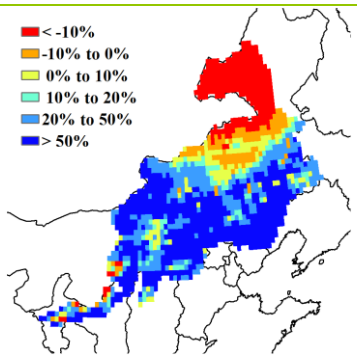

(e) Biomass

Huanghuaihai

Crop condition in Huanghuaihai was generally below the recent five-year average, although it exceeded that level in January. Unfavorable meteorological conditions during the last monitoring period may have impacted crop sowing and crop development at early growing stages. In addition, dry weather from July to October hindered the germination of winter wheat, which is confirmed by the well below average NDVI value before January in the NDVI development graph. Significantly above average rainfall (RAIN, +107%) from October to January provides sufficient soil moisture for winter wheat to develop after the wintering period, resulting in a marked increase in the biomass production potential (BIOMSS, +99%).

As shown in the spatial pattern of the NDVI departure map, crop condition was slightly below average before the middle of October in almost the whole region, and well below the average since November in scattered locations across the region, especially in eastern Henan and northern Anhui provinces. Since December, crops in the region have been recovering, turning to average condition by January, mainly due to abundant rainfall. The maximum VCI presents low values in eastern and northern Henan, northern Anhui, and central Hebei, which is consistent with the spatial distribution of the crop condition. Overall, climatic conditions so far will benefit the development of the winter wheat after dormancy.

Figure 4.9. Crop condition China Huanghuaihai, October 2016-January 2017

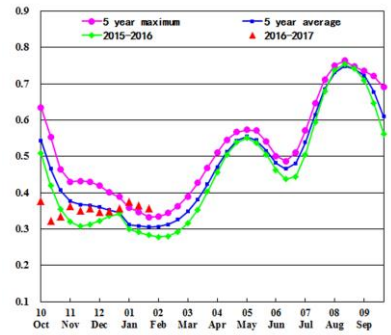

(a) Crop condition development graph based on NDVI

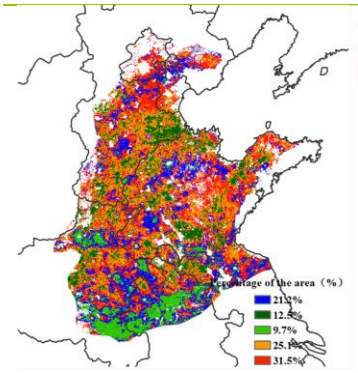

(b) Spatial NDVI patterns compared to 5YA

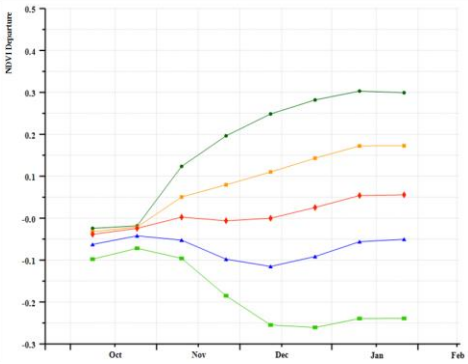

(c) NDVI profiles

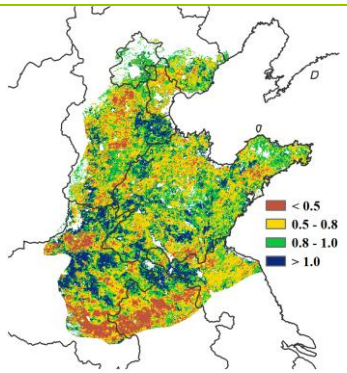

(d) Maximum VCI

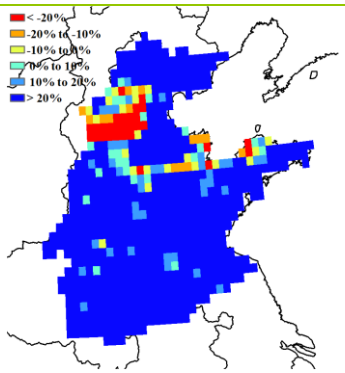

(e) Biomass

Loess region

The most relevant crop during the monitoring period was currently hibernating winter wheat. From the beginning of October to early-December, crop condition was inferior to last year's and below the five-year average. However, from mid-December to the end of the monitoring period crop condition recovered to exceed both last year's and the five-year average. Radiation (RADPAR, -9%) was below average for the region, while temperature (TEMP, +1.3°C) was above and precipitation (RAIN, +121%) far above, which gave rise to a potential biomass (BIOMSS) far above average as well (+101%).

In most of the region, the analyses based on spatial NDVI clusters and profiles are consistent with VCIx. The most favorable conditions occurred mainly in the north of Shanxi and Shaanxi provinces and in the east of Gansu province, due to the abundant rainfall and suitable sunlight. On the contrary—and mostly because of drought during the monitoring period (as confirmed by the maps of potential biomass)—crops were in poor condition in the middle of Gansu and Shaanxi provinces and in the east of Shanxi. The seemingly above average crop condition in some areas from mid-December may be the result of rapid growth due to high temperature. Altogether, crop prospects in the region are favorable.

Figure 4.10. Crop condition China Loess region, October 2016-January 2017

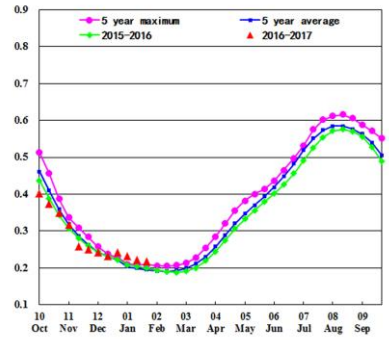

(a) Crop condition development graph based on NDVI

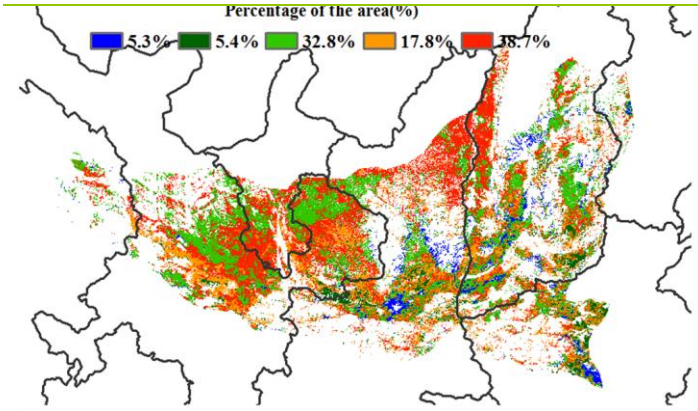

(b) Spatial NDVI patterns compared to 5YA

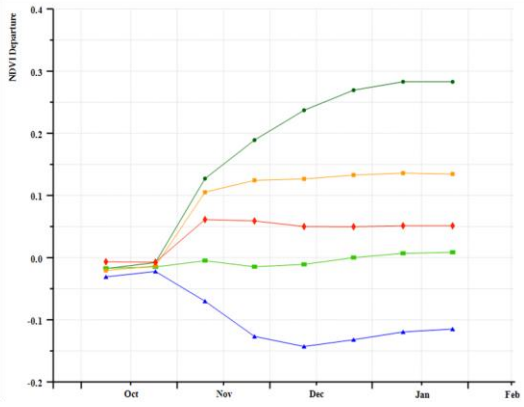

(c) NDVI profiles

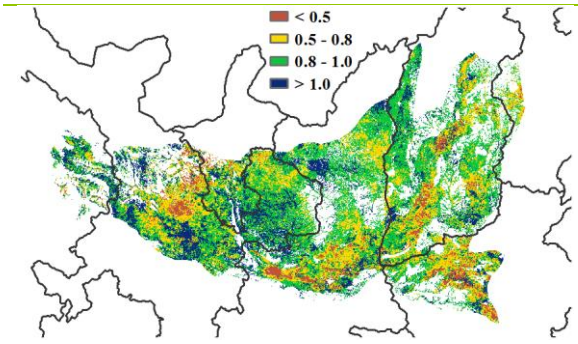

(d) Maximum VCI

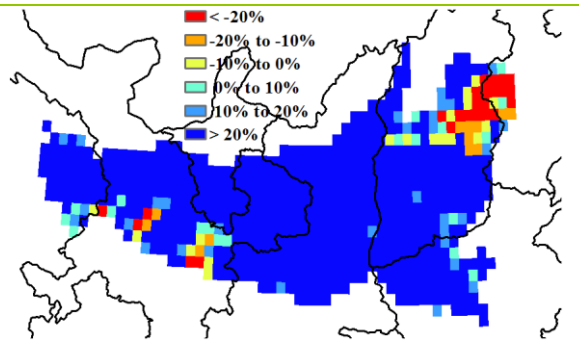

(e) Biomass

Lower Yangtze region

During the monitoring period, few crops were in the field except for winter wheat growing in the northeast and northern part of the region. Rainfall (RAIN, -12%) and radiation (RADPAR, -21%) were below average according to the CropWatch agroclimatic indicators, while temperature was above average (+1°C). Somewhat unfavorable rainfall and radiation and favorable temperature condition brought about a slight increase in the biomass production potential (BIOMSS, +6%). Based on NDVI, crop condition was below average compared to the five-year average. The BIOMSS map shows that almost half of the region suffered a marked decrease of 20% in BIOMSS this period, while an increase of 20% occurred in the north and southeast of the region. NDVI profiles show that the crop condition was predominantly poor in 36.5% of the region's cropped areas, located in the south of Jiangsu, middle of Anhui, and in Hubei province, which was confirmed by the VCIx maps. Prospects for crops in the region are mixed and vary spatially.

Figure 4.11. Crop condition Lower Yangtze region, October 2016-January 2017

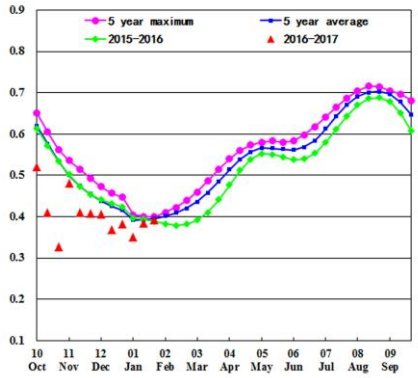

(a) Crop condition development graph based on NDVI

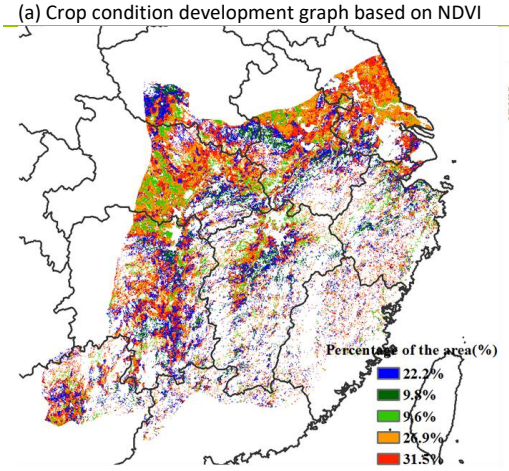

(b) Spatial NDVI patterns compared to 5YA

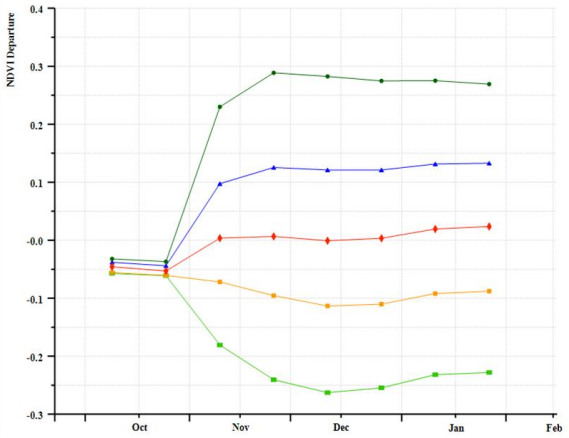

(c) NDVI profiles

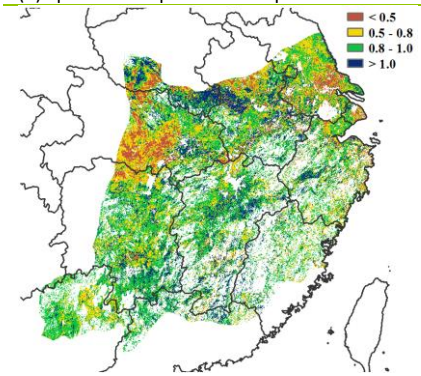

(d) Maximum VCI

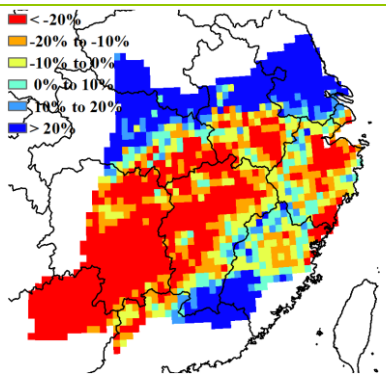

(e) Biomass

Southwest China

The overall crop condition in the region is locally below average compared with the recent five-year average, at a time that coincides with the planting season of winter wheat. NDVI was generally below average by about 0.1 units during most of the time. Agroclimatic indices show a 12% decrease of radiation (RADPAR), accompanied by a positive temperature (TEMP) anomaly of 0.9°C. The cropped arable land fraction (CALF) remains at the same level as the five-year average.

According to the spatial NDVI patterns and profiles, winter wheat condition is below average in western Chongqing, western Guizhou, parts of western Hubei, Hunan, and especially in eastern Sichuan areas, where the maximum VCI was mainly in the range of 0.5 to 0.8. This can probably be assigned to low RADPAR in Chongqing (-22%), Guizhou (-16%), Hubei (-22%), and Hunan (-24%), and increased air temperature (Sichuan: +0.9°C; Chongqing: +0.7°C; and Guizhou: +1.2°C). Crop condition is generally favorable, with the exception of the listed areas where the final outcome will depend on conditions prevailing during the coming months.

Figure 4.12. Crop condition Southwest China region, October 2016-January 2017

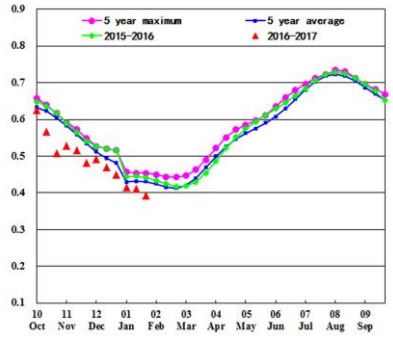

(a) Crop condition development graph based on NDVI

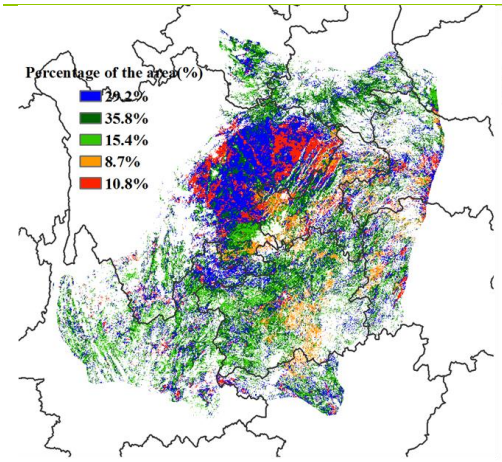

(b) Spatial NDVI patterns compared to 5YA

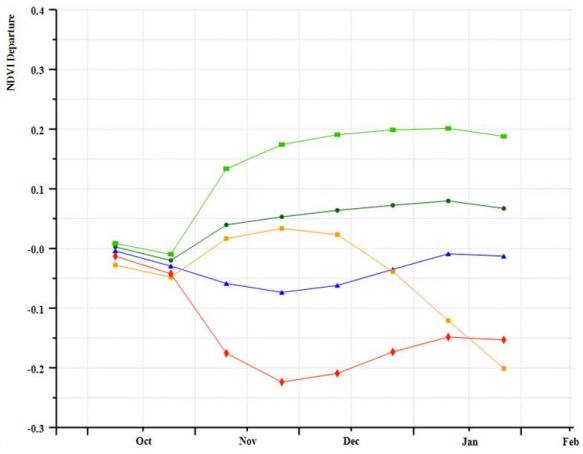

(c) NDVI profiles

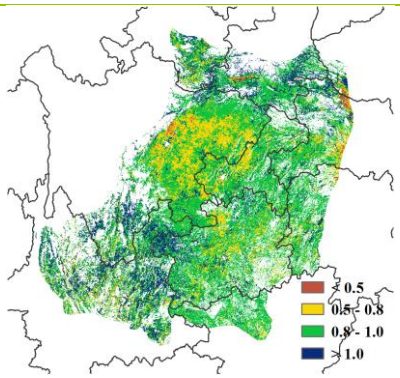

(d) Maximum VCI

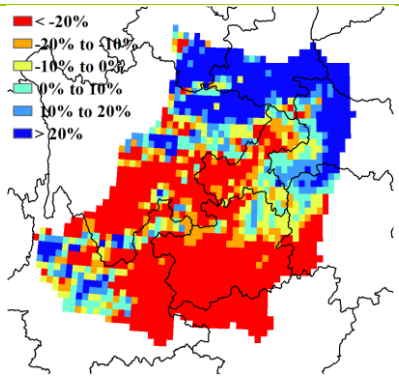

(e) Biomass

Southern China

According to the NDVI-based crop condition development graph, the overall crop condition is slightly below average compared to the recent five-year average. The monitoring period covers the harvest of late rice and the planting of winter wheat. NDVI remained below average in October and the first half of November, then increased to average at the end of December, and finally reached even the five-year maximum level. Low radiation (RADPAR) (Fujian, -20%; Guangdong, -14%; and Guangxi,-11%) and high temperature (Fujian, +1.7°C; Guangdong, +1.0°C; Guangxi, +1.2°C; and Yunnan, +0.8°C) led to this partly below average situation. As a result, the general maximum VCI reached only 0.6 with the cropped arable land fraction (CALF) staying at the same level as the five-year average.

Crop condition in central Guangdong deserves close monitoring due to its obvious below average condition during the whole period, with maximum VCI below 0.5; this is also reflected by the NDVI spatial patterns and profiles. Overall expectations for the forthcoming winter wheat, however, remain fair.

Figure 4.13. Crop condition Southern China region, October 2016-January 2017

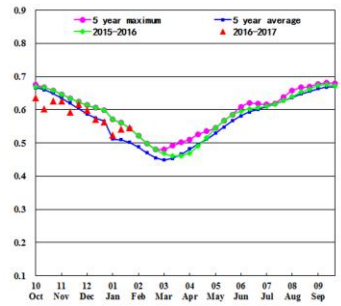

(a) Crop condition development graph based on NDVI

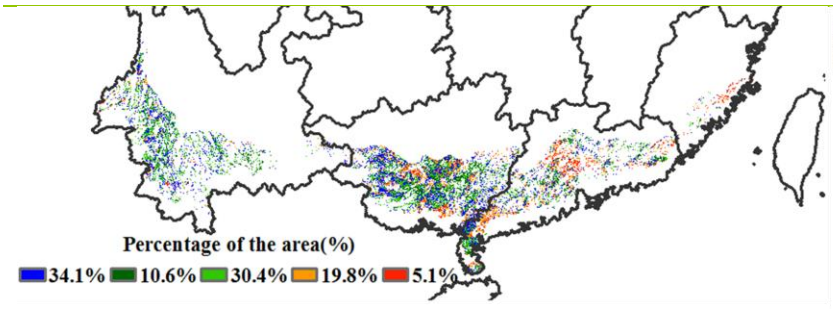

(b) Spatial NDVI patterns compared to 5YA

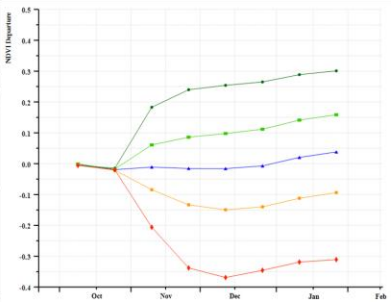

(c) NDVI profiles

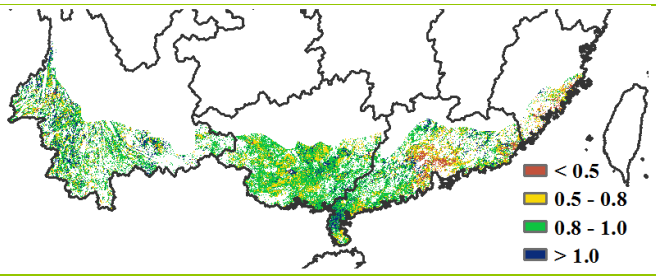

(d) Maximum VCI

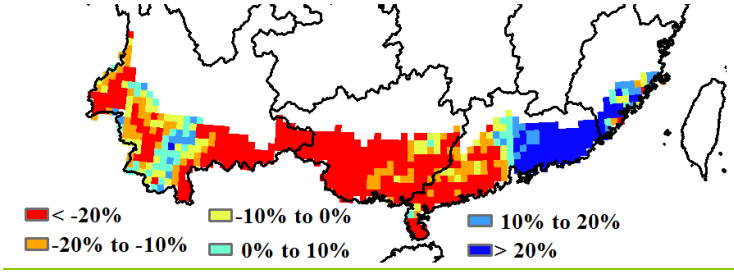

(e) Biomass

Chapter 5. Focus and perspectives

Building on the CropWatch analyses presented in chapters 1 through 4, this chapter includes an updated production outlook for 2016 focused on wheat (section 5.1), as well as sections on recent disaster events (section 5.2), a focus on agriculture in the East and Southeast Asia (5.3) and an update on El Niño (5.4).

5.1 CropWatch production outlook

The production outlook for the current bulletin includes only the major producers in the southern hemisphere, as assessments for the northern hemisphere would be too hypothetical at this early stage in the season.

For Argentina, CropWatch puts its winter wheat production of 2016 at 11.245 million tons, an increase of 5.0% over the previous year resulting from increases in the major production area. This year, however, provinces that generally contribute relatively little to the global output outperformed the traditional “big” wheat producers from Córdoba to Buenos Aires. The same occurred in Australia where the wheat production increased more in minor producing areas (+45.1% over last year) than nationwide (+24.3%). The total output in Australia exceeds that of Argentina by a factor 3 and reaches 32.066 million tons. Finally, at 7.747 million tons, the output of Brazil stays behind that of its southern neighbor, increasing however 10.0% over the previous season. Contrary to the situation in Australia and Argentina, minor wheat producing areas in Brazil did poorly (-29%). Wheat production results for Argentina, Australia and Brazil are listed in Annex B.

5.2 Disaster events

Introduction

According to a recent World Bank study (Hallegatte et al, 2017), economic losses from natural disasters totaled US$92 billion in 2015, mostly in the building, infrastructure and agricultural production sectors.

For many people, a disaster is the beginning of the poverty spiral, as assets—such as farm tools and animals, often acquired over many years, are abruptly lost in one disaster event. For instance, there are indications that the losses to the livestock sector during the Sahelian droughts of the 1960s to mid-1980s are still not completely recovered from in terms of per capita meat and milk production.

The World Bank study found that the effect of disasters on well-being, measured in terms of lost consumption, is larger than asset losses. This results in long-term effects on health, education, ability to work productively and to restore pre-disaster conditions. It also precipitates many people into debt when assets had to be sold to survive. Therefore, the report estimates that impact on well-being in affected countries is equivalent to consumption losses that far exceed direct impact losses and reach about US$520 billion a year, far larger than any earlier estimates.

Overview

This section of the CropWatch bulletin provides an overview of disasters that occurred during the reporting period. It is sometimes based on early reports, as well as early impact assessments, as the full measure of impacts becomes available long after the impacting factor itself has subsided. The report also focuses on disasters that have the potential to directly affect agriculture. Volcanic eruptions in non-

agricultural areas, earthquakes and man-made disasters are thus mostly not mentioned, even if they have the potential to lead to long-term effects that are very comparable to those listed in the just mentioned World Bank report. Importantly, all disasters can be made worse by mismanagement as it often affects rescue operations.

The recent El Niño, which has led to misery in large regions worldwide, was the first occurrence of a large-scale geophysically caused disaster in many years, probably going back to the mid-1980s and the well-known Ethiopian droughts.

The most significant disasters of the reporting period include floods in southeastern Africa (especially Mozambique) and Hurricane Matthew, which affected Haiti at the beginning of October.

Cyclones and storms

Hurricane Matthew (September 28-October 10, 2016) was one of the strongest and long-lived Atlantic cyclones in ten years, starting its trajectory off the Venezuelan coast and dissipating east of Canada. It crossed the Caribbean between Cuba and Haiti, which were the most severely affected developing countries (damages estimated at US$2.6 billion and US$1.9 billion, respectively). Total economic loss, including between US$5 and 8 billion in the United States) is currently put as about US$13 billion. In the Caribbean, the period coincides with the maize and rice harvests and the planting of the second maize crops. According to FAO, the most affected areas in Haiti have lost up to 100% of crops, and pastures to feed livestock have also been affected. The organization puts the total value of crop losses at US$360 million and damages to irrigation and fishing equipment at US$178 million. The final estimate by government and FAO puts annual crops losses due to Matthew at 116,000 tons of food, while also about 16,500 tons of food in stock was lost. Fruit losses until recovery are estimated at over 100 million tons. About 2 million birds, 500,000 goats, 163,000 pigs, 102,000 heads of cattle, 74,000 sheep and 23,000 horses were killed, which will affect protein availability for several years. In total, 1.4 million people, or 13% of Haiti's population, were in need of food assistance at the beginning of October. In Cuba (Guantanamo, Holguin, and Las Tunas provinces) the impact was more limited; the production loss is estimated to reach 10,000 tons of maize, as the affected provinces represent a small fraction of total national maize and rice output. Horticultural crops, however, are deemed to have been more severely impacted, as were plantain and bananas. Plantain and bananas suffered as well from wind damage in several Caribbean islands.

Figure 5.1. Damage to bananas in Hainan as a result of typhoon Sarika

Source: Wikipedia

Typhoon Sarika (October 13-19, 2016) affected the Philippines (crop loss: 250,000 tons), South China, and Vietnam (provinces of Nghe An, Ha Tinh, Quang Tri, Thua Thien Hue, and Quang Binh), for a total estimated loss of US$760 million (of which US$680 in Hainan) and 34 fatalities (figure 5.1). The typhoon formed east of the Philippines where it made landfall in Quezon and moved west-northwest in the general direction of China's Hainan province. A twin typhoon (Haima) developed between 14 and 26 October in the same general area, making landfall over northern Luzon in the Philippines and then progressing to China and eventually reaching Japan. The total damage is estimated at 18 casualties and US$1.93 billion damage, including US$70 million in the Philippines and more than US$1 billion in China. Precise impact estimates for the agricultural sector are still missing. In Guangdong, agricultural and economical losses were in excess of US$500 million. Just under 200,000 ha of crops were destroyed in

Hainan (worth just over US$600 million), with more limited impacts in Fujian (200 hectares and an economic loss of US$5 million).

Hurricane Otto affected Costa Rica, Nicaragua, and Panama between November 20 and 26 in 2016. Total damage is estimated at US$50 million. No specific agricultural impact assessments are available from FAO, but the damage to the sector was limited and certainly much less severe than the destruction brought about by Matthew.

Typhoon Nock Ten was the third cyclone that affected the Philippines this season. It lived from the 20th to the 28th of December and affected, next to the Philippines, Vietnam as well, with wind speeds reaching just short of 300 km/h in the early stages. Nearly 3 million people have been affected in Bicol region, Mimaropa, Calabarzon and Eastern Visayas, but casualties remained low and damage relatively contained (US$ 100 million), mostly comprising of about 200,000 tons of rice, maize, and some high value crops totaling US$90 million.

At the end of January, about 20 people died in Georgia and Mississippi in the United States after multiple tornadoes rattled the region. In total, at least 62 tornadoes touched down across the states of Texas, Louisiana, Mississippi, Alabama, Georgia, Florida, and South Carolina from January 21 to 23.

Excess rainfall and landslides

Abundant precipitation leading to floods have occurred on all continents, forcing people to evacuate and destroying homes and crops. Example of this are in Egypt (late October, killing 30), Indonesia (mid-November in Karawang, West Java), the Dominican Republic (mid-November, affecting several provinces with frequent landslides), and in central Vietnam (early December, with losses valued at more than US$309 million). In Argentina, a storm surge on December 26 caused flooding and heavy damage in the provinces of Buenos Aires and Rosario, with 10 towns still flooded in January. On January 9, floods affecting 13 provinces killed 19 people in the lower-central region and mostly the south of Thailand. Some days later (January 20 to 26), the Philippines were hit by floods and landslides that resulted in 9 deaths, mainly in Davao and northern Mindanao regions, affecting 1.5 million people; early estimates indicated that the cost of damage to agriculture is about US$1 million.

Figure 5.2. Map of estimated precipitation between 12 and 18 January 2017 in Mozambique and Zimbabwe

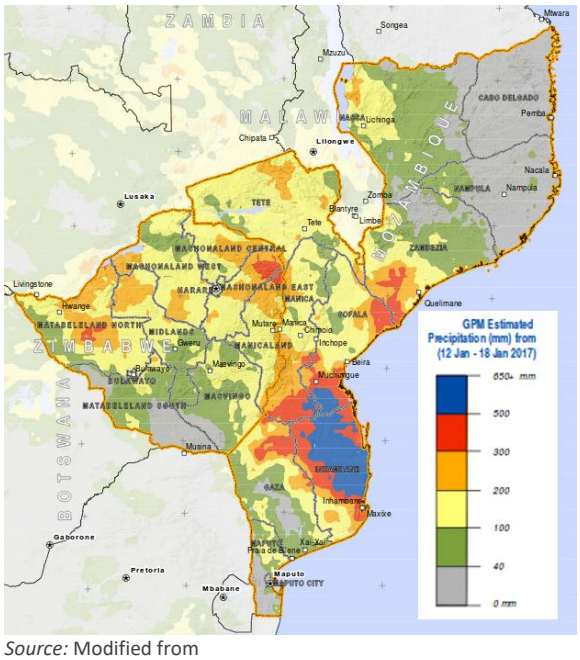

Source: Modified from http://www.unitar.org/unosat/node/44/2535.

The most severe and widespread floods are those that befell southern Africa, after a drought year brought about by El Niño and reported on in previous CropWatch bulletins. Countries affected include mostly Mozambique and Zimbabwe, and—to a lesser degree—Angola where 10,000 people were made homeless. The region is at the peak of its agricultural season, with cassava and maize being the main crops. Torrential rains started early in the month, and more than 600,000 people were affected by as much as 600 mm in one week (12 to 18 January) in Mozambique, while 44 people were killed, mostly in the provinces of Maputo, Gaza, Inhambane, and Nampula (figure 5.2). According to ACAPS, the Zambezi river burst its banks on January 24 in the central province of Sofala. Two million people are expected to

be affected in Mozambique (IPC phase 3 level)[3]. The floods occurred when about 1 million people were still receiving food assistance as a result of last year's drought and at a time the price of maize was already 20% to 100% (according to the market) above normal seasonal values. Many of the affected areas are semi-arid (especially in the south) and are not well prepared nor equipped for excess precipitation. Although thousands of hectares of crops have been lost, it is likely that the precipitation will benefit crop production at the national level.

Drought, heatwaves, and fire

On November 8, wild fires started in the central provinces of Chile. By mid-December, 49 fires had been reported; by mid-January, 32 fires (out of a total of 100) were still active. In total, about 250,000 hectares of vegetation were lost in seven regions: Valparaiso, Metropolitan, O'Higgins, Maule, Bío-Bío, Aracuanía, and Los Lagos, and 11 people have died. According to Chile's fire brigade chiefs, poor preparation for climate change and large monoculture plantations were to blame for the disaster (see figure 5.3).

An extreme heat wave has hit parts of New South Wales and Queensland in Australia at mid-January, with temperatures reaching close to 50°C.

Figure 5.3. Dramatic night view of wild fires in Chile

Source: https://www.theguardian.com/world/2017/jan/29/chiles-forest-fires-poor-planning-fire-chiefs-monoculture-fire-breaks.

Cold wave

At mid-December, a dzud (an extreme cold wave) affected 13 provinces in northern Mongolia.

A cold wave affected a large area spanning the Mediterranean and parts of central Europe; the conditions started in early January and the cold wave was accompanied by snowstorms, strong winds, and very cold freezing temperatures by local standards (reaching -35°C). Disaster monitoring systems single out Macedonia and Belarus. In North Africa, Morocco reports a less intense but nevertheless severe cold wave from mid-January, affecting particularly regions in the east, north, and south. Neighboring Algeria was affected in its eastern, central and the high plateau regions. In Libya, cold weather was reported from late December. It is unknown whether agricultural impacts are to be expected.

5.3 East and Southeast Asia

General geographic setting

East and South-East Asia[4] (hereafter referred to as "the region"[5]) are home to about 31% of the world population distributed among 17 countries, including some of the most populated ones such as China (ranking first), Indonesia (fourth), and Japan (tenth). Figure 5.4 shows the location of the countries in this region, identifying them by their three-letter ISO codes. The countries together span a huge climate and

[3] IPC stands for Integrated Phase Classification, a standardized code to report food insecurity. See also, http://www.ipcinfo.org/ipcinfo-detail-forms/ipcinfo-resource-detail0/en/c/162270/.
[4] Unless otherwise specified, the data used for section 5.2 is taken from FAO (FAOSTAT, http://www.fao.org/faostat/en/#data) and the World Bank (http://data.worldbank.org/indicator).
[5] Eastern Asia and South-East Asia are referred to as "sub-regions". "Recent rate of change" refers to the percent change between 2001-2005 and 2011-15.

ecological gradient as their latitudes vary from about -19°S to 50°N, and close to 85° in longitude from Xinjiang in China to the islands of New Ireland in Papua New-Guinea.

Figure 5.4. Location of countries in East and Southeast Asia

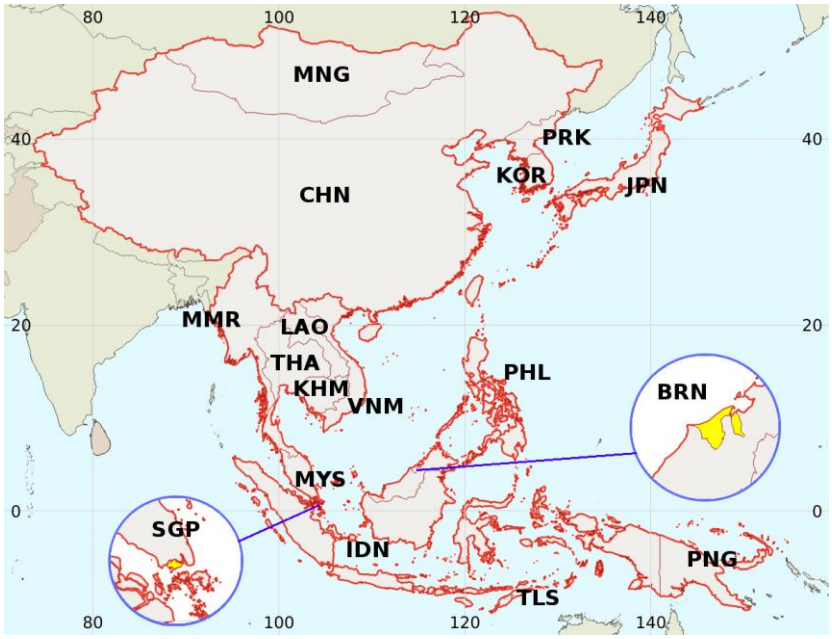

Note: BRN: Brunei Darussalaam; CHN: China; IDN: Indonesia; JPN: Japan; KHM: Cambodia; KOR: Republic of Korea; LAO: Lao People's Democratic Republic; MMR: Myanmar; MNG: Mongolia; MYS: Malaysia; PNG: Papua New-Guinea; PHL: Philippines; PRK: Democratic People's Republic of Korea; SGP: Singapore; THL: Thailand; TLS: Timor Leste; and VNM: Vietnam. Mostly for ethnic reasons, PNG is often considered part of Oceania, although it shares the island of Papua with Indonesia. The line between CHN and MMR, LAO and VNM marks the separation between East Asia and South-East Asia. Boundaries modified from GAUL_0 (FAO, 2017).

The largest share of the population (1,594 million or 72% of the region's total population) occurs in Eastern Asia, including China, Myanmar, the Democratic Republic of Korea, Republic of Korea, and Japan (table 5.1). In both sub-regions of Eastern Asia and Southeast Asia, the rate of urbanization is close to 50%, with rates of 58% and 45% respectively,[6]resulting from a recent rate of change of about 30%. Overall, however, the population in Eastern Asia grew only 5% since 2001, which is less than the growth in world population of 12%. Needless to say, since China's population represents 87% of the East Asian population, all trends affecting the sub-region are *de facto* Chinese trends. This applies, in particular, to the sharp rate of decrease in the rural population since 2001-2005 (-17%) due to a combination of factors, including foremost the recently relaxed one-child policy.

Table 5.1. Comparison of selected agricultural indicators in Eastern Asia, Southeast Asia and the world

Region		Eastern Asia		South-East Asia		World	
Variable		**Average**	**C%**	**Average**	**C%**	**Average**	**C%**
Population (million)	Total	1594	5	615	12	7140	12
	Urban	925	32	284	30	3764	23
	Rural	691	−17	331	1	3357	2
Land (million ha)	Total	1156	0	640	0	13009	0
	Forest	253	7	94	4	4009	−1
	Agricultural	638	−2	316	−5	4885	−1
	Arable	116	−6	221	−2	1404	0
	Irrigated	73	13	109	10	327	8
Production (million tons)	Cereals	558	31	248	32	2639	22

[6] Urbanization keeps increasing in most areas (with rates as high as 94% in Japan and 100% in Singapore, where crop agriculture disappeared in the 1990s), while the share of agriculture GNP drops. For example, in Vietnam this share today is 17%, down from 40% in the late 1980s; in Cambodia it is still 90%.

Region		Eastern Asia		South-East Asia		World	
Variable		Average	C%	Average	C%	Average	C%
	Fiber crops	7	5	0	0	31	14
	Fruits	154	71	54	24	654	29
	Oil crops	17	10	58	75	187	49
	Pulses	5	−21	6	83	74	25
	Roots and tubers	177	−8	79	54	805	13
	Sugar	14	19	15	28	172	20
	Vegetables	597	34	41	37	1110	29
	Maize	204	62	39	63	933	41
	Rice, paddy	223	14	208	28	727	21
	Wheat	122	31	0	45	690	16
	Potatoes	96	28	2	21	367	14
	Soybeans	14	−17	2	11	271	39
Local Food Availability (LFA) ratio	Cereals	0.91		0.96			
	Oil	0.18		0.85			
	Sugar	0.67		1.09			

Note: "Average" stands for the average of whichever years are available in FAOSTAT between 2011 and 2015. "Irrigated" stands for "equipped for irrigation," which may differ from "actually irrigated". C% is the percentage of change between the average of 2001-2005 and 2011-15; it is thus not the annual rate of change. The local food availability ratio (LFA ratio) was computed as local production divided by availability, which in turn is obtained as local production plus imports minus exports.

The climatic environment and agriculture

Due to the wide geographic extension, combined with a very varied topography (figure 5.5), the region covers about 15 climate classes (figure 5.6) conditioned by altitude and continentality in east Asia, while topography has a limited influence on the prevailing tropical (continental Southeast Asia) and equatorial conditions (maritime Southeast Asia). The climate range results in a similarly complex agricultural environment ranging from cold desert conditions in the north (too cold for winter crops, but favorable for irrigated summer crops or livestock husbandry; D and B climates) to temperate conditions that can accommodate both winter and summer crops. (Additional detail will be provided below in the comments about the crop distribution map (figure 5.9) after examining the constraints linked to water shortage, which are dominant in the northern sub-region.)

Figure 5.5. Topography

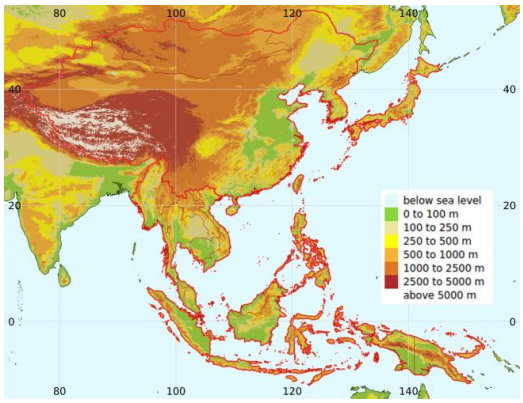

Figure 5.6. Köppen 1971-2000 Climate map

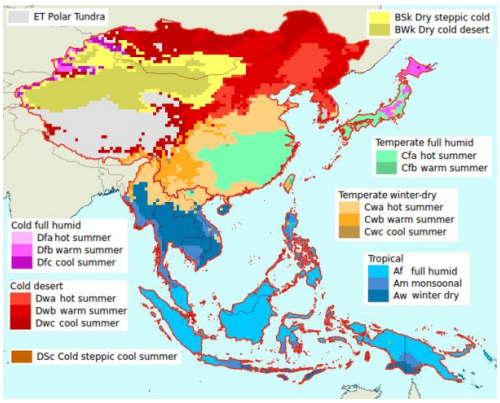

Note: Köppen 1971-2000 climate map based on Kottek et al., 2006.

Figures 5.7 and 5.8 illustrate the water availability in the region. Significant amounts of rainfall in excess of 1000 mm annually occur in areas roughly south of the Yangtze in China, the Korean peninsula and Japan. They are the same areas where a weak positive water balance (rainfall-evapotranspiration, see figure 5.8) appears along a north-south gradient, reaching large excesses in Indonesia (Borneo, Papua province and, to some extent, western Java), parts of the Philippines, and in Papua New-Guinea. A climates are typical tropical forest areas, which are also conducive to plantation crops such as rubber and

oil palm. This directly influences the ratio between arable land and permanently cropped land, which reaches high values in some countries in the region, for instance 1/1 in Papua New-Guinea or 1/5 in Malaysia.

A large share of the population actually lives in the basin of the rivers that flow from the Himalayas, creating some complex situations that typically characterize international rivers (see the Mekong in Figure 5.9) in that climate in one location, for example in Tibet and Yunnan, can affect crops at far distances, such as in the Mekong Delta, more than 3000 km away.

Overall, the distribution of rainfall during the year—either in winter (parts of Mindanao, Sumatra, and most of the Cf climates in China), summer (most of Cw climate in China), or throughout the year (much of the equatorial belt), the length of the growing season and rainless periods (just two or three winter months in Hainan), cold weather, and the availability of non-rain sources of water, together result in a large diversity of crop growing seasons.

Figure 5.7. Annual precipitation (mm)

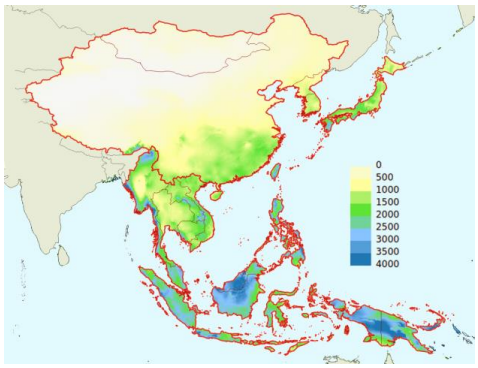

Note: Based on data in Kritikos et al., 2012.

Figure 5.8. Annual water balance as rainfall-Potential Evapotranspiration (PET) (mm)

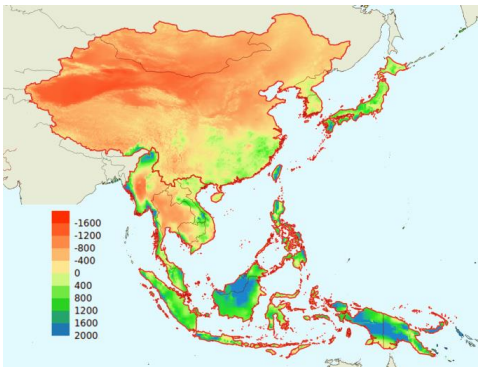

Note: Prepared with data from Kritikos et al., 2012, and Zomer et al (2006, 2008) for PET.

Crop distribution and irrigation

As mentioned, climate and irrigation water availability largely condition the distribution of the crops cultivated in the region (figure 5.9). While the highest latitudes can cultivate only summer crops due to cold winter (such as in Northeast China), more temperate areas grow mostly winter wheat and summer crops (especially rice and maize, and frequently soybean, sunflower and potatoes as well) until tropical climates are reached along a latitudinal gradient in continental Southeast Asia. Here, in A climates, the main crop is usually harvested at the end of the year around the time that a secondary crop is planted, to be harvested in May or June. In the Cf climates of eastern Asia, multiple crops are practiced under irrigated conditions, often involving a winter crop and one or two summer crops.

Rice, the preferred cereal in eastern and southeastern Asia, dominates the agricultural landscape from the south of Japan, the southern Korean Peninsula, and the remaining region approximately south of the Yangtze. Wheat still remains confined to higher latitudes but, as also discussed below, the continental Southeast Asian countries are making efforts to develop the crop. The recent trends also show that maize is likely to continue expanding, essentially at the expense of rice, in most of the region where the crop is climatically suitable, with or without irrigation, a concept that covers several levels of water control.

In the driest areas, where natural moisture is always in short supply, water can be obtained only from rivers, where available, or from aquifers, at least during part of the year if temperature conditions permit. It is typical, in tropical areas (Am or Aw in figure 5.6), that irrigation is applied during the season when rainfall is insufficient, but temperature is conducive to plant growth. It is common, in all A climates, to

have the dominant rice crop cultivated behind bunds that retain rainfall. Strictly speaking, the rice cultivated under those conditions (lowland rice) is rainfed and may occasionally suffer drought, just as upland rice, which is also cultivated using only rainfall.[7]

As shown in figure 5.10, Irrigation percentages up to 25% are common along the Pacific coast of the region in Northeast China, the Loess region, Southeastern China, and most of the region south of the Yangtze, including continental Southeast Asia from Vietnam to Myanmar. Higher irrigation percentages (>25% to 50%) occur along the Yangtze and in patches in western Gansu-Xinjiang, southern Sagaing and southern Ayeyawaddy delta in Myanmar, and the Red River area in Vietnam. Next, even higher irrigation densities (>50% of land irrigated) are most relevant in China (Huanghuaihai and the Yangtze delta) and Vietnam (Mekong delta). Highest irrigation percentages (75% and above, sometimes reaching more than 90%) occur in central Liaoning province (Northeast China) and in northern-central Thailand where double and triple rice cropping is practiced in Suphanburi, NakhonPathom, Nonthaburi, PathumThani, PhraNakhon, and Si Ayudhya and adjacent areas. The listed areas in Thailand and China are somehow comparable to central California and the Nile delta, but very far from reaching the level of irrigation occurring in the area from Punjab (Pakistan and India) and Haryana and Uttar Pradesh, where virtually all land is irrigated.

In maritime Southeast Asia, irrigation is less widespread due to equatorial conditions with regular water supply throughout the year. It is, however, practiced in the northern Philippines (central Luzon and the Cagayan valley), as well as in limited areas in Indonesia (Tengah and Timur at Java), which happen to be areas where the full humid tropical climate (Af) gives way to winter dry climate as the distance to the equator increases.

Figure 5.9. Distribution of main cereals (rice, wheat, maize)

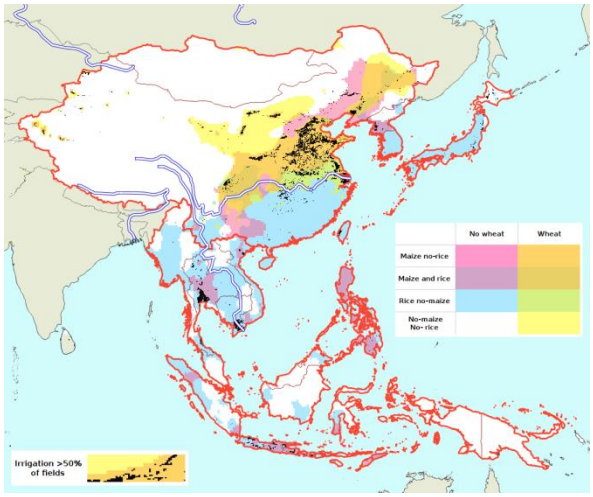

Figure 5.10. Percentage of irrigated crop area according to GMIA (2017)

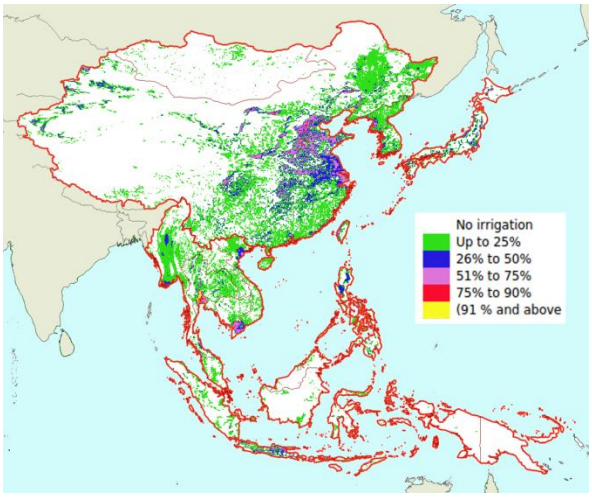

Note: Based on crop distribution data from JRC (Vancutsem et al., 2013). The large rivers relevant for the region are the west-east flowing Yangtze (entirely in China) and the north-south flowing Brahmaputra and Mekong.

[7] Upland Rice is often cultivated at high elevations, where precipitation is abundant. The defining factor, however, is not elevation but the fact that the crop is rainfed and not cultivated in flooded fields. Upland rice can thus be cultivated at sea level if precipitation permits.

Crop production

China not only "dominates" all population statistics in Eastern Asia (87% or the people in the sub-region are Chinese), but the same is true for agriculture. China produces an even larger share (96%) of both cereals and tubers, indicating that, in spite of fast industrial and economic growth, agriculture retains a larger importance than in some other countries in the sub-region, especially Japan and the Republic of Korea. When considering the larger region, the share of China decreases to 67% and 65% (cereal and roots and tuber production), with Indonesia and Thailand coming next with 11% and 5% shares for cereals and 11% for roots and tubers in both countries. Vietnam comes third with shares of 6% and 4%, respectively. When compared to the Southeast Asian sub-region alone, the percentages for Thailand, Indonesia, and Vietnam increase about threefold.

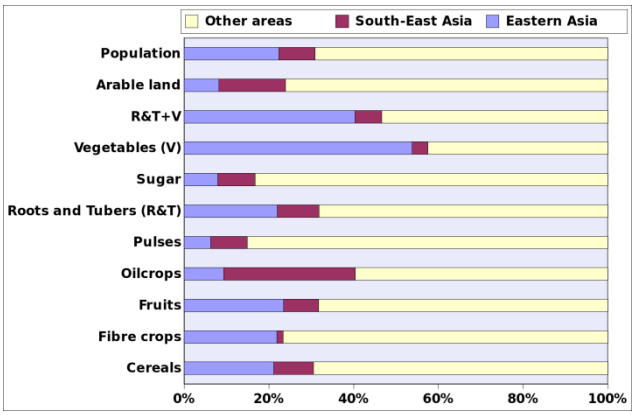

Figure 5.11. Relative contribution of East and Southeast Asia to the global production of major crops

*Note: "*Other areas" was obtained by subtracting eastern and southeastern Asia data from worldwide data.
Source: Data source is FAOSTAT.

Figure 5.11 shows the relative contribution of the region and the two sub-regions to the global production of main crop groups, while table 5.1 adds detail about recent change dynamics. Due to the specific features of diets in the region, where meat plays a subordinate role compared with plants, vegetables is the only category where the region produces more than half of the world output (58%) while vegetables in the broad sense (that is, including roots and tubers) reach 47%. As far as dynamics are concerned, the increase in production of cereals (+31% in eastern Asia and +32% in the southeast of the region), fruits (+71% in eastern Asia), and potatoes (+28% and +21%) all exceed the worldwide recent growth rates of +22%, +29%, and +14% respectively).

The figure given for cereals hides the fact that wheat (31% and 45% for the two regions respectively vs. 16% globally) and especially maize (+62% and +63% vs. 41%) are growing fast, while rice is lagging behind in eastern Asia (+14%). Together with the southeastern Asian countries, the regional increase of rice production reaches 20%, a value close to the worldwide value of 21%. The most significant decreases are those of pulses and especially soybeans. For pulses, the 14% increase over the last 15 years (to be compared with +25% for worldwide production) was brought about by a decrease in eastern Asia that reached 21%. Similarly, the stagnation of soybean (0% change since 2001-2005) is due to a large decrease in all eastern Asian countries and a modest increase of 11% in the southeast. This compares with the spectacular worldwide increase (+39%) of a crop which, together with maize, is one of the favorite crops of the moment, largely owing to the large demand precisely in eastern Asia. In 2016, however, due to changes in policy, soybean production increased for the first time in China after a more than decade-long decrease that was compensated by massive imports.

Owing mainly to climate conditions, oil crops (in particular oil palm, a typical plantation crop in A climates) are the only category where southeast Asia out-produces the eastern sub-region (58 vs 17 million tons of output) and where the rate of change since 2001-2005 is one of the highest (+75% or 53% above the global rate of change). This comes, however, at a large environmental cost as deforestation rather than agricultural land reallocation is the source for the new land.

Statistics do confirm the liking of the region for maize with a number of countries increasing their production by more than 50% (China, 68%; Indonesia, 74%; Lao, 534%; Myanmar, 125%; Philippines, 53%; Papua New-Guinea, 66%, and Vietnam, 68%). The list includes Vietnam, a significant exporter of maize, next to Thailand (+14% "only"). Actually, Thailand and neighboring Myanmar both put a lot of emphasis on cassava (+50% and +1286% increases in production, respectively, with +92% in Vietnam) and, interestingly, in wheat (+44% both), of which the production is currently insignificant in Southeast Asia,[8] among others because the crop cannot compete with other commodities in the Af climates of maritime Southeast Asia. For roots and tubers, in addition to cassava, farmers in the region have also increased the production of potatoes (Thailand, +50%) and sweat potatoes (Malaysia, +94%), as well as other traditional crops such as yams in Laos (+587%) and Cambodia (+2120%), as well as Myanmar (+109%), confirming the come-back of a country that used to be a major exporter of rice thirty years ago.

Finally, rice production doubled in Cambodia, an isolated observation regarding a crop that is so well established in the region (59% of world production) that it dominates the landscape, the diet, and the culture… while at the same time losing ground to other summer crops, especially in the eastern Asian sub-region.

Trade

Figures 5.12 and 5.13, based on FAOSTAT data, represent sums of exports/imports of the individual countries inside the two sub-regions. However, as such they do not take into consideration that exports to or imports from countries inside the group do not actually leave the group and should not be counted.

Figure 5.12. Exports of major crop categories by Eastern and Southeastern countries compared with the rest of the world

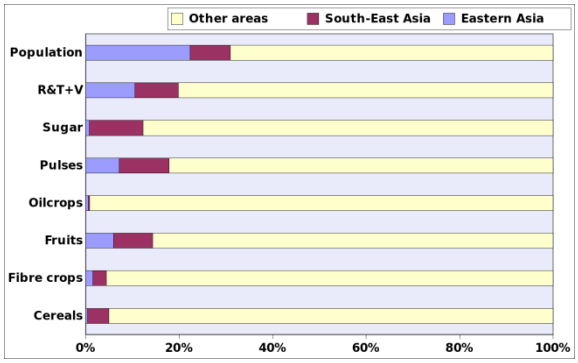

Source of data: FAOSTAT.

Figure 5.13. Imports of major crop categories by Eastern and Southeastern countries compared with the rest of the world

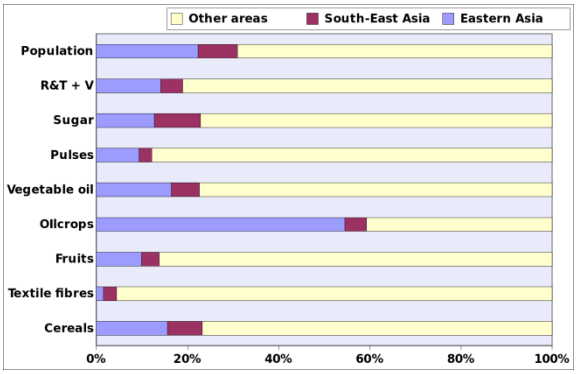

Source of data: FAOSTAT.

Nevertheless, the figures show that *exports* from Southeast Asia, for instance for sugar (sugarcane), exceed those of Eastern Asia, while food *imports* in all categories tend to be largest in Eastern Asia, again reflecting the weight of China in terms of production and trade as well. Eastern Asia imports about 60 million tons of soybeans, which is almost entirely absorbed by China (90%) with the rest going to Japan. Of the 56 million tons of cereals that go to Eastern Asia, 26 go to Japan, while the Republic of Korea absorbs 13 million tons and China (including the province of Taiwan) 17 million tons. In all Eastern Asian countries, the cereal imports are made up by approximately one-third of wheat and two-thirds of maize, while China usually also imports some other coarse grains next to maize (such as barley and sorghum as animal feeds) and about 2 million tons of rice as well. The most remarkable—and often quoted—success

[8] In tropical countries, wheat and other temperate cereals (such as barley) are typically grown as an irrigated crop in Aw climates where the cold and dry seasons coincide.

stories in the region include the export of refined sugar from Thailand (up 29% from the early 2000s) as well as rice exports from Vietnam, which rose 77% in about 15 years. During the same period, Japan reduced soybean imports by 45% to 3 million tons, and maize imports by 10% to 15 million ton.

Southeast Asia imports 28 million tons of cereals distributed as follows: Indonesia, 11 million tons; Malaysia, 5 million; Vietnam, 4 million; the Philippines, 4 million; and Thailand, 2 million. The volume is made up (approximately half) by wheat, with the difference shared equally between maize and rice. Southeastern Asia imports 6 million ton of soybean, which go mostly to Indonesia and Thailand in about equal shares (2 million tons) and to Vietnam and Malaysia. The sharpest changes in food imports over the recent decade include a 129% increase in maize imports to reach 3 million tons in Indonesia, a doubling of wheat imports to Vietnam (which now exceed 2 million ton annually), as well as the already mentioned soybean bought by China. Wheat imports where quintupled in a decade in China, while maize climbed from 50 thousand tons in 2008 to 5 million tons in 2012, equivalent to a more than hundredfold increase in just five years, mostly to take advantage of favorable international prices and to pave the way for some internal reforms.

5.4 Update on El Niño

El Niño has continued to be neutral during the fourth quarter of 2016 and the start of 2017. The eastern tropical Pacific sea surface temperatures have kept cooling between July and January according to the Optimum Interpolation Sea Surface Temperature (OISST). Temperatures are predicted to rise moderately while staying altogether average until the third quarter of 2017 according to the Beijing Climate Center (figure 5.14).

Figure 5.15 illustrates the behavior of the standard Southern Oscillation Index (SOI) of the Australian Bureau of Meteorology (BOM) from January 2016 to January 2017. During the current season, SOI has increased rapidly from -4.3 in October to +2.6 in December, followed by a minor decreased +1.3 in January, 2017, indicating neutral conditions of El Niño.

NOAA confirms the cooler-than-average sea temperature in the central-eastern tropical Pacific Ocean and that La Niña is no longer present (figure 5.16). BOM and NOAA agree on a neutral El Niño for 2017. CropWatch will nevertheless keep monitoring El Niño trends.

Figure 5.14. Tropical Pacific SSTA (Forecasted and monitored datasets)

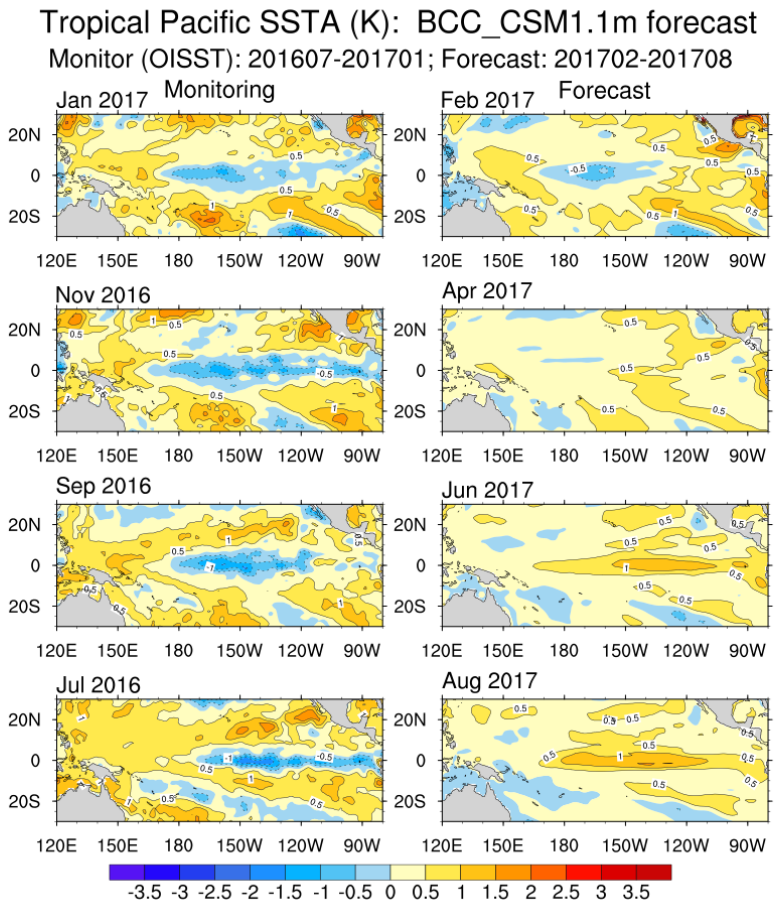

Source: http://cmdp.ncc-cma.net/download/ENSO/Variables_evolution/ENSO_SSTA_Patterns_O7P7_20170201.png

Figure 5.15. MonthlySOI-BOM time series for January 2016 to January 2017

Source: http://www.bom.gov.au/climate/current/soi2.shtml.

Figure 5.16. Average sea surface temperature (SST) anomalies (°C) for the week of February 1, 2017

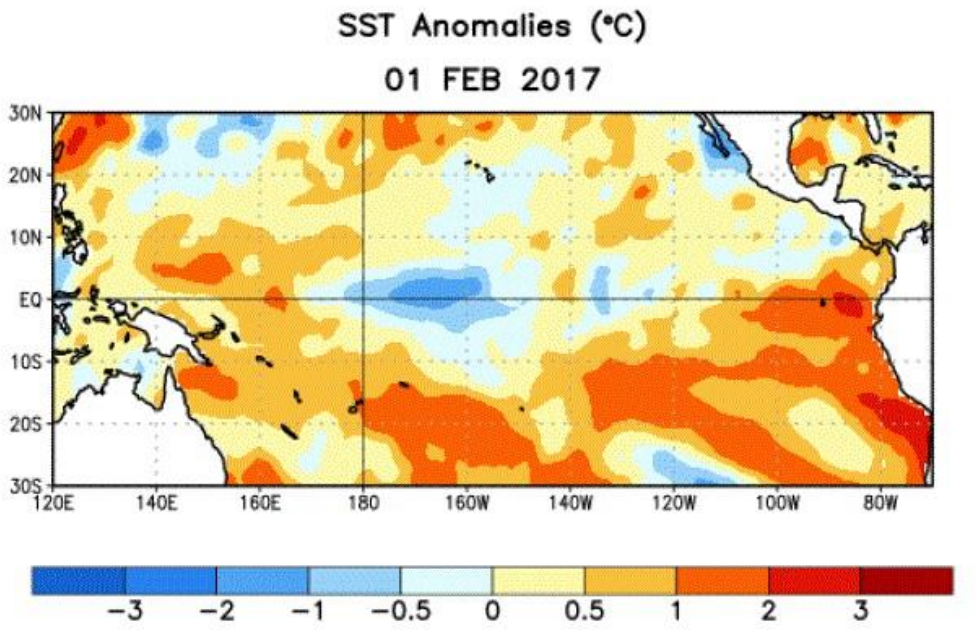

Note: Anomalies are computed with respect to the 1981-2010 base period weekly means.

Annex A. Agroclimatic indicators and BIOMSS

Table A.1. October 2016-January 2017 agroclimatic indicators and biomass by global Monitoring and Reporting Unit

		RAIN		TEMP		RADPAR		BIOMSS	
	65 Global MRUs	Current (mm)	15YA dep. (%)	Current (°C)	15YA dep. (°C)	Current (MJ/m^2)	15YA dep. (%)	Current (gDM/m^2)	5YA dep. (%)
1	Equatorial central Africa	510	-8	25.9	0.4	1225	8	1496	-4
2	East African highlands	121	-40	19.8	0.1	1317	7	467	-30
3	Gulf of Guinea	251	7	27.1	-0.2	1148	0	685	3
4	Horn of Africa	189	-44	24.8	-0.3	1360	6	619	-37
5	Madagascar (main)	449	-41	24.3	-0.7	1381	8	1299	-21
6	Southwest Madagascar	353	-20	24.8	-0.9	1478	3	1089	-10
7	North Africa-Mediterranean	163	-7	13.2	-0.3	698	-1	566	-2
8	Sahel	41	-19	28.0	0.2	1276	1	135	-19
9	Southern Africa	474	7	24.9	-0.6	1369	2	1308	3
10	Western Cape (South Africa)	44	-65	18.6	0.0	1598	4	221	-55
11	British Columbia to Colorado	330	32	-3.8	-0.2	444	-4	509	11
12	Northern Great Plains	213	35	1.3	1.0	477	-5	647	28
13	Corn Belt	371	1	3.7	1.5	431	-5	885	11
14	Cotton Belt to Mexican Nordeste	344	-8	13.5	1.4	667	-2	957	-1
15	Sub-boreal America	180	18	-6.0	1.9	231	-13	451	15
16	West Coast (North America)	425	20	6.7	-0.4	496	-8	825	15
17	Sierra Madre	104	-18	15.6	0.4	1024	0	384	-11
18	SW U.S. and N. Mexican highlands	145	51	9.0	0.8	753	-4	459	22
19	Northern South and Central America	472	2	25.8	-0.2	961	2	1139	3
20	Caribbean	328	-2	24.4	-0.7	903	-2	798	-14
21	Central-northern Andes	598	5	16.6	0.0	1172	4	1282	1
22	Nordeste (Brazil)	196	-30	28.6	0.8	1378	1	550	-28
23	Central eastern Brazil	720	-4	26.2	-0.6	1268	4	1801	-2
24	Amazon	962	20	27.8	-0.5	1098	1	2054	5
25	Central-north Argentina	453	4	25.1	-1.3	1351	5	1366	3
26	Pampas	759	19	22.5	-0.7	1379	1	1717	7
27	Western Patagonia	86	-44	13.4	0.0	1410	-2	377	-28
28	Semi-arid Southern Cone	102	-17	18.6	-0.6	1543	4	412	-5
29	Caucasus	266	-6	2.1	-1.6	554	1	684	-11
30	Pamir area	246	77	2.8	0.3	709	-2	517	24
31	Western Asia	156	17	6.5	-0.5	653	0	453	1
32	Gansu-Xinjiang (China)	135	156	-3.6	0.3	564	-4	400	127
33	Hainan (China)	536	46	22.3	0.5	669	-15	935	41
34	Huanghuaihai (China)	168	107	6.7	0.6	566	-13	639	99
35	Inner Mongolia (China)	123	151	-5.2	0.7	548	-4	410	91
36	Loess region (China)	159	121	2.8	1.3	614	-9	582	101
37	Lower Yangtze (China)	221	-12	12.5	1.0	552	-21	790	6
38	Northeast China	172	90	-8.7	-0.6	472	-3	345	7
39	Qinghai-Tibet (China)	120	17	2.4	1.1	864	2	354	15
40	Southern China	170	-7	17.4	1.0	726	-9	577	4
41	Southwest China	149	-5	10.3	0.9	529	-12	527	0
42	Taiwan (China)	250	33	19.3	0.7	741	-3	694	17
43	East Asia	174	-18	-1.4	-0.2	499	-4	515	-5
44	Southern Himalayas	136	-4	18.5	0.7	885	0	384	-4
45	Southern Asia	122	-48	23.8	-0.2	1068	4	343	-39

	65 Global MRUs	RAIN		TEMP		RADPAR		BIOMSS	
		Current (mm)	15YA dep. (%)	Current (°C)	15YA dep. (°C)	Current (MJ/m²)	15YA dep. (%)	Current (gDM/m²)	5YA dep. (%)
46	Southern Japan and Korea	303	-25	9.6	0.5	573	-4	1056	-6
47	Southern Mongolia	140	366	-9.9	0.3	462	-4	340	168
48	Punjab to Gujarat	84	201	21.3	-0.1	964	0	226	114
49	Maritime Southeast Asia	1285	15	25.5	-0.5	928	-5	2345	6
50	Mainland Southeast Asia	631	79	25.3	0.0	906	-8	1138	44
51	Eastern Siberia	116	-31	-13.0	-2.3	292	4	220	-33
52	Eastern Central Asia	52	-3	-16.8	-0.9	358	0	151	-21
53	Northern Australia	676	13	26.9	-0.7	1258	-3	1506	5
54	Queensland to Victoria	195	-21	20.5	-0.4	1494	1	772	-6
55	Nullarbor to Darling	61	-40	18.8	-1.0	1609	2	240	-44
56	New Zealand	145	-52	13.4	-0.3	1274	-2	667	-36
57	Boreal Eurasia	258	-2	-4.2	-0.7	130	0	455	-13
58	Ukraine to Ural mountains	212	4	-2.8	-1.6	192	-5	552	-12
59	Mediterranean Europe and Turkey	244	-24	7.9	-1.4	542	1	796	-16
60	W. Europe (non Mediterranean)	231	-20	3.9	-2.1	299	-3	797	-14
61	Boreal America	276	-12	-7.5	0.6	145	-1	375	7
62	Ural to Altai mountains	175	32	-9.8	-1.9	241	-7	314	-20
63	Australian desert	135	45	20.9	-1.1	1569	-1	564	39
64	Sahara to Afghan deserts	59	-5	17.8	0.0	975	1	187	-6
65	Sub-arctic America	121	91	-15.2	3.6	38	6	166	205

Table A.2. October 2016-January 2017 agroclimatic indicators and biomass by country

	31 Countries	RAIN		TEMP		RADPAR		BIOMSS	
		Current (mm)	15YA Departure (%)	Current (°C)	15YA Departure (°C)	Current (MJ/m²)	15YA Departure (%)	Current (gDM/m²)	5YA Departure (%)
[ARG]	Argentina	608	23	22.1	-0.9	1417	2	1466	8
[AUS]	Australia	216	-15	20.9	-0.5	1499	1	705	-8
[BGD]	Bangladesh	240	5	22.4	-0.2	922	0	613	16
[BRA]	Brazil	769	5	26.4	-0.4	1233	2	1719	-2
[CAN]	Canada	259	12	-4.1	1.5	282	-9	508	17
[CHN]	China	176	12	7.5	0.7	577	-12	531	25
[DEU]	Germany	194	-24	3.2	-1.4	228	-8	828	-11
[EGY]	Egypt	37	-35	17.5	-0.6	798	0	153	-3
[ETH]	Ethiopia	116	-26	20.2	0.2	1310	8	446	-20
[FRA]	France	201	-36	5.6	-3.5	357	3	683	-35
[GBR]	UK	255	-31	6.4	-2.3	200	-1	967	-18
[IDN]	Indonesia	1251	13	25.6	-0.6	946	-5	2357	6
[IND]	India	101	-30	21.9	0.1	1017	3	287	-21
[IRN]	Iran	188	-1	7.5	-0.3	751	1	482	-15
[KAZ]	Kazakhstan	170	41	-7.3	-1.3	301	-8	394	-7
[KHM]	Cambodia	784	120	27.1	-0.3	934	-10	1449	62
[MEX]	Mexico	148	-24	19.7	0.6	969	1	449	-8
[MMR]	Myanmar	248	7	22.7	0.2	913	-3	713	10
[NGA]	Nigeria	170	-5	27.2	0.0	1218	0	387	-9
[PAK]	Pakistan	85	30	15.2	0.4	860	-1	213	20
[PHL]	Philippines	1354	50	25.3	-0.5	858	-6	2099	20
[POL]	Poland	250	31	1.9	-1.0	197	-14	794	-2
[ROU]	Romania	242	11	0.9	-2.2	347	-6	733	-2
[RUS]	Russia	176	-1	-7.2	-1.8	221	-2	380	-18
[THA]	Thailand	581	82	25.4	0.0	930	-7	1006	38
[TUR]	Turkey	272	-15	3.9	-1.3	594	2	745	-16

31 Countries		RAIN		TEMP		RADPAR		BIOMSS	
		Current (mm)	15YA Departure (%)	Current (°C)	15YA Departure (°C)	Current (MJ/m²)	15YA Departure (%)	Current (gDM/m²)	5YA Departure (%)
[UKR]	Ukraine	249	33	0.2	-1.7	260	-7	695	-4
[USA]	USA	317	5	6.7	1.1	554	-3	781	12
[UZB]	Uzbekistan	300	100	3.9	-0.8	551	-2	725	51
[VNM]	Vietnam	750	74	22.7	0.7	723	-11	1218	38
[ZAF]	South Africa	402	9	20.9	-0.2	1416	1	1179	-1

See note table A.1.

Table A.3. Argentina, October 2016-January 2017 agroclimatic indicators and biomass (by province)

	RAIN		TEMP		RADPAR		BIOMSS	
	Current (mm)	15YA Departure (%)	Current (°C)	15YA Departure (°C)	Current (MJ/m²)	15YA Departure (%)	Current (gDM/m²)	5YA Departure (%)
Buenos Aires	474	7	20.0	-0.4	1488	0	1336	0
Chaco	764	37	24.8	-1.5	1360	1	1904	25
Cordoba	456	3	21.8	-1.1	1461	3	1351	-4
Corrientes	1072	42	23.9	-1.2	1365	0	2039	18
Entre Rios	849	47	22.3	-1.0	1420	0	1790	14
La Pampa	460	18	21.0	-0.5	1572	3	1433	15
Misiones	939	4	23.8	-0.8	1342	4	2098	8
Santiago Del Estero	480	9	24.7	-1.4	1345	2	1472	9
San Luis	389	-4	21.0	-1.0	1547	6	1360	2
Salta	482	6	24.1	-1.2	1301	7	1350	2
Santa Fe	817	48	23.0	-1.1	1412	0	1859	18
Tucuman	352	-18	23.1	-1.2	1322	8	1136	-13

See note table A.1.

Table A.4. Australia, October 2016-January 2017 agroclimatic indicators and biomass (by state)

	RAIN		TEMP		RADPAR		BIOMSS	
	Current (mm)	15YA Departure (%)	Current (°C)	15YA Departure (°C)	Current (MJ/m²)	15YA Departure (%)	Current (gDM/m²)	5YA Departure (%)
New South Wales	196	-19	21.3	-0.3	1527	2	776	-4
South Australia	136	23	18.3	-0.9	1491	-2	641	28
Victoria	148	-25	17.0	-0.8	1435	-2	704	-8
W. Australia	110	-10	19.6	-0.9	1594	2	284	-36

See note table A.1.

Table A.5. Brazil, October 2016-January 2017 agroclimatic indicators and biomass (by state)

	RAIN		TEMP		RADPAR		BIOMSS	
	Current (mm)	15YA Departure (%)	Current (°C)	15YA Departure (°C)	Current (MJ/m²)	15YA Departure (%)	Current (gDM/m²)	5YA Departure (%)
Ceará	166	-11	28.8	0.2	1369	-2	513	0
Goias	737	-14	25.7	-0.7	1315	8	2022	-4
Mato Grosso do Sul	740	6	26.2	-1.5	1306	3	1961	4
Mato Grosso	1057	6	27.3	-0.5	1184	3	2347	2
Minas Gerais	719	-12	24.8	0.1	1299	5	1738	-8
Parana	719	-8	23.1	-0.7	1267	4	1917	0
Rio Grande do Sul	977	30	22.7	-0.4	1316	0	1858	7
Santa Catarina	846	2	21.2	-0.1	1187	-1	1811	-8
Sao Paulo	821	4	24.3	-0.7	1272	4	2062	5

See note table A.1.

Table A.6. Canada, October 2016-January 2017 agroclimatic indicators and biomass (by province)

	RAIN		TEMP		RADPAR		BIOMSS	
	Current (mm)	15YA Departure (%)	Current (°C)	15YA Departure (°C)	Current (MJ/m²)	15YA Departure (%)	Current (gDM/m²)	5YA Departure (%)
Alberta	101	-5	-5.8	0.9	255	-9	407	3
Manitoba	198	63	-4.7	2.6	276	-13	541	29
Saskatchewan	149	50	-5.9	1.7	271	-13	457	18

See note table A.1.

Table A.7. India, October 2016-January 2017 agroclimatic indicators and biomass (by state)

	RAIN		TEMP		RADPAR		BIOMSS	
	Current (mm)	15YA Departure (%)	Current (°C)	15YA Departure (°C)	Current (MJ/m²)	15YA Departure (%)	Current (gDM/m²)	5YA Departure (%)
Arunachal Pradesh	217	1	16.4	1.3	812	1	684	1
Andhra Pradesh	67	-71	25.0	-0.4	1104	6	221	-60
Assam	168	-7	22.8	1.2	851	1	506	0
Bihar	66	-23	21.4	-0.2	936	1	203	-27
Chhattisgarh	79	-25	21.8	-0.4	1062	3	223	-37
Daman and Diu	84	84	24.5	-1.4	1083	0	239	42
Delhi	127	240	19.9	0.5	918	1	425	148
Gujarat	142	473	24.3	-0.2	1052	-1	344	264
Goa	63	-69	24.5	-0.4	1160	3	293	-46
Himachal Pradesh	218	84	4.4	1.3	857	-2	415	13
Haryana	125	201	18.9	0.4	902	0	376	125
Jharkhand	48	-58	21.0	0.2	998	2	181	-51
Kerala	205	-62	25.4	-0.2	1097	2	695	-40
Karnataka	53	-74	24.1	-0.2	1159	5	203	-64
Meghalaya	184	-28	19.4	1.5	875	0	509	4
Maharashtra	59	-42	23.4	-0.5	1095	3	192	-39
Manipur	206	8	17.3	1.2	891	1	579	-1
Madhya Pradesh	39	-34	21.4	0.0	1037	3	166	-24
Mizoram	303	17	18.5	0.2	935	0	716	6
Nagaland	148	-15	17.4	1.9	841	1	466	-20
Orissa	126	-28	23.1	0.0	1042	4	324	-33
Puducherry	260	-82	27.0	-0.1	1059	9	957	0
Punjab	107	73	17.8	0.6	849	0	300	23
Rajasthan	66	292	21.0	-0.3	981	0	205	192
Sikkim	56	-62	6.1	1.2	908	3	208	-45
Tamil Nadu	216	-60	26.6	0.1	1084	9	748	-34
Tripura	396	60	22.1	0.2	912	-1	789	31
Uttarakhand	153	41	11.0	3.1	898	0	399	22
Uttar Pradesh	86	31	20.4	0.3	946	1	263	12
West Bengal	146	-18	23.0	0.5	948	2	380	-17

See note table A.1.

Table A.8. Kazakhstan, October 2016-January 2017 agroclimatic indicators and biomass (by oblast)

	RAIN		TEMP		RADPAR		BIOMSS	
	Current (mm)	15YA Departure (%)	Current (°C)	15YA Departure (°C)	Current (MJ/m²)	15YA Departure (%)	Current (gDM/m²)	5YA Departure (%)
Akmolinskaya	139	33	-9.0	-1.1	235	-12	325	-18
Karagandinskaya	146	50	-8.8	-1.1	295	-11	320	-20
Kustanayskaya	135	22	-8.8	-1.9	233	-8	349	-17
Pavlodarskaya	129	58	-9.1	-1.3	234	-12	316	-15
Severo	143	33	-9.9	-1.9	200	-9	306	-22
Vostochno	219	45	-10.0	-1.0	330	-11	308	-16
Zapadno	128	-2	-4.8	-2.0	272	-3	502	-8

See note table A.1.

Table A.9. Russia, October 2016-January 2017 agroclimatic indicators and biomass (by oblast, kray and republic)

	RAIN		TEMP		RADPAR		BIOMSS	
	Current (mm)	15YA Departure (%)	Current (°C)	15YA Departure (°C)	Current (MJ/m²)	15YA Departure (%)	Current (gDM/m²)	5YA Departure (%)
Bashkortostan	220	17	-8.4	-2.3	192	-4	352	-22
Chelyabinskaya	137	17	-9.3	-2.4	203	-6	328	-19
Gorodovikovsk	254	3	1.4	-2.2	323	-1	778	-7
Krasnodarskiy	181	-23	-4.8	-1.5	286	1	432	-19
Kurganskaya	127	7	-10.7	-3.2	189	-2	298	-26
Kirovskaya	169	-27	-8.4	-3.0	134	4	354	-25
Kurskaya	221	18	-2.0	-1.5	214	-5	585	-14
Lipetskaya	205	8	-2.9	-1.6	206	-4	545	-16
Mordoviya	162	-21	-4.6	-1.6	184	1	480	-16
Novosibirskaya	180	24	-11.8	-2.1	192	-2	247	-33
Nizhegorodskaya	169	-22	-5.2	-1.9	155	2	458	-18
Orenburgskaya	179	15	-7.0	-1.8	230	-7	408	-16
Omskaya	148	14	-12.1	-2.8	183	0	255	-32
Permskaya	187	-13	-10.5	-3.4	146	5	297	-29
Penzenskaya	168	-17	-4.5	-1.6	199	-2	488	-15
Rostovskaya	159	-29	0.1	-1.7	303	0	656	-12
Ryazanskaya	178	-11	-3.6	-1.5	177	-1	515	-16
Stavropolskiy	208	5	1.7	-2.2	337	-5	731	-4
Sverdlovskaya	139	-2	-11.5	-3.8	156	-1	280	-30
Samarskaya	187	9	-6.1	-2.1	213	-1	438	-17
Saratovskaya	138	-16	-4.1	-1.7	242	-1	518	-12
Tambovskaya	190	-5	-3.4	-1.5	207	-3	530	-15
Tyumenskaya	143	10	-12.2	-3.5	168	-2	265	-31
Tatarstan	176	-9	-6.8	-2.5	180	1	404	-23
Ulyanovskaya	163	-8	-5.4	-1.9	198	-1	456	-17
Udmurtiya	180	-16	-8.8	-3.1	151	4	341	-27
Volgogradskaya	153	-11	-2.0	-1.8	271	-1	607	-8
Voronezhskaya	192	3	-2.1	-1.4	233	-3	592	-11

See note table A.1.

Table A.10. United States, October 2016-January 2017 agroclimatic indicators and biomass (by state)

	RAIN		TEMP		RADPAR		BIOMSS	
	Current (mm)	15YA Departure (%)	Current (°C)	15YA Departure (°C)	Current (MJ/m²)	15YA Departure (%)	Current (gDM/m²)	5YA Departure (%)
Arkansas	416	-20	11.5	1.6	604	-3	1261	2
California	348	45	7.9	-0.2	600	-8	757	26
Idaho	367	75	-2.9	-1.1	454	-7	601	11
Indiana	360	-8	6.1	1.4	484	-5	1075	8
Illinois	318	-10	5.8	1.5	490	-6	1024	7
Iowa	299	36	3.0	1.6	473	-8	921	32
Kansas	189	11	6.3	1.0	616	-2	538	-11
Michigan	364	16	2.8	1.6	365	-9	890	16
Minnesota	293	63	-1.0	1.7	395	-5	718	35
Missouri	304	-14	7.5	1.4	535	-6	985	0
Montana	268	115	-2.8	-0.9	427	-4	620	43
Nebraska	186	38	3.0	1.1	555	-3	724	44
North Dakota	250	113	-2.8	1.0	398	-5	642	57
Ohio	346	0	5.9	1.5	465	-4	1074	10
Oklahoma	248	-7	10.1	1.0	655	-2	828	1
Oregon	429	22	2.4	-1.1	397	-10	811	9
South Dakota	241	86	0.4	0.7	488	-2	775	75
Texas	271	2	14.7	1.4	704	-4	754	7
Washington	407	13	1.5	-0.9	335	-8	797	11
Wisconsin	353	35	0.9	1.5	402	-5	805	19

See note table A.1.

Table A.11. China, July 2016 - October 2016 agroclimatic indicators and biomass (by province)

	RAIN		TEMP		RADPAR		BIOMSS	
	Current (mm)	15YA Departure (%)	Current (°C)	15YA Departure (°C)	Current (MJ/m²)	15YA Departure (%)	Current (gDM/m²)	5YA Departure (%)
Anhui	245	15	10.2	0.6	524	-23	915	32
Chongqing	176	1	9.9	0.7	396	-22	567	-8
Fujian	286	19	15.0	1.7	604	-20	832	22
Gansu	122	110	1.6	1.3	650	-6	462	115
Guangdong	221	25	18.0	1.0	706	-14	707	41
Guangxi	141	-36	17.0	1.2	644	-11	500	-19
Guizhou	141	-25	11.3	1.2	460	-16	503	-16
Hebei	90	83	1.0	0.6	578	-6	401	83
Henan	189	110	-11.4	-1.3	443	-1	290	-6
Heilongjiang	206	91	8.0	0.6	551	-18	785	79
Hubei	222	22	9.5	0.5	502	-22	774	17
Hunan	177	-32	11.6	0.5	501	-24	670	-16
Jilin	285	85	9.8	0.7	523	-22	1005	82
Jiangsu	224	-26	13.4	1.2	562	-22	791	-5
Jiangxi	192	104	-6.8	-0.1	494	-5	421	20
Liaoning	140	47	-1.6	0.5	543	-5	543	42
Inner Mongolia	121	147	-8.3	0.2	508	-3	335	65
Ningxia	122	182	1.1	1.8	671	-3	457	171
Sichuan	207	102	4.5	1.2	541	-15	730	91
Shandong	162	114	6.7	0.8	575	-11	658	115
Shaanxi	117	85	0.9	1.6	605	-8	485	77
Shanxi	102	-1	9.0	0.9	563	-7	387	-1
Yunnan	134	-20	12.9	0.8	772	0	472	-11
Zhejiang	222	-26	12.5	1.6	525	-22	835	-2

See note table A.1.

Annex B. 2016-2017 Southern hemisphere wheat production estimates

Tables B.1-B.3 present 2016-2017 CropWatch production estimates for wheat in Argentina, Australia, and Brazil.

Table B.1. Argentina, 2016-2017 wheat production, by province (thousand tons)

	Wheat	
	2016-2017	Δ%
Buenos Aires	7268	4
Córdoba	768	7
Entre Rios	1109	3
Santa Fe	1265	5
Sub total	10410	4
Others	835	18
Argentina	11245	5

Δ% indicates percentage difference with previous year.

Table B.2. Australia, 2016-2017 wheat production, by state (thousand tons)

	Wheat	
	2016-2017	Δ%
New South Wales	9839	39.8
South Australia	4794	15.0
Victoria	4354	29.1
Western Australia	12304	15.1
Sub total	31291	23.8
Other states	774	45.1
Australia	32066	24.3

Δ% indicates percentage difference with previous year.

Table B.3 Brazil, 2016-2017 wheat production, by state (thousand tons)

	Wheat	
	2016-2017	Δ%
Parana	2549	14
Rio Grande Do Sul	4528	12
Santa Catarina	357	23
Sub total	7433	13
Others	314	-29
Brazil	7747	10

Δ% indicates percentage difference with previous year.

Annex C. Quick reference to CropWatch indicators, spatial units, and production estimation methodology

The following sections give a brief overview of CropWatch indicators and spatial units, along with a description of the CropWatch production estimation methodology. For more information about CropWatch methodologies, visit CropWatch online at www.cropwatch.com.cn.

CropWatch indicators

The CropWatch indicators are designed to assess the condition of crops and the environment in which they grow and develop; the indicators—RAIN (for rainfall), TEMP (temperature), and RADPAR (photosynthetically active radiation, PAR)—are not identical to the weather variables, but instead are value-added indicators computed only over crop growing areas (thus for example excluding deserts and rangelands) and spatially weighted according to the agricultural production potential, with marginal areas receiving less weight than productive ones. The indicators are expressed using the usual physical units (e.g., mm for rainfall) and were thoroughly tested for their coherence over space and time. CWSU are the CropWatch Spatial Units, including MRUs, MPZ, and countries (including first-level administrative districts in select large countries). For all indicators, high values indicate "good" or "positive."

INDICATOR			
BIOMSS			
Biomass accumulation potential			
Crop/ Ground and satellite	Grams dry matter/m^2, pixel or CWSU	An estimate of biomass that could potentially be accumulated over the reference period given the prevailing rainfall and temperature conditions.	Biomass is presented as maps by pixels, maps showing average pixels values over CropWatch spatial units (CWSU), or tables giving average values for the CWSU. Values are compared to the average value for the last five years (2011-15), with departures expressed in percentage.
CALF			
Cropped arable land and cropped arable land fraction			
Crop/ Satellite	[0,1] number, pixel or CWSU average	The area of cropped arable land as fraction of total (cropped and uncropped) arable land. Whether a pixel is cropped or not is decided based on NDVI twice a month. (For each four-month reporting period, each pixel thus has 8 cropped/ uncropped values).	The value shown in tables is the maximum value of the 8 values available for each pixel; maps show an area as cropped if at least one of the 8 observations is categorized as "cropped." Uncropped means that no crops were detected over the whole reporting period. Values are compared to the average value for the last five years (2011-15), with departures expressed in percentage.
CROPPING INTENSITY			
Cropping intensity Index			
Crop/ Satellite	Number of crops growing over a year for each pixel	Cropping intensity index describes the number of times the same hectare is used over a year. It is the ratio of the total crop area of all planting seasons in a year to the total area of arable land. It can be expressed as a dimensionless number (e.g., 1.85) or percentage (185%).	Cropping intensity is presented as maps by pixels or spatial average pixels values for MPZs, 31 countries, and 7 regions for China. Values are compared to the average of the previous five years, with departures expressed in percentage.

INDICATOR			
NDVI			
Normalized Difference Vegetation Index			
Crop/ Satellite	[0.12-0.90] number, pixel or CWSU average	An estimate of the density of living green biomass.	NDVI is shown as average profiles over time at the national level (cropland only) in crop condition development graphs, compared with previous year and recent five-year average (2011-15), and as spatial patterns compared to the average showing the time profiles, where they occur, and the percentage of pixels concerned by each profile.
RADPAR			
CropWatch indicator for Photosynthetically Active Radiation (PAR), based on pixel based PAR			
Weather /Satellite	W/m^2, CWSU	The spatial average (for a CWSU) of PAR accumulation over agricultural pixels, weighted by the production potential.	RADPAR is shown as the percent departure of the RADPAR value for the reporting period compared to the recent fifteen-year average (2001-15), per CWSU. For the MPZs, regular PAR is shown as typical time profiles over the spatial unit, with a map showing where the profiles occur and the percentage of pixels concerned by each profile.
RAIN			
CropWatch indicator for rainfall, based on pixel-based rainfall			
Weather /Ground and satellite	Liters/m^2, CWSU	The spatial average (for a CWSU) of rainfall accumulation over agricultural pixels, weighted by the production potential.	RAIN is shown as the percent departure of the RAIN value for the reporting period, compared to the recent fifteen-year average (2001-15), per CWSU. For the MPZs, regular rainfall is shown as typical time profiles over the spatial unit, with a map showing where the profiles occur and the percentage of pixels concerned by each profile.
TEMP			
CropWatch indicator for air temperature, based on pixel-based temperature			
Weather /Ground	°C, CWSU	The spatial average (for a CWSU) of the temperature time average over agricultural pixels, weighted by the production potential.	TEMP is shown as the departure of the average TEMP value (in degrees Centigrade) over the reporting period compared with the average of the recent fifteen years (2001-15), per CWSU. For the MPZs, regular temperature is illustrated as typical time profiles over the spatial unit, with a map showing where the profiles occur and the percentage of pixels concerned by each profile.
VCIx			
Maximum vegetation condition index			
Crop/ Satellite	Number, pixel to CWSU	Vegetation condition of the current season compared with historical data. Values usually are [0,1], where 0 is "NDVI as bad as the worst recent year" and 1 is "NDVI as good as the best recent year." Values can exceed the range if the current year is the best or the worst.	VCIx is based on NDVI and two VCI values are computed every month. VCIx is the highest VCI value recorded for every pixel over the reporting period. A low value of VCIx means that no VCI value was high over the reporting period. A high value means that at least one VCI value was high. VCI is shown as pixel-based maps and as average value by CWSU.
VHI			
Vegetation health index			
Crop/ Satellite	Number, pixel to CWSU	The average of VCI and the temperature condition index (TCI), with TCI defined like VCI but for	Low VHI values indicate unusually poor crop condition, but high values, when due to low temperature, may be difficult to interpret. VHI is

INDICATOR			
		temperature. VHI is based on the assumption that "high temperature is bad" (due to moisture stress), but ignores the fact that low temperature may be equally "bad" (crops develop and grow slowly, or even suffer from frost).	shown as typical time profiles over Major Production Zones (MPZ), where they occur, and the percentage of pixels concerned by each profile.
VHIn			
Minimum Vegetation health index			
Crop/ Satellite	Number, pixel to CWSU	VHIn is the lowest VHI value for every pixel over the reporting period. Values usually are [0, 100]. Normally, values lower than 35 indicate poor crop condition.	Low VHIn values indicate the occurrence of water stress in the monitoring period, often combined with lower than average rainfall. The spatial/time resolution of CropWatch VHIn is 16km/week for MPZs and 1km/dekad for China.

Note: Type is either "Weather" or "Crop"; source specifies if the indicator is obtained from ground data, satellite readings, or a combination; units: in the case of ratios, no unit is used; scale is either pixels or large scale CropWatch spatial units (CWSU). Many indicators are computed for pixels but represented in the CropWatch bulletin at the CWSU scale.

CropWatch spatial units (CWSU)

CropWatch analyses are applied to four kinds of CropWatch spatial units (CWSU): Countries, China, Major Production Zones (MPZ), and global crop Monitoring and Reporting Units (MRU). The tables below summarize the key aspects of each spatial unit and show their relation to each other. For more details about these spatial units and their boundaries, see the CropWatch bulletin online resources.

SPATIAL LUNITS	
CHINA	
Overview	*Description*
Seven monitoring regions	The seven regions in China are agro-economic/agro-ecological regions that together cover the bulk of national maize, rice, wheat, and soybean production. Provinces that are entirely or partially included in one of the monitoring regions are indicated in color on the map below.

Countries (and first-level administrative districts, e.g., states and provinces)	
Overview	*Description*
"Thirty plus one" countries to represent main producers/exporters and other key countries.	CropWatch monitored countries together represent more than 80% of the production of maize, rice, wheat and soybean, as well as 80% of exports. Some countries were included in the list based on criteria of proximity to China (Uzbekistan, Cambodia), regional importance, or global geopolitical relevance (e.g., four of five most populous countries in Africa). The total number of countries monitored is "thirty plus one," referring to thirty countries and China itself. For the nine largest countries—, United States, Brazil, Argentina, Russia, Kazakhstan, India, China, and Australia, maps and analyses may also present results for the first-level administrative subdivision. The CropWatch agroclimatic indicators are computed for all countries and included in the analyses when abnormal conditions occur. Background information about the countries' agriculture and trade is available on the CropWatch Website, **www.cropwatch.com.cn**.

Major Production Zones (MPZ)	
Overview	*Description*
Seven globally important areas of agricultural production	The six MPZs include West Africa, South America, North America, South and Southeast Asia, Western Europe and Central Europe to Western Russia. The MPZs are not necessarily the main production zones for the four crops (maize, rice, soybean, wheat) currently monitored by CropWatch, but they are globally or regionally important areas of agricultural production. The seven zones were identified based mainly on production statistics and distribution of the combined cultivation area of maize, rice, wheat and soybean.

Global Monitoring and Reporting Unit (MRU)	
Overview	*Description*
65 agro-ecological/agro-economic units across the world	MRUs are reasonably homogeneous agro-ecological/agro-economic units spanning the globe, selected to capture major variations in worldwide farming and crops patterns while at the same time providing a manageable (limited) number of spatial units to be used as the basis for the analysis of environmental factors affecting crops. Unit numbers and names are shown in the figure below. A limited number of units (e.g., MRU-63 to 65) are not relevant for the crops currently monitored by CropWatch but are included to allow for more complete coverage of global production. Additional information about the MRUs is provided online under **www.cropwatch.com.cn** .

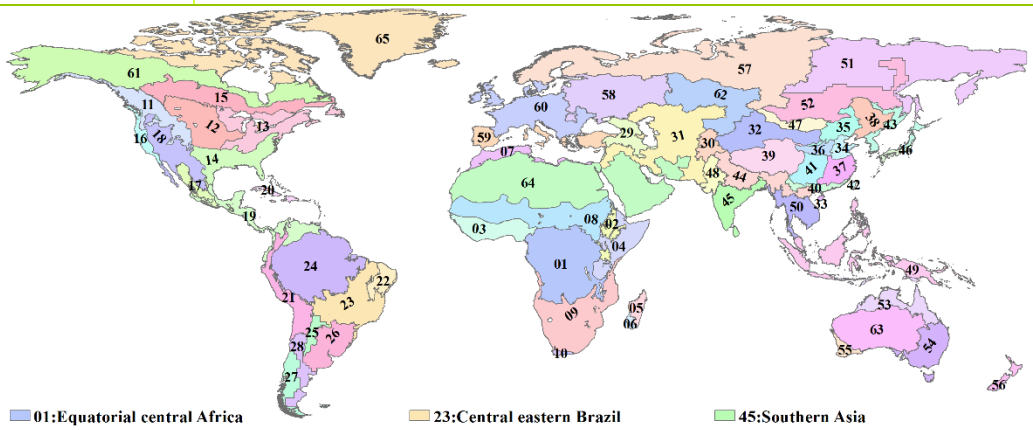

01:Equatorial central Africa
02:East African highlands
03:Gulf of Guinea
04:Horn of Africa
05:Madagascar (main)
06:Southwest Madagascar
07:North Africa Mediterranean
08:Sahel
09:Southern Africa
10:Western Cape (South Africa)
11:British Columbia to Colorado
12:Northern Great Plains
13:Corn Belt
14:Cotton Belt to Mexican Noreste
15:Sub-boreal America
16:West Coast (North America)
17:Sierra Madre
18:Southwest U.S. and north Mexican highlands
19:Northern South and Central America
20:Caribbean
21:Central-northern Andes
22:Nordeste (Brazil)
23:Central eastern Brazil
24:Amazon
25:Central-north Argentina
26:Pampas
27:Western Patagonia
28:Semi-arid Southern Cone
29:Caucasus
30:Pamir area
31:Western Asia
32:Gansu-Xinjiang (China)
33:Hainan (China)
34:Huanghuaihai (China)
35:Inner Mongolia (China)
36:Loess region (China)
37:Lower Yangtze (China)
38:Northeast China
39:Qinghai-Tibet (China)
40:Southern China
41:Southwest China
42:Taiwan (China)
43:East Asia
44:Southern Himalayas
45:Southern Asia
46:Southern Japan and Korea
47:Southern Mongolia
48:Punjab to Gujarat
49:Maritime Southeast Asia
50:Mainland Southeast Asia
51:Eastern Siberia
52:Eastern Central Asia
53:Northern Australia
54:Queensland to Victoria
55:Nullarbor to Darling
56:New Zealand
57:Boreal Eurasia
58:Ukraine to Ural mountains
59:Mediterranean Europe and Turkey
60:W. Europe (non Mediterranean)
61:Boreal America
62:Ural to Altai mountains
63:Australian desert
64:Sahara to Afghan deserts
65:Sub-arctic America

Production estimation methodology

The main concept of the CropWatch methodology for estimating production is the calculation of current year production based on information about last year's production and the variations in crop yield and cultivated area compared with the previous year. The equation for production estimation is as follows:

$$Production_i = Production_{i-1} * (1 + \Delta Yield_i) * (1 + \Delta Area_i)$$

Where i is the current year, $\Delta Yield_i$ and $\Delta Area_i$ are the variations in crop yield and cultivated area compared with the previous year; the values of $\Delta Yield_i$ and $\Delta Area_i$ can be above or below zero.

For the 31 countries monitored by CropWatch, yield variation for each crop is calibrated against NDVI time series, using the following equation:

$$\Delta Yield_i = f(NDVI_i, NDVI_{i-1})$$

Where $NDVI_i$ and $NDVI_{i-1}$ are taken from the time series of the spatial average of NDVI over the crop specific mask for the current year and the previous year. For NDVI values that correspond to periods after the current monitoring period, average NDVI values of the previous five years are used as an average expectation. $\Delta Yield_i$ is calculated by regression against average or peak NDVI (whichever yields the best regression), considering the crop phenology of each crop for each individual country.

A different method is used for areas. For China, CropWatch combines remote-sensing based estimates of the crop planting proportion (cropped area to arable land) with a crop type proportion (specific type area to total cropped area). The planting proportion is estimated based on an unsupervised classification of high resolution satellite images from HJ-1 CCD and GF-1 images. The crop-type proportion for China is obtained by the GVG instrument from field transects. The area of a specific crop is computed by multiplying farmland area, planting proportion, and crop-type proportion of the crop.

To estimate crop area for wheat, soybean, maize, and rice outside China, CropWatch relies on the regression of crop area against cropped arable land fraction of each individual country (paying due attention to phenology):

$$Area_i = a + b * CALF_i$$

where a and b are the coefficients generated by linear regression with area from FAOSTAT or national sources and CALF the Cropped Arable Land Fraction from CropWatch estimates. $\Delta Area_i$ can then be calculated from the area of current and the previous years.

The production for "other countries" (outside the 31 CropWatch monitored countries) was estimated as the linear trend projection for 2014 of aggregated FAOSTAT data (using aggregated world production minus the sum of production by the 31 CropWatch monitored countries).

Data notes and bibliography

ACAPS, https://www.acaps.org/.

China Meteorological Administration (CMA), http://www.scio.gov.cn/xwfbh/gbwxwfbh/xwfbh/qxj/Document/1473467/1473467.htm).

Climate gov. 2016. https://www.climate.gov/sites/default/files/geopolar-ssta-monthly-nnvl--1000X555--2016-07-00.png and https://www.climate.gov/enso.

CRED: http://www.cred.be/.

Disaster report, http://www.disaster-report.com/.

FAO, 2016. Global map of irrigated agriculture, GMIA, version 4.0.1. http://www.fao.org/nr/water/aquastat/irrigationmap/index.stm.

FAO, 2017. Global Administrative Units Layers (GAUL). http://www.fao.org/geonetwork/srv/en/metadata.show?currTab=simple&id=12691.

FAOSTAT, http://faostat3.fao.org/faostat-gateway/go/to/home/E.

GEO5 2012. Global environmental outlook: environment for the future we want. UNEP, Nairobi. 528 pp.

GMIA, 2017. Global map of irrigated areas, available from http://www.fao.org/nr/water/aquastat/irrigationmap/index10.stm.

Guardian, https://www.theguardian.com/world/natural-disasters?page=1.

Hallegatte, Stephane; Vogt-Schilb, Adrien; Bangalore, Mook; Rozenberg, Julie. 2017. Unbreakable : Building the Resilience of the Poor in the Face of Natural Disasters. Climate Change and Development;. Washington, DC: World Bank. World Bank. https://openknowledge.worldbank.org/handle/10986/25335.

Hendrix, C and Brinkman, H 2013 Food Insecurity and Conflict Dynamics: Causal Linkages and Complex Feedbacks. Stability: International Journal of Security & Development, 2(2): 26, pp. 1-18, DOI: http://dx.doi.org/10.5334/sta.bm.

Irin, http://www.irinnews.org/.

Kottek, M., J. Grieser, C. Beck, B. Rudolf, and F. Rubel. 2006: World Map of Köppen-Geiger Climate Classification updated. Meteorol. Z., 15, 259-263. The map used in this note is based on 1971 to 2000 data.

Kriticos, D.J., Webber, B.L., Leriche, A., Ota, N., Macadam, I., Bathols, J. & Scott, J.K. (2012) CliMond: global high resolution historical and future scenario climate surfaces for bioclimatic modelling. Methods in Ecology & Evolution 3: 53-64. DOI: 10.1111/j.2041-210X.2011.00134.x.

NOAA, Snow Cover Maps, https://www.ncdc.noaa.gov/snow-and-ice/snow-cover/.

RCRC 2008. Public health guide for emergencies. The Johns Hopkins and the International Federation of Red Cross and Red Crescent Societies, Geneva, Switzerland. 603 pp. http://www.jhsph.edu/research/centers-and-institutes/center-for-refugee-and-disaster-response/publications_tools/publications/_CRDR_ICRC_Public_Health_Guide_Book/Forward.pdf.

Reliefweb http://reliefweb.int/ and http://reliefweb.int/map/mongolia/mongolia-dzud-response-planning-22-december-2016.

Unitar, United Nations Institute for Training and Research. Population Exposure Heavy Rains in Mozambique and Zimbabwe, January 2017, http://unosat-maps.web.cern.ch/unosat-maps/MZ/FL20170118MOZ/UNOSAT_Pop_Exposure_Analysis_FL20170118MOZ_Mozambique_Zimbabwe.pdf; http://www.unitar.org/unosat/maps/MOZ.

Vancutsem, C., Marinho, E., Kayitakire, F., See, L., & Fritz, S. , 2013. Harmonizing and combining existing land cover/land use datasets for cropland area monitoring at the African continental scale. Remote Sensing,5(1), 19-41.

Wikipedia, https://en.wikipedia.org/wiki/Hurricane_Matthew; https://en.wikipedia.org/wiki/Typhoon_Sarika_(2016); https://en.wikipedia.org/wiki/Typhoon_Nock-ten_(2016).

World Bank, 2016, http://data.worldbank.org/indicator.

Zomer R J, Trabucco A, Bossio D A, Verchot L V. 2008. Climate change mitigation: A spatial analysis of global land suitability for clean development mechanism afforestation and reforestation. Agriculture, Ecosystems and Environment 126:67–80.

Zomer, R. J.; Trabucco, A.; van Straaten, O.; Bossio, D. A. 2006. Carbon, land and water: A global analysis of the hydrologic dimensions of climate change mitigation through afforestation/reforestation. Colombo, Sri Lanka: International Water Management Institute. 44p. (IWMI Research Report 101). http://www.cgiar-csi.org/wp-content/uploads/2012/11/Zomer-et-al-2007-A-Global-Analysis-of-the-Hydrologic-Dimensions-of-Climate-Change-Mitigation-through-Afforestation-and-Reforestation.pdf.

Acknowledgments

This bulletin is produced by the CropWatch research team at the Institute of Remote Sensing and Digital Earth (RADI), at the Chinese Academy of Sciences in Beijing, China. The team gratefully acknowledges the active support of a range of organizations and individuals, both in China and elsewhere.

Financial and programmatic support is provided by the Ministry of Science and Technology of the People's Republic of China, National Natural Science Foundation of China, State Administration of Grain, and the Chinese Academy of Sciences. We specifically would like to acknowledge the financial support through the National High Technology Research and Development Program of China (863 program), Grant No. 2012AA12A307; the International Science & Technology Cooperation Program of China, Grant No. 2011DFG72280; National Natural Scientific Foundations of China, Grant No. 91025007; China Grains Administration Special Fund for Public Interest, Grant No. 201313009-02, 201413003-7; CAS global food production monitoring and customization service, Grant No. KFJ-EW-STS-017; Visiting Professorships for Senior International Scientists, Grant No. 2013T1Z0016; National Natural Science Foundation, Grant No: 41561144013 and RADI funding in the form of the "Global Spatial Information System for Environment and Resources" project, Grant No: Y6SG0300CX.

The following contributions by national organizations and individuals are greatly appreciated: China Center for Resources Satellite Data and Application for providing the HJ-1 CCD data; China Meteorological Satellite Center for providing FY-2/3 data; China Meteorological Data Sharing Service System for providing the agro-meteorological data; and Chia Tai Group (China) for providing GVG (GPS, Video, and GIS) field sampling data.

The following contributions by international organizations and individuals are also recognized: François Kayitakire at FOODSEC/JRC for making available and allowing use of their crop masks; Ferdinando Urbano also at FOODSEC/JRC for his help with data; Herman Eerens, Dominique Haesen, and Antoine Royer at VITO, for providing the JRC/MARS SPIRITS software, Spot Vegetation imagery and growing season masks, together with generous advice; Patrizia Monteduro and Pasquale Steduto for providing technical details on GeoNetwork products; and IIASA and Steffen Fritz for their land use map.

Online resources

This bulletin is only part of the CropWatch resources available. Visit www.cropwatch.com.cnfor access to additional resources, including the methods behind CropWatch, country profiles, and other CropWatch publications. For additional information or to access specific data or high-resolution graphs, simply contact the CropWatch team at cropwatch@radi.ac.cn.

Online Resources posted on www.cropwatch.com.cn:

- ✓ **Definition of spatial units**
  A description of the four spatial levels of analysis: Monitoring and Reporting Units (MRU), Major Production Zones (MPZ), selected countries, and the use of sub-national administrative areas.
- ✓ **Methodology**
  Overview of CropWatch data sources and methods.
- ✓ **Time series of indicators**
  Background data on agroclimatic indicators presented in a series of tables.
- ✓ **Country profiles**
  Short profiles for each of the 30 countries and China highlighting key facts of interest to agriculture.
- ✓ **Country long term trends**
  Quick overview of average crop area, yield, and production values for maize, rice, soybean, and wheat for recent years, along with long-term (2001-12) trends (based on FAOSTAT data).

CropWatch bulletins introduce the use of several new and experimental indicators. We would be very interested in receiving feedback about their performance in other countries. With feedback on the contents of this report and the applicability of the new indicators to global areas, please contact:

Professor Bingfang Wu
Institute of Remote Sensing and Digital Earth
Chinese Academy of Sciences, Beijing, China
E-mail: cropwatch@radi.ac.cn, wubf@radi.ac.cn